VOL. 5 NO. 6 JUNE 1963

Journal of

ELECTROANALYTICAL CHEMISTRY

International Journal Dealing with all Aspects of Electroanalytical Chemistry, Including Fundamental Electrochemistry

ELSEVIER

GENERAL INFORMATION

Types of contributions

(a) Original research work not previously published in other periodicals.
(b) Reviews on recent developments in various fields.
(c) Short communications.
(d) Bibliographical notes and book reviews.

Languages

Papers will be published in English, French or German.

Submission of papers

Papers should be sent to one of the following Editors:

Professor J. O'M. Bockris, John Harrison Laboratory of Chemistry, University of Pennsylvania, Philadelphia 4, Pa., U.S.A.
Dr. R. Parsons, Department of Chemistry, The University, Bristol 8, England.
Professor C. N. Reilley, Department of Chemistry, University of North Carolina, Chapel Hill, N.C., U.S.A.

Authors should preferably submit two copies in double-spaced typing on pages of uniform size. Legends for figures should be typed on a separate page. The figures should be in a form suitable for reproduction, drawn in Indian ink on drawing paper or tracing paper, with lettering etc. in thin pencil. The sheets of drawing or tracing paper should preferably be of the same dimensions as those on which the article is typed. Photographs should be submitted as clear black and white prints on glossy paper.
All references should be given at the end of the paper. They should be numbered and the numbers should appear in the text at the appropriate places.
A summary of 50 to 200 words should be included.

Reprints

Twenty-five reprints will be supplied free of charge. Additional reprints can be ordered at quoted prices. They must be ordered on order forms which are sent together with the proofs.

Publication

The *Journal of Electroanalytical Chemistry* appears monthly and has six issues per volume and two volumes per year, each of approx. 500 pages.

Subscription price (post free): £ 10.15.0 or $ 30.00 or Dfl. 108.00 per year; £ 5.7.6 or $ 15.00 or Dfl. 54.00 per volume.
Additional cost for copies by air mail available on request.
For advertising rates apply to the publishers.

Subscriptions

Subscriptions should be sent to:

ELSEVIER PUBLISHING COMPANY, P.O. Box 211, Spuistraat 110-112, Amsterdam-C., The Netherlands.

TECHNIQUES IN PROTEIN CHEMISTRY

by J. LEGGETT BAILEY
Twyford Laboratories, London, Great Britain

4th volume in a series of monographs on New Frontiers in Molecular Biology

The principal aim of this monograph is to offer guidance to biochemists who have limited practical experience of protein chemistry, and yet wish to undertake tentative characterization and structural investigation of the proteins or peptides which interest them. Such workers will clearly require assistance in the selection of suitable techniques because of the variety of applications and modifications developed in recent years, and because these have not hitherto been comprehensively and critically surveyed in a single publication.

The result of selective condensation of a large body of literature, this essentially practical handbook should enable the non-specialist to try out the analytical procedures described without recourse to original sources. At the same time, advanced workers will be interested to have preliminary details of promising new methods. Finally, the simple presentation of the subject matter should appeal to scientists in related fields who require a concise up-to-date summary of the experimental techniques currently used in protein chemistry.

CONTENTS

5½ × 8½″ viii + 307 pages 42 tables 90 illus. 537 refs. 1963 60s.

ELSEVIER PUBLISHING COMPANY
AMSTERDAM LONDON NEW YORK

134 E

THE CAPACITY OF AN ELECTRODE IN THE PRESENCE OF AN ADSORBED SUBSTANCE OBEYING SIMPLE LAWS*

ROGER PARSONS

Department of Physical and Inorganic Chemistry, The University, Bristol

(Received January 28th, 1963)

1. INTRODUCTION

In a previous paper[1] we have discussed the possibility of obtaining the amount of a surface-active material adsorbed at an electrode surface directly from the differential capacity of the electrode. In that paper the form of the potential (or charge) dependence of the free energy of adsorption was not specified. Here we assume two simple forms for this dependence and investigate whether the capacity curves predicted as a result are in reasonable agreement with those observed experimentally.

2. THE FREE ENERGY OF ADSORPTION

The free energy of specific adsorption of both ions and molecules at an electrode must depend on the electrical state of the electrode since the adsorbed material is held partly by short-range forces and hence must be present in the inner region of the double layer where there is a large electrostatic field which may be varied by changing the potential of the electrode. In general this might be expressed by writing the standard free energy of adsorption as a power series in the field X:

$$-\ln \beta = \overline{\Delta G}^{\ominus}/kT = \Delta G^{\ominus}/kT + aX + bX^2 + cX^3 + \ldots \qquad (2\text{-}1)$$

Here $\Delta G^{\ominus}$ represents the part of the standard free energy of adsorption which does not vanish as the field becomes zero, *i.e.* the 'chemical' part. This 'chemical' part of the free energy may itself depend on the field, but this dependence may formally be included in the terms of higher powers of X. The main contribution to the linear term aX arises from the electrostatic interaction of the charge of an ion or the permanent dipole (with fixed orientation) of an ion or molecule with the field in the double layer.

However, the field in the inner region is not measurable directly and it is necessary to relate it to a quantity which is accessible such as the potential drop across the inner layer, *e.g.* by assuming a linear potential drop across the inner region, or the charge on the metal *e.g.* by assuming Gauss's law and a dielectric constant independent of the distance from the electrode surface. The choice between these two variables cannot be made with certainty. For the adsorption of ions the charge is the clearer

* Presented at a Symposium on 'Some Aspects of Electrochemistry' on October 6th, 1961 in New Delhi under the auspices of the National Institute of Sciences of India.

concept with which to work and the easier to obtain from experiment. This is because the observed potential differences include the potential across the diffuse layer which changes with the amount of ionic adsorption. In the adsorption of uncharged substances the diffuse layer correction is more easily made; nevertheless the charge is still probably the more satisfactory variable. In the adsorption of iodide ion on mercury from aqueous KI it has been found[1] that the standard free energy of adsorption is very closely represented by a linear function of the charge. This behaviour can be explained with a very simple model representing the inner region of the double layer as a parallel plate condenser of constant thickness containing a dielectric of constant properties. The adsorbed ion then behaves as a point charge located on a fixed plane parallel to the plates of the condenser. On the other hand a similar behaviour should be found for the adsorption of a dipole with constant orientation. In fact for the adsorption of thiourea[2] some deviation was found from the linear dependence of the standard free energy of adsorption with charge. This was interpreted in terms of a change in the dielectric constant of the inner layer, which is in reasonable agreement with theoretical expectations[3]. Hence the simpler behaviour of the adsorbed ion may be a result of the compensation of the effect of the dielectric constant variation with the effect of a change in the distance of the ion from the electrode.

For the majority of systems in which an uncharged substance is adsorbed at a mercury electrode, it is found that the capacity curve or the electrocapillary curve at the extreme ends of the potential range coincides with the curve for the base solution. Hence the neutral substance becomes desorbed at large values of the charge on the mercury whether positive or negative. For this reason it is unlikely that the odd powers in the series (2-1) have any importance for the adsorption of many types of uncharged molecules. The theories of FRUMKIN[4] and of BUTLER[5] are both based on the assumption that a quadratic function is adequate to represent the variation of standard free energy with field. At first sight BUTLER's theory appears the more realistic as it expresses the energy in terms of the interaction of the field with the permanent and induced dipoles of the adsorbed molecules. However, it is more difficult to relate to the dimensions of the double layer since these enter only implicitly. FRUMKIN's theory leads more directly to some insight into the structure of the double layer. There is also a difference in the form of the adsorption isotherm used. BUTLER assumed an ideal form with the lowering of the interfacial tension proportional to the surface concentration while FRUMKIN assumed a more realistic isotherm allowing for the size of the adsorbate and the interaction between the particles.

FRUMKIN considered the energy change when, as a result of the adsorption of a molecule, the capacity of an element of the double layer of area S changes from the value C per unit area appropriate to the base solution to the value C' appropriate to the electrode saturated with adsorbed material. The energy change is:

$$\overline{\Delta G}^{\ominus} = \Delta G^{\ominus} + \tfrac{1}{2}E^2(C - C')S + E\{\mu/l - \mu'/l'\}, \qquad (2\text{-}2)$$

where E is the potential drop across the inner region of the double layer whose thickness is l in the absence of adsorbate and l' in its presence. μ is the component of the dipole moment of the double layer element perpendicular to the condenser plates in the absence of adsorbate and μ' is the same quantity when the element is filled with adsorbate.

It follows from (2-2) that $\overline{\Delta G}^{\ominus}$ has a maximum value* when E has the value

$$E_{max} = -(\mu/l - \mu'/l')/(C - C')S\,, \tag{2-3}$$

so that if we define

$$\overline{\Delta G}^{\ominus}_{max} = \Delta G^{\ominus} - (\mu/l - \mu'/l')^2/2(C - C')S \tag{2-4}$$

and

$$\Delta = E - E_{max}\,, \tag{2-5}$$

we can rewrite (2-2) in the form

$$\overline{\Delta G}^{\ominus} = \overline{\Delta G}^{\ominus}_{max} + \tfrac{1}{2}(C - C')S\Delta^2\,, \tag{2-6}$$

which is analogous to that used by BUTLER.

On the other hand if we consider the energy of adsorption to be determined by the charge on the metal, we can write

$$\overline{\Delta G} = \Delta G + \tfrac{1}{2}q^2\left\{\frac{1}{C'} - \frac{1}{C}\right\}S + 4\pi q\{\mu/\varepsilon - \mu'/\varepsilon'\}\,, \tag{2-7}$$

where ε and ε' are the dielectric constants in the presence and absence of adsorbate, respectively. Now the maximum in the standard free energy of adsorption occurs at

$$q_{max} = -4\pi(\mu/\varepsilon - \mu'/\varepsilon')/\left\{\frac{1}{C'} - \frac{1}{C}\right\}S\,, \tag{2-8}$$

and

$$\overline{\Delta G}^{\ominus}_{max} = \Delta G^{\ominus} - [4\pi(\mu/\varepsilon - \mu'/\varepsilon')]^2/2\left\{\frac{1}{C'} - \frac{1}{C}\right\}S\,. \tag{2-9}$$

If

$$\delta = q - q_{max} \tag{2-10}$$

$$\overline{\Delta G}^{\ominus} = \overline{\Delta G}^{\ominus}_{max} + \tfrac{1}{2}\left\{\frac{1}{C'} - \frac{1}{C}\right\}S\delta^2\,. \tag{2-11}$$

Thus in either method of analysis the shape of the free energy curve depends only on the change in the capacity caused by adsorption, while the position of the maximum adsorption (minimum standard free energy of adsorption) on the potential or charge scale depends on the permanent dipole moment of the adsorbed species**. This conclusion is analogous to that made by Butler because, in effect, he described the capacity in terms of the polarizability per unit volume of the medium within the double layer condenser. However, on FRUMKIN's model it is clear, as he pointed out, that the change from C to C' may occur as a result of a change of either the polarizability of the dielectric or the thickness of the condenser or both simultaneously.

* BREITER AND DELAHAY[6] state the BUTLER's theory predicts a maximum adsorption at the apex of the electrocapillary curve. In fact the maximum adsorption occurs at a potential determined by the polarity of the adsorbed molecules in a way very similar to that described by (2-3).

** In effect, any variation in the component of the dipole moment perpendicular to the electrode surface is treated as a contribution to the dielectric constant, or, in BUTLER's theory, to the polarizability. Hence the values of μ and μ' may not have a close relation to the molecular dipole moment but will depend on the amount of re-orientation undergone by the adsorbed molecule when the potential changes.

Consequently a free energy which is quadratic in the electrical parameter can occur with saturated dielectries, if the thickness of the inner layer is increased by the adsorbed substance. Hence the adsorption of large ions like the tetra-alkyl-ammonium ions will show similar behaviour to that of neutral substances because their distance of closest approach to the electrode is greater than that of the inorganic ions used in the base solution.

3. THE FORM OF THE CAPACITY CURVE WHEN THE STANDARD FREE ENERGY IS LINEARLY DEPENDENT ON THE FIELD IN THE DOUBLE LAYER

We have shown previously[1] that for an adsorption isotherm of the form

$$\Gamma_i = \Gamma_i\,(\beta a_i)\,, \tag{3-1}$$

The change in the capacity on adsorption is

$$\Delta C = C - C^b = kT\left\{\frac{\partial}{\partial E}\left(\Gamma\frac{\partial \ln \beta}{\partial E}\right)\right\}_{T,p,\mu_i},$$

$$= kT\left\{\Gamma\left(\frac{\partial^2 \ln \beta}{\partial E^2}\right)_{T,p} + \left(\frac{\partial \Gamma}{\partial \ln \beta}\right)_{T,p,\mu_i}\left(\frac{\partial \ln \beta}{\partial E}\right)^2_{T,p}\right\}, \tag{3-2}$$

if β is considered as a function of E. Now if we put

$$-\ln \beta = \overline{\Delta G}^{\ominus}/kT = \Delta G^{\ominus}/kT + aE\,, \tag{3-3}$$

it follows that

$$(\partial \ln \beta/\partial E)_{T,p} = -a\,; \quad (\partial^2 \ln \beta/\partial E^2)_{T,p} = 0\,, \tag{3-4}$$

so that

$$\Delta C = a^2 kT\,(\partial \Gamma/\partial \ln \beta)_{T,p}\,. \tag{3-5}$$

This enables us to calculate the form of the relation between ΔC and the potential since $\partial \Gamma/\partial \ln \beta$ can be calculated from the isotherm equation and expressed as a function of potential using (3-3). We now describe the result of this procedure for some simple adsorption isotherms*.

For the Henry's Law isotherm the capacity equation is

$$\Delta C = a^2 kT A e^{-aE} \tag{3-6}$$

where $A = a_i \exp[-\Delta G^{\ominus}/kT]$. It is clear that a plot of log ΔC against E, should be a straight line of slope $-a/2.303$. Similarly for the Freundlich isotherm we obtain

$$\ln \Delta C - \ln(a^2 kTA/x) = -aE/x\,, \tag{3-7}$$

i.e. the slope of the log $\Delta C - E$ plot is reduced by the factor $1/x$. The Langmuir adsorption isotherm leads to the expression

$$\Delta C = Aa^2 kT e^{-aE}/\{1 + (A/\Gamma_s)e^{-aE}\}^2\,. \tag{3-8}$$

* The isotherm equations are given in ref. 2.

This may be plotted as a single function by plotting ln $(\Delta C/\Gamma_S a^2 kT)$ against aE + ln (A/Γ_S). Such a plot is shown in Fig. 1. We note that the slope of this curve approaches the ideal value when adsorption is small (negative E, since the curve is plotted for anion adsorption and for this a is negative), because the Langmuir isotherm reduces to Henry's law at low coverages. A maximum value of ΔC is reached when the surface is half covered and further increase in the amount of adsorption results in a decrease of ΔC. Eventually a second region is reached where log ΔC is proportional to E but the slope is of opposite sign to that at low coverages.

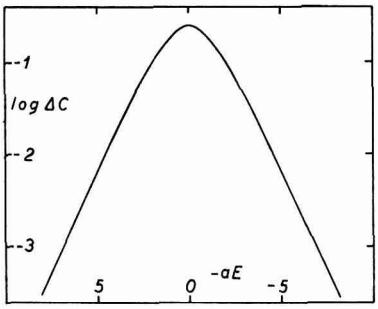

Fig. 1. Relation between change of capacity and the potential for the adsorption of a substance obeying a Langmuir isotherm with a free energy of adsorption linearly dependent on potential.

The change in capacity when the adsorbed substance obeys a virial adsorption isotherm cannot be expressed simply in terms of the potential because the equation for Γ in terms of β is transcendental. However the calculation can be carried out numerically and the results plotted in the form of $\log_{10} \Delta C$ + const. against aE + const. This is done in Fig. 2 for positive and negative values of the second virial coefficient B. If B is positive, ΔC approaches a constant value as the coverage increases; this type of behaviour was discussed previously[2] for the adsorption of thiourea. On the other hand if B is negative (corresponding to attraction between the adsorbed particles) the slope of the log ΔC — E curve becomes numerically greater.

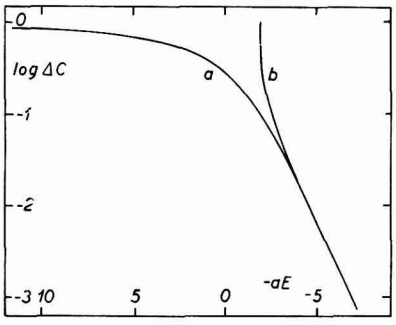

Fig. 2. Relation between change of capacity and the potential for the adsorption of a substance obeying a virial isotherm with a free energy of adsorption linearly dependent on potential. (a) second virial coefficient positive; (b) second virial coefficient negative.

It is clear that the Langmuir and the virial isotherms take into account two different properties of the adsorbed molecules: the former allows for the size of the molecules, *i.e.* the short-range repulsive forces which can be represented as an abrupt increase in the potential energy; while the latter allows (at small coverages) for repulsive (or attractive) forces which vary appreciably as the distance between the adsorbed particles changes. The simplest isotherm allowing for the two effects simultaneously is that proposed by TEMKIN[7] which leads to the expression (*cf.* ref. 1)

$$\Delta C = \frac{a^2 kT\,\Gamma_s}{f}\left\{\frac{A\,e^{-aE}}{1+A\,e^{-aE}} - \frac{A\,e^{-aE-f}}{1+A\,e^{-aE-f}}\right\} \tag{3-9}$$

Since this equation has two parameters, Γ_s the saturation coverage and f describing the interaction energy, we cannot plot a universal log $\Delta C - E$ curve as for the simpler isotherms. In Fig. 3 is shown a plot of this function for several values of f. It is evident that as f (which is analogous to B in the virial isotherm) increases the region of the maximum of the curve becomes broader. For very large values of f the curve would have an almost horizontal region (like that of the ririal curve) separating the two parts of the curve where log ΔC is proportional to E.

It seems probable that most experimental curves will have the general form of those shown in Fig. 3 although minor deviations may occur as a result of deviations from the Temkin isotherm or from (3-3). In particular we may expect that so long as

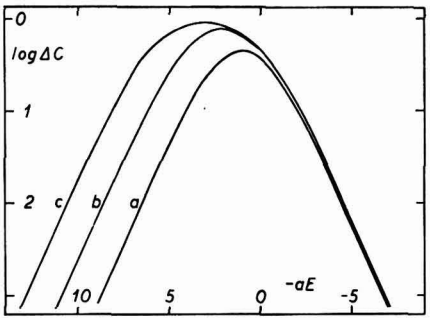

Fig. 3. Relation between change of capacity and potential for the adsorption of a substance obeying a Temkin isotherm with a free energy of adsorption linearly dependent on potential (a) $f = 2$; (b) $f = 4$; (c) $f = 6$.

(3-3) is obeyed, all systems should have a linear relation between log ΔC and E at the beginning of adsorption. No large deviation from linearity is observed in the plots of Figs. 1–3 until the coverage is greater than about 10% of saturation (or $\Gamma > 0.1/B$). It is possible that deviation will also occur if the capacity becomes so large that it is comparable to the capacity of the diffuse layer which has been ignored here.

It was noted previously[1] that the equations deduced by assuming that $\overline{\Delta G}^{\ominus}$ is a function of electrode charge have precisely the same form as those using potential as the electrical variable, if $-1/C$ is substituted for C and q for E. Consequently Figs. 1–3 predict the results of a plot of log $[-\Delta(1/C)]$ against q for adsorption isotherm which have a free energy which is linearly dependent upon q.

Data for the examination of these relations are not plentiful. Recently BARKER AND FAIRCLOTH[8] have studied the capacity of mercury in contact with 1.5 M $HClO_4$ to which small quantities of a chloride or a bromide have been added. Their results are plotted in the form of $\log_{10} \Delta C$ against E in Fig. 4. It is evident that all these results

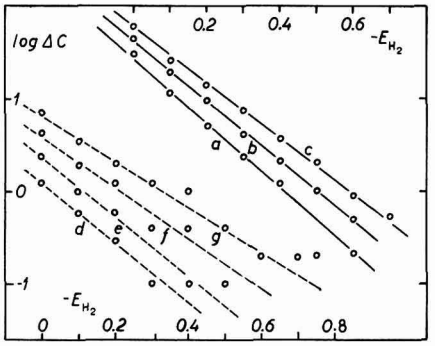

Fig. 4. Relation between change of capacity and the potential for the adsorption of bromide (full lines) and chloride (dotted lines) on mercury from a solution of aqueous 1.5 M $HClO_4$ (BARKER AND FAIRCLOTH[8])
(a) 0.02 M; (b) 0.05 M; (c) 0.1 M; (d) 0.025 M; (e) 0.05 M; (f) 0.1 M; (g) 0.2 M.

lead to an essentially linear relation with a about -6.6 V^{-1} for chloride and about -7.5 V^{-1} for bromide. There appears to be a change of slope with concentration, and although this may be due to the scatter of the points, it probably reflects the over-simplification of the theory. On the other hand, if we plot $\log [-\Delta(1/C)]$ against q, the linearity of the plots is not nearly so satisfactory. On this evidence, therefore, it must be concluded that it is preferable to represent the data in terms of E.

A similar result is found for the adsorption of thiourea on mercury using the data of Schapink *et al.*[9]. The plots of $\log \Delta C$ against E are remarkably well represented by a set of parallel straight lines as shown in Fig. 5. However, when $\log [-\Delta(1/C)]$ is plotted against q the lines are distinctly curved and only at the most negative charges is the slope as large as would be expected from the detailed analysis of this system[2]. Consequently, it appears that results of the kind shown in Figs. 4 and 5 must be regarded with caution though they may provide some preliminary information about an adsorption system.

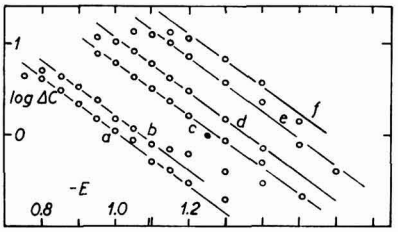

Fig. 5. Relation between the change of capacity and the potential in the adsorption of thiourea on mercury from aqueous NaF (SCHAPINK *et al.*[9]).
(a) 0.005 M; (b) 0.01 M; (c) 0.05 M; (d) 0.1 M; (e) 0.25 M; (f) 0.5 M.

4. THE FORM OF THE CAPACITY CURVE WHEN THE FREE ENERGY IS DEPENDENT ON THE SQUARE OF THE FIELD IN THE DOUBLE LAYER

It follows from equation (2-6) that

$$(\partial \ln \beta/\partial E)_{T,p} = -b\Delta \; ; \quad (\partial^2 \ln \beta/\partial E^2)_{T,p} = -b \, , \tag{4-1}$$

if we put

$$b = (C - C')S/kT \, .$$

Consequently, from (3-2)

$$\Delta C = kT\{-b\Gamma + (b\Delta)^2(\partial \Gamma/\partial \ln \beta)_{T,p}\} \, . \tag{4-2}$$

This is a more complicated function than (3-5) as it has two maxima and three minima. The minima occur at $\Delta = 0$ and $\Delta = \pm\infty$, while the condition for the maxima is

$$b\Delta^2 = 3(\partial \Gamma/\partial \ln \beta)_{T,p}/[\partial^2 \Gamma/(\partial \ln \beta)^2]_{T,p} \, . \tag{4-3}$$

The minima at $\Delta = \pm\infty$ occur as a result of complete desorption of the adsorbate while that at $\Delta = 0$ corresponds to the maximum adsorption Γ_{max} for a given concentration. It follows that

$$\Delta C_{min} = -bkT\,\Gamma_{max} \tag{4-4}$$

for any isotherm of type (3-1) for which (4-1) is valid at the potential of maximum adsorption. This fact was pointed out by LORENZ, MÖCKEL AND MÜLLER[10] and used by them in their study of adsorption isotherms on mercury.

The potential dependence of an adsorption obeying Henry's law may be written:

$$\Gamma = \Gamma_{max}\, e^{-b\Delta^2/2} \tag{4-5}$$

which, together with the fact that for this isotherm $(\partial \Gamma/\partial \ln \beta)_{T,p} = \Gamma$ leads to the expression

$$\Delta C/bkT\,\Gamma_{max} = e^{-b\Delta^2/2}(1 - b\Delta^2) \tag{4-6}$$

for the change in capacity as a function of potential. This is plotted in Fig. 6. We note that the maxima on the ΔC curves occur at $\Delta = \pm\sqrt{3/b}$ and that it follows from (4-5) that the amount adsorbed at the potential of these peaks is $e^{-3/2}\,\Gamma_{max}$ or 0.223 Γ_{max}. Since the value of ΔC at the peak (ΔC_p) obtained from (4-6) is $+ 2bkTe^{-3/2}\,\Gamma_{max}$ we see that the ratio $\Delta C_p/\Delta C_{min}$ is $-2\,e^{-3/2}$ or -0.446. Thus if the adsorbate obeys a Henry's law isotherm, the position of the peaks depends only on the value of b and not on the concentration of the adsorbate in solution; also there is a constant ratio of peak height to the lowering of the capacity at the minimum. The Freundlich isotherm leads to the capacity – potential curve expressed by

$$\Delta C/bkT\,\Gamma_{max} = e^{-b\Delta^2/2x}(1 - b\Delta^2/x) \, . \tag{4-7}$$

Thus the difference from Henry's law is the same as if the constant b is divided by x. The ratio $\Delta C_p/\Delta C_{min}$ remains the same.

The Langmuir isotherm leads to a capacity–potential curve which may be expressed in the form

$$\Delta C/bkT\,\Gamma_{max} = [\theta_m - (1-\theta_m)e^{b\Delta^2/2}]^{-1}\left\{1 - b\Delta^2\left[1 + \frac{\theta_m}{1-\theta_m}e^{-b\Delta^2/2}\right]^{-1}\right\} \qquad (4\text{-}8)$$

from which it is clear that the form of the curve depends on the value of θ_m the degree of coverage at the maximum amount adsorbed; this is, of course, determined for a given electrode by the concentration of the adsorbate in solution. Some curves for different values of θ_m are shown in Fig. 6. As already noted by LORENZ AND MÖCKEL[11],

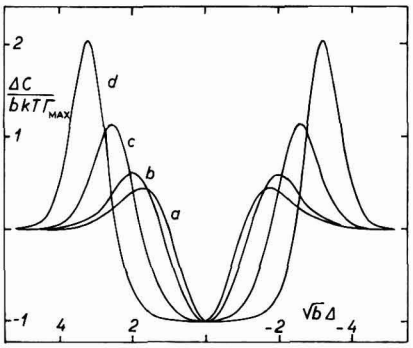

Fig. 6. Relation between the change of capacity and the potential for the adsorption of a substance obeying a Henry's law isotherm or a Langmuir isotherm with a free energy of adsorption dependent on the square of the potential.
(a) Henry's law; (b) Langmuir $\theta_m = 0.50$; (c) Langmuir $\theta_m = 0.91$; (d) Langmuir $\theta_m = 0.99$.

the peaks in the curve become higher and move apart as the concentration (and hence θ_m) increases. The potential of the maximum of the peak Δ_p may be found (4-3) which leads to the transcendental equation

$$\frac{1-\theta_m}{\theta_m}e^{b\Delta_p^2/2} = \frac{b\Delta_p^2 + 3}{b\Delta_p^2 - 3}, \qquad (4\text{-}9)$$

or, since the coverage at the maximum is related to the activity of the adsorbate a_i by

$$(1-\theta_m)/\theta_m = e^{\overline{\Delta G}^{\ominus}_{max}/kT}/a_i$$

this may be expressed

$$b\Delta_p^2/2 = -\overline{\Delta G}^{\ominus}_{max}/kT + \ln a_i - \ln\left[\frac{b\Delta_p^2 + 3}{b\Delta_p^2 - 3}\right]. \qquad (4\text{-}10)$$

When the concentration is high so that $a_i \gg \exp(\overline{\Delta G}^{\ominus}/kT)$ the last term is (4-10) becomes unimportant and the linear relation between Δ_p^2 and $\ln a_i$ found by LORENZ AND MÖCKEL[11] is obeyed. Equation (4-10) was solved by a graphical method and Fig. 7 shows the solution. We note that at low concentrations $b\Delta_p^2$ becomes asymptotic to the value 3 which is that found for the Henry's law isotherm. This suggests that the deviation from their linear plot found by LORENZ AND MÖCKEL are not necessarily due to deviations from the Langmuir isotherm as they suggested.

The capacity curve for an adsorbed substance obeying a virial adsorption isotherm may be expressed in the form

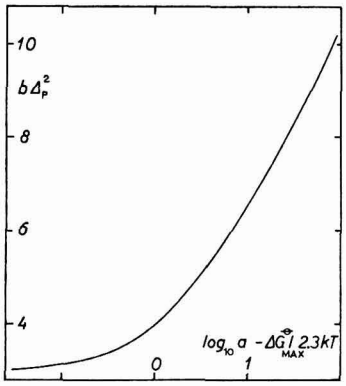

Fig. 7. Relation between the potential at which the change of capacity is a maximum and the concentration of adsorbing substance when the latter obeys a Langmuir isotherm with a free energy dependent on the square of the potential.

$$\Delta C/bkT\,\Gamma_{max} = -(\Gamma/\Gamma_{max})\left\{1 - \frac{b\Delta^2}{1 + B\Gamma}\right\}. \qquad (4\text{-}11)$$

As we mentioned earlier, Γ cannot be expressed simply in terms of the potential for this isotherm. Some curves calculated from this equation are shown in Fig. 8. In common with the curves based on the Langmuir isotherm, the peaks in the capacity move apart as the concentration of the adsorbate in solution increases, if the second virial coefficient is positive. However, the peaks are broader and not so high as

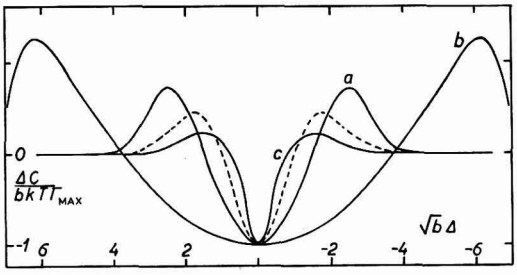

Fig. 8. Relation between the change of capacity and the potential for the adsorption of a substance obeying a virial isotherm with a free energy dependent on the square of the potential.
(a) $\Gamma_{max} = 1/B$; (b) $\Gamma_{max} = 10/B$; (c) $\Gamma_{max} = -0.5/B$.
Dotted line shows relation for Henry's law.

those of Fig. 6; this is because the chemical potential of the adsorbed species changes more rapidly with coverage when a virial isotherm is obeyed than when a Langmuir is obeyed at medium coverages. On the other hand, if the second virial coufficient is negative, then the peaks tend to become lower and to approach one another as the concentration is increased. The curve shown in Fig. 8 corresponds to $\Gamma_{max} = -0.5/B$ which is the limiting value. It can be seen that the change from the Henry's law curve is small. The upper limit of the ratio $\Delta C_p/\Delta C_{min}$ is about -0.23.

The equation for the capacity curve of a substance obeying Temkin's isotherm is

$$\Delta C/bkT\,\Gamma_{max} = -\frac{\theta}{\theta_m}\left[1 - \frac{b\Delta^2}{f\theta}\left\{\frac{\beta a_i}{1+\beta a_i} - \frac{\beta a_i\,e^{-f}}{1+\beta a_i\,e^{-f}}\right\}\right], \tag{4-12}$$

where

$$\theta = \frac{1}{f}\ln\left[(1+\beta a_i)/(1+\beta a_i\,e^{-f})\right].$$

As pointed out in the previous section this is a more realistic type of isotherm Variation in two parameters which we take as θ_m and f is possible. The curve in Fig. 9 is calculated for $f = 4$ and $\theta_m = 0.99$. Comparison with the Langmuir curve for

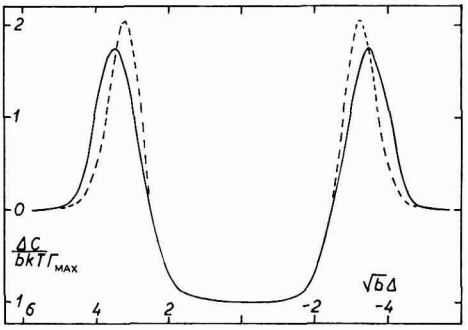

Fig. 9. Relation between the change in capacity and the potential for the adsorption of a substance obeying a Temkin isotherm with a free energy dependent on the square of the potential and $f = 4$, $\theta_m = 0.99$. Dotted line shows relation for Langmuir isotherm with $\theta_m = 0.99$.

$\theta_m = 0.99$ shows that the difference in the region between the peaks where ΔC is negative is negligible. This is the region of high coverage where the forces between adsorbed particles become virtually constant. Hence the adsorption follows the Langmuir isotherm well and the value of f has no effect on the shape of the curve. On the other hand in the region of the peaks, the coverage is moderate and increase of f tends to lower and broaden the peaks in the same way as the increase of B in the virial isotherm.

5. THE INTERPRETATION OF EXPERIMENTAL RESULTS FOR THE ADSORPTION OF NEUTRAL MOLECULES

It is clear from the results of the previous section that there is not likely to be a simple way of comparing experimental capacity curves with the theoretical predictions in order to identify the isotherm and to determine its parameters; this is in contrast with the results of section 3. There are some approximations which can be made to simplify the procedure. First, measurements can be made at very high frequency when, as pointed out by FRUMKIN AND MELIK-GAIKAZYAN[12] the second term in the bracket of (4-2) vanishes. The observed ΔC is then simply proportional to the amount adsorbed. Second, measurements can be made at small values of Δ so that the second term in the bracket of (4-2) is negligible. The region of potential over

which this approximation is valid depends on the amount adsorbed. For the Langmuir and Temkin isotherms the error is less than 1% at $|\Delta| < 0.8/\sqrt{b}$ if $\theta_m = 0.99$; at $|\Delta| < 0.4/\sqrt{b}$ if $\theta_m = 0.91$ and $|\Delta| < 0.1/\sqrt{b}$ if $\theta_m = 0.5$. Hence, it seems likely that this method will give reliable results near to saturation, but not at the lower coverages, except, of course at $\Delta = 0$.

Thus only values of the capacity at $\Delta = 0$ are of real use in identifying the isotherm directly from low frequency capacity measurements. Third, measurements at very large values of Δ can be used. Under these conditions the amount of adsorption is small and all isotherms approach the Henry's law isotherm (4-6) which approximates to the form:

$$\Delta^2 = -(2/b) \ln (\Delta C/bkT\, \Gamma_{max}) . \qquad (5\text{-}1)$$

Hence the slope of a plot of log ΔC against Δ^2 gives the value of b and the intercept gives Γ_{max} though the extrapolation may be unreliable. However, if b is constant throughout the potential range, the value found from (5-1) may be used to calculate Γ_{max} from ΔC_{min} using (4-4). These values may be used to identify the isotherm and to calculate the reminder of the capacity curve.

This last method is illustrated in Fig. 10 where the results plotted are those obtained by BREITER AND DELAHAY[6] for the adsorption of amyl alcohol on mercury from 1 M $NaClO_4$. The points for the far cathodic region agree satisfactorily with equation (5-1) although there is some scatter. The value of b found is 10 V^{-2}. A similar plot for the far anodic region does not give such good linearity, but there are some indications that the results are not so reliable in this region. If we substitute this value of b into (4-4) we find the value of Γ_{max} for the solution of 0.1 M amyl alcohol to be 0.047 molecules/A^2. This is not in very good agreement with the value of 0.062 molecules /A^2 obtained from BREITER AND DELAHAY's interfacial tension measurements, but it compares well with that found from the area of long chain alcohols by insoluble film technique[13] 21 A^2/molecules (0.048 molecules/A^2). However, it seems likely that this value of b is too low. We have seen that the value of Δ_p is $\pm\sqrt{3/b}$ for an ideal adsorbed film; with $b = 10$ V^{-2}, Δ_p is $\pm$ 0.55 V. According to BREITER AND DELAHAY's results Δ_p reaches this value when the concentration of amyl alcohol is 0.05 M. But $\Delta C_p/\Delta C_{min}$ for this solution is -1.64 *i.e.* much smaller than the value -0.45 for an ideal surface layer. Hence this peak must occur at a potential greater than $\sqrt{3/b}$ so that b must be greater than 10 V^{-2}. A similar conclusion is reached from the curve in the most dilute solution (0.006 M amyl alcohol) for which the adsorbed layer is probably close to ideality. Here the cathodic peak probably occurs at $\Delta_p \simeq -0.35$ V, corresponding to a value of $b \simeq 24$ V^{-2}. On the other hand $\Delta C_p/\Delta C_{min}$ for this curve is about -0.21 which is larger than the ideal value. It is possible that this value could indicate attraction between adsorbed molecules, but even with the limiting curve of $\Gamma_{max} = -0.5/B$ shown in Fig. 8 this would lead to $b \simeq 19$ V^{-2}.

A more probable explanation is that in spite of the extrapolation used by BREITER AND DELAHAY, the capacities in the region of the peaks are not zero-frequency capacities. If this is so the values of the capacity in the region of the peak are too low by an amount which increases as the potential of the peak is approached. The slope of the curves in Fig. 10 could then be too low.

An examination of published capacity curves for systems of this type reveals that the ratio $\Delta C_p/\Delta C_{min}$ is often greater than -0.446 for the solutions dilute in the adsorbing substance. This may be due to the fact that they are not zero-frequency capacities. On the other hand the ΔC curve is rarely symmetrical about its minimum, nor is the potential of the minimum independent of the concentration of adsorbed substance. Hence the simple quadratic expression (2-6) is unlikely to give a precise representation of the experimental results. These deviations could also be due to the change of the constants of the isotherm with potential. If this is so, the isotherm is no

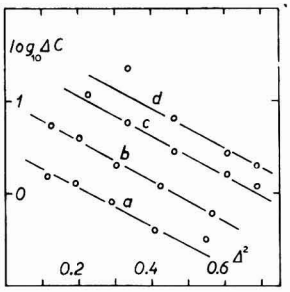

Fig. 10. Relation between the change in capacity and the potential for the adsorption of amyl alcohol on mercury from 1 M $NaClO_4$ (BREITER AND DELAHAY[6])
(a) 0.006 M; (b) 0.012 M; (c) 0.024 M; (d) 0.05 M.

longer of the form (3-1). The asymmetry does not vanish if we represent the capacity as a function of q instead of E. Hence we must conclude that it is an intrinsic property of the systems which have been studied. This is not so surprising when we note that in all the measurements a specifically adsorbed anion is present. It is possible that the use of NaF as a base electrolyte might lead to some improvement in the agreement with a simple theory of the form outlined here. On the other hand the capacity for pure aqueous sodium fluoride solution is by no means symmetrical so that it may be essential to develop expressions allowing for a more complex dependence of the free energy of adsorption on the field in the double layer.

I would like to express my gratitude to Professor R. H. BUSCH and his colleagues for providing congenial surroundings in his department at the University of Buenos Aires where part of this paper was written.

SUMMARY

The form of the dependence on field of the standard free energy of adsorption at an electrode is discussed. Linear and quadratic laws are considered to be reasonable first approximations for two types of adsorption. The form of the capacity curve is calculated using these two laws together with some simple adsorption isotherms. Comparison with experiment confirms the suggestion that these are only first approximations.

REFERENCES

1 R. PARSONS, *Trans. Faraday Soc.*, 55 (1959) 999.
2 R. PARSONS, *Proc. Roy. Soc.*, A261 (1961) 79.
3 R. J. WATTS-TOBIN, *Phil. Mag.*, 61 (1961) 133.
4 A. N. FRUMKIN, *Z. Physik.*, 35 (1926) 792.
5 J. A. V. BUTLER, *Proc. Roy. Soc.*, A122 (1929) 399.
6 M. BREITER AND P. DELAHAY, *J. Amer. Chem. Soc.*, 81 (1959) 2938.
7 M. I. TEMKIN, *Zhur. Fiz. Khim.*, 15 (1941) 296.
8 G. C. BARKER AND R. FAIRCLOTH, *Advances in Polarography*, 1 (1961) 313.
9 F. W. SCHAPINK, K. W. OUDEMAN, K. W. LEU AND I. N. HELLE *Trans. Faraday Soc.*, 56 (1960) 415.
10 W. LORENZ, F. MÖCKEL AND N. MÜLLER, *Z. physik. Chem.*, 25 (1960) 145.
11 W. LORENZ AND F. MÖCKEL, *Z. Elektrochem.*, 60 (1956) 507
12 A. N. FRUMKIN AND V. I. MELIK-GAIKAZYAN, *Doklady Akad. Nauk*, 78 (1951) 885.
13 N. K. ADAM, *Physics and Chemistry of Surfaces*, Oxford, 3rd edition, (1941) p. 50.

CHRONOPOTENTIOMETRY OF HYDROGEN PEROXIDE WITH A PLATINUM WIRE ELECTRODE

JAMES J. LINGANE AND PETER JAMES LINGANE*

Department of Chemistry, Harvard University, Cambridge 38, Mass.

(Received January 18th, 1963)

In a previous study in this laboratory[5] it was found that the reduction of oxygen at a platinum cathode under chronopotentiometric conditions produces only a single wave in both strongly acid and strongly alkaline media, and the diffusion-controlled transition time corresponds to a 4-electron reduction. This indicates that under chronopotentiometric conditions any hydrogen peroxide transiently formed is immediately reduced. It was of interest, therefore, to examine the chronopotentiometric behaviour of hydrogen peroxide itself, and this has been done in the present study.

EXPERIMENTAL

Merck 30% "Superoxal" was used as the source of hydrogen peroxide. After suitable dilutions, the hydrogen peroxide solutions were standardized spectrophotometrically via the peroxy titanium sulfate complex or by titration with ceric sulfate or potassium permanganate. All chemicals were of reagent grade quality and were used without further purification. Prepurified nitrogen was used to purge the electrolysis solutions.

Authentically pure (99.99%) platinum wire was obtained from Englehard Industries, Inc., Newark 2, New Jersey. The working electrode was prepared by sealing this platinum wire into the end of 6 mm soft glass tubing. The finished electrode measured 2.27 cm in length, was 0.0495 cm in diameter and hence had a projected area, excluding the end, of 0.333 cm^2.

The general electrical circuitry employed in chronopotentiometry and the particular cell employed in this investigation have been described elsewhere[1]. A Sargent model MR recording potentiometer was used to obtain the curves reproduced in this paper. Separate experiments have shown that the chart drive of this instrument is accurate to ± 0.1 sec; therefore, transition times were interpolated directly from the chart paper. Transition time measurements were also made by manually opening the electrolysis circuit at the "transition potential" and thus stopping a stop clock[1]. In conjunction with this latter technique, either the Sargent recorder, a Leeds and Northrup Model 7664 pH indicator, or a Dumont Model 403 oscilloscope were employed as visual voltmeters. The oscilloscope was always employed for transition time measurements below about three seconds.

* Present address: *Division of Chemistry and Chemical Engineering, California Institute of Technology, Pasadena* (Calif., USA).

The solutions were thermostated at 25.0 ± 0.1°C.

All potentials were measured with respect to the saturated calomel electrode (S.C.E.).

In the course of this discussion, it will be convenient to refer to "active" and to "clean" electrodes. An active electrode is one which has been anodized and cathodized several times. The extent of surface oxidation is constant under these conditions and corresponds to about 500 μC/cm²*. A clean electrode is one whose surface is completely free of all oxide(s) and finely divided metal. The clean state is most conveniently achieved by soaking the electrode in 1 *F* sulfuric acid for twenty-four hours.

RESULTS AND DISCUSSION

The general characteristics of the anodic and cathodic chronopotentiograms of hydrogen peroxide in 0.5 *F* perchloric acid and 1.0 *F* sulfuric acid are shown in Figs. 1 and 2. The chronopotentiograms were recorded *seriatim* and are separated by one minute of vigorous stirring with nitrogen followed by one minute of quiescence. Curves 12 through 21 have been omitted since they represent the repeated anodic and cathodic cycling of the electrode. Cycling the electrode means that it was anodized to the transition potential (+1.30 V in these media), reduced to the cathodic transition potential (—0.20 V), reanodized, etc. The solution was then stirred for one minute and allowed to become quiet for one minute before curve 22 was recorded.

The behavior in perchloric and sulfuric acids is similar except for the potential fluctuations observed only in perchloric acid (curve 23, Fig. 1). Discussion of this phenomenon is reserved for a later section.

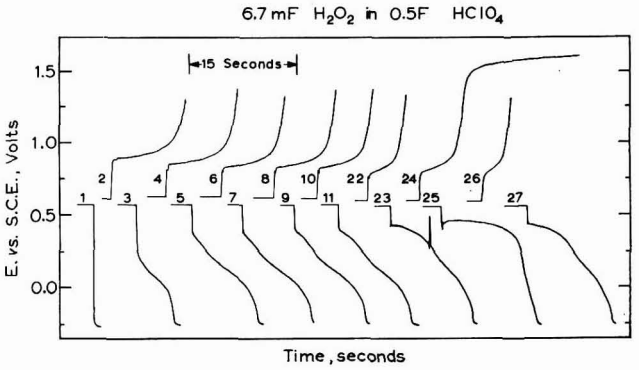

Fig. 1. Oxidation and reduction of 6.7 m*F* hydrogen peroxide in 0.5 *F* perchloric acid at a current density of 1.7 mA/cm². The curves were recorded *seriatim*, and are separated by one minute of vigorous nitrogen stirring followed by one minute of quiescence. Curve 1 was recorded with a "clean" electrode. Curves 12–21 were omitted, and correspond to the repeated anodic and cathodic cycling of the electrode.

Curve 1 of Fig. 1, demonstrates that hydrogen peroxide does not show a reduction wave on a clean electrode (defined above); the potential drops immediately to the value at which hydrogen ion is reduced. Curve 2 shows a well developed wave for the

* ANSON AND LINGANE[2] and LINGANE[1] have reported larger values. This discrepancy is to be expected since the ratio of projected to microscopic area differs with individual electrodes[1].

oxidation of hydrogen peroxide. The potential at which this wave begins (+0.89 V *vs.* S.C.E.) is about 0.4 V more oxidizing than the standard potential of the O_2-H_2O_2 couple (+0.44 V *vs.* S.C.E.); and it corresponds to the potential at which the platinum electrode is itself oxidized to form a film of platinum oxides[2,3]. As HICKLING AND WILSON[3] pointed out, this clearly suggests that the electron-transfer reaction is the oxidation of the platinum itself to form a film of PtO + PtO_2, and these platinum oxides are then "chemically" reduced by hydrogen peroxide. We have confirmed that the platinum oxide film is readily reduced by hydrogen peroxide. Thus the oxidation of hydrogen peroxide proceeds via the reduction of these platinum oxides and the primary electron-transfer reaction is the oxidation of the platinum metal. The rate of diffusion of hydrogen peroxide governs the transition time under this condition even though the hydrogen peroxide is undergoing a "chemical" rather than an "electrochemical" (electron-transfer) oxidation at the electrode surface.

Curve 3 and subsequent cathodic trials, exhibit waves for the reduction of hydrogen peroxide. This is in sharp contrast with the behavior on a clean electrode (curve 1). These reduction waves are produced only after activation of the electrode by the anodic trials. With increasing number of anodic and cathodic trials, the activity of the electrode increases. Because of this, the cathodic transition time increases until it stabilizes at a value (curve 7) about equal to the anodic transition time for curve 2. This increased activity of the electrode is also reflected by a decrease in the overpotential for the reduction of hydrogen peroxide.

The film of PtO + PtO_2 formed during the anodic trial is reduced to finely divided platinum during the subsequent cathodization. Very probably the reduction mechanism involves the preliminary oxidation of the platinum itself by the hydrogen peroxide (or a strong oxidant derived therefrom, *vide infra*) and the electron-transfer step is reduction of the oxidized platinum species. We believe that the preliminary "chemical" reaction, rather than the subsequent electron-transfer reaction is rate determining.

This chemical step is too slow on a clean electrode to prevent the potential from dropping immediately to the value for hydrogen ion reduction (curve 1). As the activity of the electrode increases, providing additional finely divided platinum, the rate of this "chemical" step increases until the chemical oxidation proceeds sufficiently rapidly so that the diffusion of hydrogen peroxide to the electrode becomes rate determining.

We subscribe to the hypothesis that the potential of any metal electrode, including the noble metals such as platinum, is always determined by the activity of the metal ions in equilibrium with it. Furthermore, as the activity of the electrode increases the rate of the chemical oxidation of the platinum surface will increase while the rate of the electron-transfer step remains constant (at constant current). Thus an increase in the activity of the electrode should produce an increase in the extant activity of the platinum species and a decrease in the overpotential for the reduction of hydrogen peroxide, as observed.

Curve 26 in Fig. 2 was recorded after the electrode had stood in the solution for thirty minutes following the recording of curve 25. Curve 26 demonstrates that the pre-activated electrode loses much of its "activity" on standing for some time in dilute acid. This treatment reproduces the same states of the electrode as correspond to curves 1, 3, 5, etc., but in reverse order. This behavior is very similar to that

previously observed in the reduction of oxygen[5], and it appears to result from the gradual oxidation and dissolution of the finely divided platinum deposit formed by the preceding anodic-cathodic cycling.

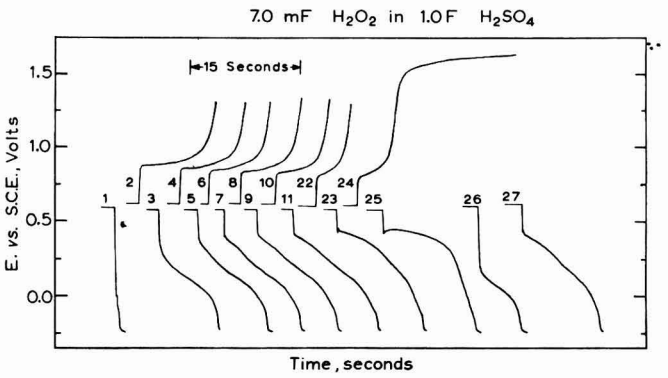

Fig. 2. Oxidation and reduction of 7.0 mF hydrogen peroxide in 1.0 F sulfuric acid at a current density of 1.7 mA/cm^2. The technique was the same as in Fig. 1. Curve 26 was recorded after the electrode had been allowed to stand for thirty minutes in a reduced condition. The electrode was reduced to hydrogen ion reduction for thirty seconds after curve 26; the solution was then stirred and allowed to become quiet before curve 27 was recorded.

After curve 26 in Fig. 2 was recorded the electrode was polarized cathodically to hydrogen ion reduction for 30 seconds, and then, after stirring for a few minutes to remove hydrogen from the electrode surface, curve 27 was recorded. It is evident that such strong pre-cathodization restores the activity of the electrode to a considerable degree. This effect has also been observed by LINGANE[5] and SAWYER *et al.*[15] in the reduction of oxygen.

In contrast to the cathodic behavior, the anodic transition times decrease as the activity of the electrode increases. Finely divided platinum is known to be an active catalyst for the disproportionation of hydrogen peroxide at the surface of the electrode. We observed that the electrode becomes sheathed in oxygen bubbles if the quiescent period is extended to ten minutes. Therefore, when electrolysis begins, the hydrogen peroxide concentration at the surface of the electrode will be less than in the bulk of the solution, and correspondingly an anodic transition time decreases.

During the cathodic electrolysis, both hydrogen peroxide and the oxygen formed by disproportionation diffuse to the electrode and are reduced there. The diffusion coefficients of hydrogen peroxide and oxygen appear to stand in such a relationship to one another that, coupled with the circumstance of a one minute quiescent period, there is no significant change in the overall cathodic transition time, *i.e.*, it corresponds to the diffusion controlled situation, *vide supra*.

Because of the disproportionation of the hydrogen peroxide at the electrode surface a definite ritual of pretreatment must be employed to obtain reproducible transition times. The procedure employed in this investigation was to maximize the transition times by the use of a clean electrode for anodic chronopotentiometry and an active electrode for cathodic chronopotentiometry.

Fig. 3 is a plot of $i\tau^{\frac{1}{2}}/CA$ *vs.* τ for the anodic and cathodic chronopotentiometry

of hydrogen peroxide in 1.0 F sulfuric acid. The anodic points have been corrected for concomitant oxidation of the electrode by the empirical relationship[1,4]
where Q is the extent of the surface oxidation of the electrode and was measured to be 152 μC (430 μC/cm^2).

$$i_{corr.} = i_{obs.} - \frac{Q}{\tau}$$

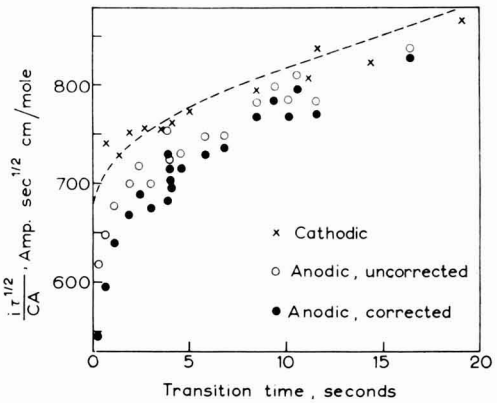

Fig. 3. Variation of $i\tau^{\frac{1}{2}}/CA$ with transition time for the oxidation and reduction of hydrogen peroxide in 1.0 F sulfuric acid. The hydrogen peroxide concentration varied between 7 and 13 mF. Anodic points have been corrected for the concomitant surface oxidation of the electrode; the uncorrected values are presented for comparison. Cathodic points correspond to the second cathodic trial after anodization. The dashed line is the plot of the Peters-Lingane equation[3] for $D = 1.55 \times 10^{-5}$ cm^2/sec.

The cathodic points correspond to the second cathodic trial after anodization. The transition times corresponding to the first cathodic trials are about 3–5% larger due to the reduction of the residual oxide film. This procedure is essentially that previously adopted in the study of oxygen reduction[5].

The dashed line in Fig. 3 corresponds to the plot of the PETERS-LINGANE eqn. (4) for $D = 1.5 \times 10^{-5}$ cm^2/sec. This is not an independent value of the diffusion coefficient but it was selected to fit the cathodic points. Unfortunately, D cannot be measured polarographically because the hydrogen peroxide wave occurs at a potential more reducing than the hydrogen wave in this medium. There are no literature values available for D in this medium, but BLACKBURN[6] determined it to be 1.6×10^{-5} cm^2/sec in 1 F perchloric acid. In spite of the lack of an independent value of D it is evident that under the conditions of Fig. 3 the oxidation and reduction of the hydrogen peroxide are both diffusion-controlled.

The anodic points in Fig. 3 fall increasingly further below the theoretical plot as the transition time decreases. That this is not caused by over-correction is evident because the uncorrected and corrected points show the same trend. Most probably this is caused by the disproportionation of hydrogen peroxide during the quiescent period. The quantity of hydrogen peroxide which disproportionates during the quiescent period is constant (for a given quiescent period), but since the quantity of hydrogen peroxide which is electrochemically oxidized up to the transition time

decreases with decreasing transition time the effect of the prior disproportionation is enhanced at shorter transition times.

Note that the cathodic waves in Figs. 1 and 2 at first show more and more doublet character as the activity of the electrode is increased by anodic-cathodic cycling. However, following very strong activation of the electrode by prolonged preanodization, the reduction process is essentially a singlet wave (curves 25). It is important to note that while the ratio of the two transition times has changed considerably between curves 7 and 25, the sum of the two transition times is approximately unchanged. This demonstrates that the diffusion of hydrogen peroxide governs the total transition time ($\tau_1 + \tau_2$), and that the factors which govern the relative ratio of the processes corresponding to τ_1 and to τ_2 operate only at the surface of the electrode. We believe that these two transition times correspond respectively to the reduction of oxygen formed by disproportionation of hydrogen peroxide and to the direct reduction of hydrogen peroxide.

Employing platinum and gold electrodes, and voltammetric techniques, KOLTHOFF AND JORDAN[7] found that the presence of trace amounts of oxygen "induces the electroreduction of hydrogen peroxide at potentials at which hydrogen peroxide is not (or very slowly) reduced...." They concluded that the electroreduction of oxygen to hydrogen peroxide proceeds in two stages, *viz.*

$$O_2 + e^- \rightarrow O_2^- \quad (1)$$

$$O_2^- + e^- \rightarrow O_2^{--} \quad (2)$$

and that the O_2^- ion so formed reacts with the hydrogen peroxide according to the Haber-Weiss mechanism

$$O_2^- + H_2O_2 \rightarrow OH^- + OH\cdot + O_2 \quad (3)$$

$$OH\cdot + e^- \rightarrow OH^- \quad (4)$$

The summation of eqns. (3) and (4), *viz.*

$$O_2^- + H_2O_2 + e^- \rightarrow 2OH^- + O_2 \quad (5)$$

is equivalent to the reduction of hydrogen peroxide catalyzed by the O_2^- ion.

KOLTHOFF AND JORDAN found that the diffusion currents for hydrogen peroxide in the presence of less than 10^{-6} *M* oxygen are linear with the hydrogen peroxide concentration up to 1.6 m*M*, the largest studied. Evidently, the presence of 10^{-6} *M* oxygen is more than sufficient to catalyze the diffusion controlled reduction of hydrogen peroxide.

Very likely a similar mechanism is operative under the conditions of our experiments, and the small amounts of oxygen formed by disproportionation at the electrode surface catalyze the reduction of hydrogen peroxide and lead to the doublet character of the reduction wave.

BLACKBURN[6] reached similar conclusions from a chronopotentiometric study of the reduction of hydrogen peroxide on palladium. On this electrode, the chronopotentiometric reduction of oxygen proceeds in two stages, presumably reduction to hydrogen peroxide and subsequent reduction to water. BLACKBURN found a doublet

wave for the reduction of hydrogen peroxide and the potentials of these two waves correspond exactly to the waves encountered in the reduction of oxygen.

These conclusions were foreshadowed as long ago as 1907 by WEIGERT[8], who studied the oxidation and reduction of hydrogen peroxide at a rotating platinum electrode, and concluded, "..... so liegt die Vermutung nahe, dass die primäre Reaktion stets der Zerfall des Wasserstoffsuperoxyds ist, und die Reduktion desselben also nichts anderes ist als die Reduktion des Sauerstoffs."

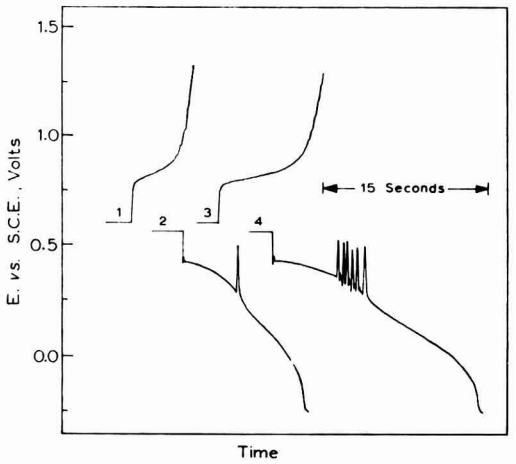

Fig. 4. Effect of current density on the potential fluctuations observed in the reduction of 6.7 mF hydrogen peroxide in 0.5 F perchloric acid. The pretreatment of the electrode was the same as that of curve 23, Fig. 1. The curves were recorded *seriatim* and are separated by one minute of vigorous nitrogen stirring and one minute of quiescence. Curves 1 and 2 were recorded at a current density of 1.7 mA/cm^2, while curves 3 and 4 were recorded at a current density of 1.4 mA/cm^2.

In perchloric acid medium (but not in sulfuric acid) with an activated electrode rapid, periodic fluctuations of the potential are observed in the cathodic wave near the end of the first part of the doublet wave. These fluctuations are noticeable on curve 23 of Fig. 1 and they are delineated more clearly by the curves in Fig. 4. The fluctuations were observed on oscilloscopic traces as well as on the curves recorded with a recording potentiometer.

The periodic change in overpotential which causes the potential fluctuations suggests the periodic accumulation at the electrode surface of an intermediate reduction species which is a more rapid oxidant than hydrogen peroxide itself. On the basis of the Haber-Weiss mechanism, the most likely such intermediates are hydroxyl radical and perhydroxyl (HO_2 or O_2^-). Either of these may either undergo further reduction as formed, or react with hydrogen peroxide. The fluctuations in overpotential may then result from periodic changes in the relative extents to which these alternate paths are followed.

Periodic chemical and electrochemical phenomena are well known, though perhaps not so thoroughly understood[10,11]. The more important of these phenomena are the periodic dissolution of metals, electrode oxidation and reduction phenomena, and

periodic catalysis. The last is especially well known in the case of the disproportionation of hydrogen peroxide[12]. Colloidal platinum is known to yield periodic catalysis, although the authors were unable to achieve periodic catalysis with platinized platinum[13]. For an excellent review, together with an attempt to relate all these phenomena to the surface activity of the electrode, the monograph of Hedges and Myers is recommended[14].

BUCK AND GRIFFITH[16] have recently reported periodic minima in the oxidation potentials of formaldehyde and methanol in strong sulfuric acid under chromopotentiometric conditions. These oscillations are strikingly similar to those reported in this communication. However, in contrast with our experience with hydrogen peroxide, the amplitude of these oscillations increases with the current density and sulfuric acid does not interfere with their production.

A qualitative investigation was undertaken to define the conditions under which these potential fluctuations occur. They are only observed with an active electrode; they are not observed until after the electrode had been cycled many times (see Fig. 1).

For each concentration of hydrogen peroxide there is a maximal current density above which the potential fluctuations do not occur at all. This maximal current density increases both with the hydrogen peroxide concentration and with the degree of activation of the electrode. Curve 2 in Fig. 4 is almost identical with curve 23 in Fig. 1. Note that under these conditions the process responsible for the potential fluctuation is relatively inhibited since only one fluctuation is observed. Curves 3 and 4 in Fig. 4 were recorded after curves 1 and 2 but at a somewhat lower current density.

The conclusion seems inescapable that these fluctuations require the presence of finely divided metal on the surface of the electrode. If, as we believe, the mechanism for the reduction of hydrogen peroxide involves the chemical oxidation of this finely divided metal, it is probable that the cause for this periodicity is to be found in the chemical step rather than in the rapid electroreduction of the resulting platinum oxides.

We were unable to observe the potential fluctuations with hydrogen peroxide concentrations smaller than about 6 mF, even with a very strongly activated electrode and with small current densities.

Since it is likely that the reduction of oxygen and hydrogen peroxide involve similar intermediates, we attempted to obtain the potential fluctuations in the presence of oxygen. We were unable to do so for solutions containing oxygen alone at one atmosphere pressure although solutions of both oxygen and hydrogen peroxide did yield the minima. The concentration of oxygen under these conditions is about 1 mM and so failure to achieve potential fluctuations may simply reflect an insufficient oxygen concentration.

The presence of more than about 25 mF sulfate completely prevents the potential fluctuations, although the reduction wave is normal in other respects. Potential fluctuations can be obtained in the presence of 50 mF borate, although only after especially strong preanodization.

We were unable to observe the potential fluctuations in the presence of 0.05 mF chloride. Furthermore, the cathodic wave is a singlet under these conditions. For chloride concentrations above about 1 mF, the anodic wave is a doublet because of the oxidation of chloride beginning at about +1.25 V.

ACKNOWLEDGEMENT

One of us (P.J.L.) would like to thank THOMAS R. BLACKBURN, DENNIS H. EVANS, and DENNIS G. PETERS for helpful discussion[1].

SUMMARY

The oxidation and reduction of hydrogen peroxide are diffusion controlled in 1.0 *F* sulfuric acid. It is believed that hydrogen peroxide is reduced by oxidizing the platinum surface; the platinum oxides are then reduced by direct electron-transfer. In both sulfuric acid and in 0.5 *F* perchloric acid, the reduction process is more rapid than diffusion only if the electrode surface is lightly platinized or "activated". This implies that the chemical step proceeds rapidly only on a platinized surface.

This lightly platinized surface causes shorter anodic transition times in both solutions because the disproportionation rate is increased on such surfaces.

A Haber-Weiss mechanism is invoked to explain the reduction process after the manner of KOLTHOFF AND JORDAN. It is thought that oxygen formed by disproportionation catalyzes the reduction of hydrogen peroxide; at more cathodic potentials, the hydrogen peroxide is reduced directly since the reduction wave displays doublet character.

Rapid decreases or fluctuations in the overpotential for the reduction of hydrogen peroxide were observed in perchloric acid for hydrogen peroxide concentrations greater than 6 m*F*. The presence of small amounts of cyanide, sulfate, borate, chloride, and methyl red inhibit the minima. Large current densities also inhibit the minima.

REFERENCES

1 J. J. LINGANE, *J. Electroanal. Chem.*, 1 (1960) 379.
2 F. C. ANSON AND J. J. LINGANE, *J. Am. Chem. Soc.*, 79 (1957) 1015, 4901.
3 A. HICKLING AND W. WILSON, *J. Electrochem. Soc.*, 98 (1951) 425.
4 D. G. PETERS AND J. J. LINGANE, *J. Electroanal. Chem.*, 2 (1961) 1.
5 J. J. LINGANE, *J. Electroanal. Chem.*, 2 (1962) 296.
6 T. R. BLACKBURN, *Ph.D. Thesis*, Harvard University, 1962. Chapters IV and V.
7 I. M. KOLTHOFF AND J. JORDAN, *J. Am. Chem. Soc.*, 74, 570, 4801 (1952).
8 F. WEIGERT, *Z. Physik. Chem.*, 60 (1907) 513.
9 *Ibid.*, P. 541.
10 E. S. HEDGES AND J. E. MYERS, *Nature*, 128 (1931) 398.
11 E. S. HEDGES AND J. E. MYERS, *J. Chem. Soc. (London)*, 127, 1013 (1925).
12 H. C. SCHUMB, C. N. SATTERFIELD AND R. L. WENTWORTH, *Hydrogen Peroxide*, Reinhold Publishing Company, New York, 1955.
13 E. S. HEDGES AND J. E. MEYERS, *J. Chem. Soc. (London)*, 125, 1282 (1924).
14 E. S. HEDGES AND J. E. MYERS, *The Problem of Physico-Chemical Periodicity*, Longmans-Green, Inc., New York, 1926.
15 D. T. SAWYER AND L. V. INTERRANTE, *J. Electroanal. Chem.*, 2 (1961) 310.
16 R. P. BUCK AND L. R. GRIFFITH, *J. Electrochem. Soc.*, 109 (1962) 1005.

MECHANISM OF THE $Zn^{II}/Zn(Hg)$ EXCHANGE

Part 1: THE $Zn^{2+}/Zn(Hg)$ EXCHANGE

N. S. HUSH AND J. BLACKLEDGE

Department of Physical and Inorganic Chemistry, The University, Bristol

(Received February 6th, 1963)

INTRODUCTION

Accurate measurement of the rates of rapid reactions involving electrodeposition of metals is a comparatively recent development in electrochemistry. Owing to the high rate of electron-exchange associated with this type of process, the overpotential results largely from concentration polarization. It is possible, by applying an a.c. voltage of sufficiently high frequency, to reduce the concentration polarization and study the primary electrode processes in more detail than is often possible by the use of d.c. techniques alone; the simplest measurements of this kind are those of the a.c. impedance of an electrode in the absence of a d.c. component (zero net current flow)[1-4]. A good deal of information about the rates of processes in which the exchange currents are not greater than 1 amp/cm^2 has already been accumulated in this way.

In the present investigation, impedance and d.c. measurements have been made on the Zn^{2+} aq./Zn(Hg) system. Previous work by RANDLES[1,5] and by ERSHLER[6] has established the general features of the electrode process, including the activation energy; d.c. measurements[7] lead to essentially the same results. In a more comprehensive study, GERISCHER[8] has identified the species involved in the reactions in complexing solutions, and has obtained the transfer coefficients for these reactions. The aim of the experiments described in this paper was to gain more information about the detailed mechanism of the $Zn^{2+}/Zn(Hg)$ exchange in non-complexing solutions through a comparison of a.c. and d.c. results, and through a study of ionic strength and temperature effects; in part 2 the catalytic effects of weakly-complexing ions will be discussed.

RATE CONSTANTS OF THE ELECTRODE PROCESSES

(*i*) *Single rate-determining step*

For a reversible reaction represented by

$$ne + O \underset{\overleftarrow{k}}{\overset{\vec{k}}{\rightleftharpoons}} R \qquad (1)$$

in which the rate-determining step involves the transfer of n electrons, the current density I at an overpotential η can be written as

$$I/n\mathrm{F} = \vec{k}' a_O \exp - n\alpha \mathrm{F}\eta/RT - \overleftarrow{k}' a_R \exp n(1-\alpha)\,\mathrm{F}\eta/RT \qquad (2)$$

where a_O and a_R are the activities of oxidised and reduced species, η is the overpotential, $\vec{k}'$ and $\overleftarrow{k}'$ are the rate constants for the forward and reverse exchange processes, and α is the transfer coefficient defined by

$$\alpha = -\frac{RT}{n\mathrm{F}}\left(\frac{\partial \ln \vec{k}'}{\partial \eta}\right)_T \tag{3}$$

The remaining symbols have their usual significance. The specific rate constants $\vec{k}$ and $\overleftarrow{k}$ differ from $\vec{k}'$ and $\overleftarrow{k}'$ by inclusion of the activity coefficients f_O and f_R of species O and R in the latter. Thus

$$\begin{aligned} \vec{k} &= f_O \vec{k}' \\ \overleftarrow{k} &= f_R \overleftarrow{k}'. \end{aligned} \tag{4}$$

The specific rate constant $\vec{k}$ is

$$\vec{k} = e\tau\varkappa \frac{kT}{h} \cdot \frac{f_O}{f_{\neq}} \cdot \exp - \Delta\vec{G}^{\neq}/RT \tag{5}$$

where $\varkappa$ is the average transmission coefficient[9] for activated complexes with energy $\geqslant$ the barrier energy, τ is the barrier penetration factor[9], $f_{\neq}$ is the activity coefficient of the activated complex, and $\Delta\vec{G}^{\neq}$ is the standard electrochemical free energy of formation[10,11] of 1 mole of activated complex from the reactants in their standard states at overpotential η.

When the system is in equilibrium ($I = 0$) we obtain from equation (2) and the Nernst equation a simple expression[12] for the exchange current density i_0.

$$i_0/n\mathrm{F} = k' a_O^{(1-\alpha)} a_R^{\alpha} \tag{6}$$

where k' is the value of $\vec{k}'$ or $\overleftarrow{k}'$ at the normal potential V_O of the system. The activation polarization resistance R_D associated with the exchange current is[1,2]

$$R_D = \left(\frac{\partial \eta}{\partial I}\right)_{\eta \to 0} = \frac{RT}{n\mathrm{F} i_0} \tag{7}$$

In the a.c. experiments described in this paper, a parallel combination of a capacity C_p and a resistance R_p (Fig. 1) were used to balance the impedance across the electrode interface, and R_D was obtained by extrapolation of the measured R_p to infinite frequency to eliminate the diffusion impedance in series with R_D.

The rate constant k' can be obtained from the exchange current density, if the activity coefficients f_O and f_R are known. A rate constant is in practice calculated for equal concentrations of O and R. Denoting this constant by k, it follows from equations (4) and (7) that

$$k = k' f_O^{(1-\alpha)} f_R^{\alpha}. \tag{8}$$

The experimental 'a.c.' rate constant k is thus in full

$$k = e\tau\varkappa \frac{kT}{h} \cdot \frac{f_R^{\alpha} f_O^{(1-\alpha)}}{f_{\neq}} \cdot \exp - \Delta\bar{G}_O^{\neq}/RT, \tag{9}$$

where $\Delta\bar{G}_O^{\neq}$ is the standard electrochemical free energy of activation at the normal potential V_O.

(ii) Consecutive steps

When the electrode reaction proceeds through two or more exchange steps of comparable rates, the analysis of the observed a.c. impedance is rather different. The theory will be briefly outlined here, as the possibility of a two-step mechanism for the $Zn^{2+}/Zn(Hg)$ exchange will be discussed later. In this case, the reaction path contains an intermediate ionic species, which will be the mono-ion M^+ if the initial ion is M^{2+}. The reaction scheme for two steps is represented as:

$$M^{2+} + e \underset{k_{-1}}{\overset{k_1}{\rightleftharpoons}} M^+ \qquad (10)$$

$$M^+ + e \underset{k_{-2}}{\overset{k_2}{\rightleftharpoons}} M(Hg)$$

In terms of the activities of the reacting species, the current I at an overpotential η (measured, as before, with respect to the normal potential of the $M^{2+}/M(Hg)$ couple) is:

$$\begin{aligned} I/2F &= k'_1 a_O \exp - \beta_1 F\eta/RT - k'_{-1} a_M \exp(1-\beta)F\eta/RT \\ I/2F &= k'_2 a_M \exp - \beta_2 F\eta/RT - k'_{-2} a_R \exp(1-\beta_2)F\eta/RT \end{aligned} \qquad (11)$$

where a_M is the activity of the intermediate species M^+ and the primed rate constants are related to those of (10) by an equation analogous to (4). The exchange current densities for the two steps are then:

$$\begin{aligned} i_1/F &= k'^2 a_O^{(1-\alpha_1)} a^{\alpha_1}{}_R \\ i_2/F &= k'^1 a_O^{(1-\alpha_2)} a^{\alpha_2}{}_R \end{aligned} \qquad (12)$$

where the coefficients α_1 and α_2 are defined as

$$\begin{aligned} \alpha_1 &= \beta_1/2 \\ \alpha_2 &= (1+\beta_6)/2 \end{aligned} \qquad (13)$$

The activation polarization resistance R_D is then[13]

$$R_D = \left(\frac{\partial\eta}{\partial I}\right)_{\eta\to o} = \frac{RT}{4F}\left(\frac{1}{i_1}+\frac{1}{i_2}\right) \qquad (14)$$

The equivalent circuit for this mechanism consists of a series combination of polarization resistances R_1 and R_2 associated with the first and second steps. The apparent exchange current density i_0^* is, for such a process,

$$\frac{1}{i_0^*} = \frac{1}{i_1} + \frac{1}{i_2} \qquad (15)$$

If α_1 and α_2 are known, the individual exchange currents and rate constants can be found. Writing the apparent (measured) transfer coefficient α^* as

$$\alpha^* = 1 - \left(\frac{\partial \ln i^*}{\partial \ln a_O}\right)_{a_R,\mu,T} \qquad (16)$$

the ratio of individual exchange currents is

$$\frac{i_1}{i_2} = \left\{\frac{\alpha^* - \alpha_1}{a_2 - \alpha^*}\right\}. \tag{17}$$

The individual rate constants k_1 and k_2 are then

$$k_1 = k^* \left\{\frac{\alpha_2 - \alpha_1}{\alpha_2 - \alpha^*}\right\}$$
$$k_2 = k^* \left\{\frac{\alpha_2 - \alpha_1}{\alpha^* - \alpha_1}\right\} \tag{18}$$

where $k^* = i_0^*/2F$. These are equal to the specific rate constants for the first and second steps multiplied by the activity coefficient factors $(f_R/f_O)^{\alpha_1}$, $(f_R/f_O)^{\alpha_2}$, respectively [*cf.* eqn. (4)].

In order to obtain sufficient data to solve these equations for a two-step process, the relative heights of the two energy barriers must be altered sufficiently for a transition from control by one to control by the other to be observed. Experimentally there are two ways in which this might be achieved at constant temperature: (1) large anodic or cathodic polarization, (2) alteration of the double-layer potential. A direct current method is useful for large overvoltages, as it is not practicable to measure a.c. impedances when the ratio C_O/C_R is either very small or very large. The region of most interest here is that of fairly high anodic overpotential, and the d.c. dissolution current of dropping zinc amalgam electrodes were measured and analysed.

EXPERIMENTAL

The same electrolytic cell was used in both a.c. and d.c. measurements; in the d.c. work, a saturated calomle reference electrode was inserted, using an NH_4ClO_4 salt bridge, to standardise the potential of the polarized electrode. In the a.c. measurements a mercury pool acted as a secondary non-polarizable electrode.

The cell was of conventional design, carrying a capillary electrode and nitrogen bubblers which enabled the contents to be either outgassed or blanketed with presaturated nitrogen. Capillaries of suitable diameter were obtained by drawing out 1 mm bore thick-walled Hysil tubing, and were sealed into the cell. Typical capillary characteristics were: drop-time t = 9.0 sec, flow-rate m = 0.34 mgm.sec^{-1}, under a pressure of 60 cm Hg.

A reservoir containing a supply of zinc amalgam was attached to the cell-head and was maintained under a pressure of nitrogen; when the capillary was not in use the pressure was reduced slightly below that required to cause the amalgam to flow. The temperature of the nitrogen was maintained equal to that of the aqueous solution by means of a large glass coil immersed in a separate thermostat bath, on order to minimise temperature gradients in the mercury or amalgam column.

Preparation of the zinc amalgam was carried out by electrolysis of a molar solution of $ZnSO_4$ (pH ~ 2) in a cell similar to that described by RANDLES[1]. Once prepared, the amalgam was run into the reservoir, which had been flushed out with oxygen-free nitrogen for 30 minutes. The concentration of each amalgam was checked polarographically at regular intervals by recording the anodic current in a 2 *M* $NaClO_4$

solution; the value of the diffusion coefficient of zinc in a dilute amalgam used in this work is that determined by STROMBERG[15] ($D_{Zn} = 1.57 \times 10^{-5} cm^2 sec^{-1}$ at 25°C)*.

A schematic diagram of the electrical circuitry associated with both a.c. and d.c. measurements is shown in Fig. 1. A Tinsley automatic polarograph, operated manually, provided the d.c. potential which was standardized against that of a Muirhead Weston cell using a Tinsley potentiometer. The current was measured by a Pye Scalamp galvanometer, the sensitivity of which could be varied from 0.10–5.6 μA/cm.

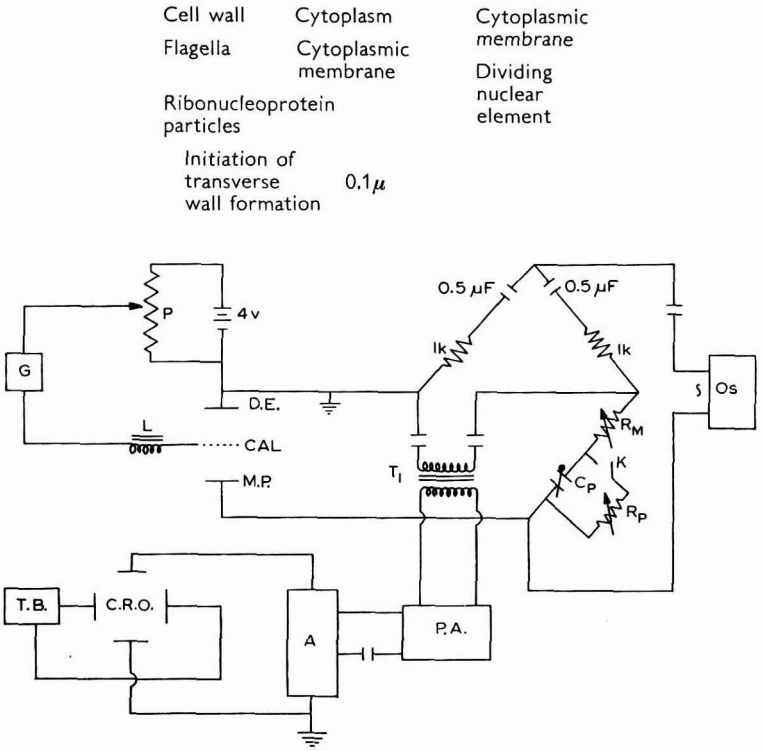

Fig. 1. Bridge circuit used in electrode impedance measurements.

The oscillator provided an a.c. voltage of variable frequency (0–16,000 cycles/sec) and amplitude (0–200 mV); the amplitude was maintained below 6 mV in these measurements. The lower (0–300 cycles/sec) and higher (500–14,000 cycles/sec) frequency ranges of the oscillator were calibrated against the frequency of the mains supply and that of a standard 1000 cycles/sec tuning-fork oscillator (Muirhead Type D-630-B) respectively.

The ratio arms of the bridge contained two 1000 Ω non-inductive resistances and two 0.5 μF non-reactive paper capacitors; both were accurate to $\pm$ 0.1%. The measuring arm of the bridge, similar to that used by GERISCHER[8], contained two

* This value was measured in the absence of a surface-active 'maximum suppressor'. From the results of other workers[16–18] and our own observations[19] it appears that surface-active agents have a marked effect on the limiting anodic current in amalgam dissolution.

non-inductive Sullivan resistance boxes (R_p, 0–10,000 Ω in steps of 0.1 Ω; R_M, 0–10,000 Ω in steps of 1.0 Ω) and a non-reactive Muirhead decade capacity box (0–1.110 μF in steps of 0.001 μF). The latter was calibrated against Sullivan standard mica capacitors and was found to be accurate to ±0.1% over the frequency range investigated.

Since it is essential to reduce to a minimum all stray capacitative and inductive effects due to the leads, all connections between circuit elements were made with screened wire; the dropping amalgam electrode was earthed because of the difficulty of screening it effectively. The out-of-balance voltage from the bridge was detected by means of a Cossor double-beam oscilloscope. A pre-amplifier was inserted between the bridge and the oscilloscope, and maximum amplification was of the order of 10^6. As one end of the bridge was earthed, an isolating transformer T (Muirhead, impedance 600 Ω) was inserted between the bridge and the detecting circuit.

A timing device was attached to the bridge, in which the second beam of the oscilloscope was used as time indicator. A delay circuit, pulsed by the fall of a drop, provided a 'pip' on the time axis; the delay was measured with a chronometer to 1/1000 sec, and the bridge could then be balanced at this pre-set time, usually just less than the drop-time. For the system studied here, however, it was often sufficiently accurate to balance at the fall of a drop, timing this with a stop-watch. This resulted in speedier operation, which is an important factor in obtaining good reproducibility. The mass of amalgam flowing through the capillary in a fixed interval of time was determined by direct weighing and in calculating surface areas it was assumed that the density of the dilute amalgam was equal to that of pure mercury.

Before determining the impedance resulting from the interfacial reaction, the ohmic resistance of the solution was measured by balancing out the impedance of the cell (with R_p out of circuit) at a potential well removed from the equilibrium potential of the system. This ensured that the reaction resistance was very large and the measured value R_M was effectively equal to the electrolyte resistance. All measurements of the latter were made at 14 kilocycles/sec. An attempt was made to use GERISCHER's method[8] of applying an a.c. of frequency 200 kilocycles/sec across the cell, which which theoretically would yield the electrolyte resistance even in the presence of a rapid exchange reaction. It was found, however, that at this radio frequency stray capacitative and inductive effects in the bridge, which was originally designed to work at audio frequencies, caused the reading to be somewhat erratic. At 25°C, the measured resistance of the cell, including that of the amalgam in the capillary, was of the order of 1–2 ohm cm^2.

In some measurements the capacity of the electrical double layer in the absence of an interfacial reaction was required. By measuring the capacity of a dropping mercury electrode over the range of potential covered in these experiments, it was possible to interpolate values of the capacity at intermediate potentials.

Measurements at 25°C (±0.01°C) were made with the cell immersed in a water thermostat. Where temperature effects were investigated, determinations were usually made in the range 0–38°C, the temperature being controlled to ±0.1°C. Also, the Zn^{2+} and Zn concentrations were usually kept high enough to eliminate the necessity of extrapolation of the measured impedance to infinite frequency. In this way it was possible to determine the impedance at 4000 cycles/sec over a temperature range without causing the run to become too protracted.

RESULTS

These measurements were primarily concerned with the $Zn^{2+}/Zn(Hg)$ exchange in the absence of complex-forming ions, and $NaClO_4$ was used as supporting electrolyte throughout.

Transfer coefficient: influence of ionic strength

Values of the transfer coefficient α were obtained by measuring the impedance R_D as a function of the concentration of zinc ion, the amalgam concentration being maintained constant. The effect of electrolyte concentration on α was measured over the range of ionic strength $\mu = 0.1$ to $\mu = 4.0$. Within limits of experimental error, α is given either by

$$\alpha = 1 + \frac{2.303RT}{n\mathrm{F}}\left(\frac{\partial \log R_D}{\partial \mathrm{V}}\right)_{C_{Zn},\mu,T} \tag{19a}$$

or

$$\alpha = 1 - \left(\frac{\partial \log R_D}{\partial \log C_{Zn^{++}}}\right)_{C_{Zn},\mu,T} \tag{19b}$$

(GERISCHER[8]).

These equations are not quite exact, but the omitted terms are estimated to be small in comparison with the limits of accuracy of the measurements. Figures 2 and 3

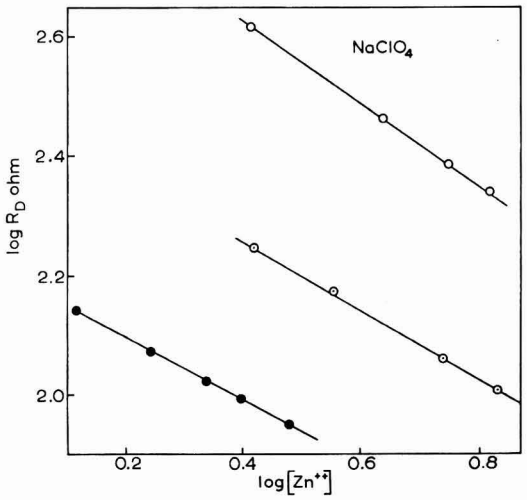

Fig. 2. The reaction resistance R_D as a function of Zn^{II} concentration, with constant Zn(Hg) concentrations, at 25°C. Base electrolyte is $NaClO_4$ throughout, at concentrations 1.2 M (points ⊙), 0.4 M (points ⊙) and 0.2 M (points ●).

illustrate some typical results; these indicate that α is approximately constant from $\mu = 1.6$ to $\mu = 4.0$, and increases sharply at lower ionic strengths, at 25°C.

The variation of α with ionic strength is illustrated in Fig. 4. The values plotted here are mostly averaged from results of both concentration and potential measure-

ments. The agreement between the two was generally good: in the region of constant α, the averaged transfer coefficients are:

	Averaged α (25°C)	
μ	eqn. (14a)	eqn. (19b)
1.6–4.0	0.31 ± 0.02	0.31 ± 0.01

The slightly lower precision of the values derived from the potential dependence of the exchange current is due to the difficulty of measuring small changes of potential very accurately at a dropping electrode.

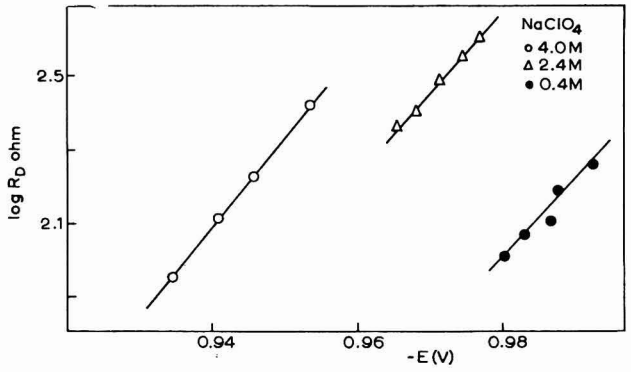

Fig. 3. The reaction resistance R_D as a function of electrode potential E at 25°C, with $NaClO_4$ base electrolyte, for the $Zn^{II}/Zn(Hg)$ exchange.

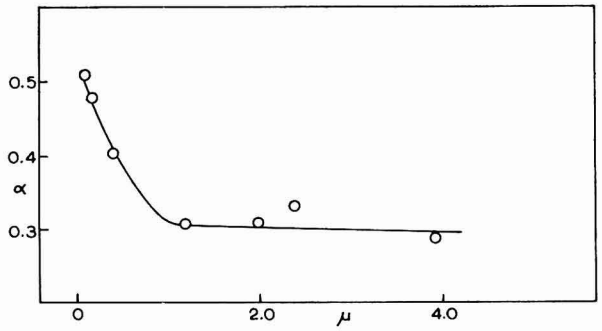

Fig. 4. The transfer coefficient α for the $Zn^{II}/Zn(Hg)$ exchange with $NaClO_4$ base electrolyte, as a function of ionic strength. (25°C) Note the decrease of α at low ionic strength.

Transfer coefficient: influence of temperature

The influence of temperature on α was examined in 2 M $NaClO_4$. Within the limits ± 0.02, α was found to be constant in the range 0–25°C.

Activation energy: influence of ionic strength

Measurements of the activation energy $\Delta H^{\neq}$ were made in the range of ionic

strength $\mu = 0.2$ to $\mu = 3.0$. The (real)[20,21] activation energy, determined at the equilibrium potential, is

$$\Delta H^{\neq} = 2.303R \frac{\mathrm{d} \log k}{\mathrm{d}(1/T)} = 2.303R \frac{\mathrm{d} \log i_0}{\mathrm{d}(1/T)}. \qquad (20)$$

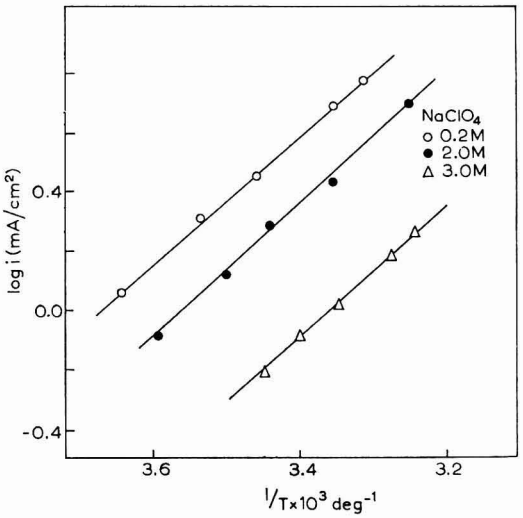

Fig. 5. Temperature-dependence of the exchange current i_0.

TABLE 1

ACTIVATION ENERGY $\Delta H^{\neq}$ OF $Zn^{2+}/Zn(Hg)$ EXCHANGE IN $NaClO_4$ DETERMINED BY IMPEDANCE MEASUREMENTS

μ	$\Delta H^{\neq}$ *kcal.mole*$^{-1}$	$k \times 10^3$ *(25°C) cm.sec*$^{-1}$
0.2	9.92	11.9
2.0	10.0	2.48
3.0	9.96	2.83

Some experimental results are shown graphically in Fig. 5, and averaged activation energies are listed in Table 1. The limits of error on the averaged values are estimated as ± 0.1 kcal.mole^{-1}, so that the value of $\Delta H^{\neq}$ can be taken to be constant over this range of ionic strength.

Rate constant

Fig. 6 illustrates the way in which the (a.c.) rate constant of the simple discharge reaction changes with ionic strength at 25°C. The majority of the values in the figure were calculated from equation (7), using the appropriate transfer coefficient interpolated from Fig. 3 and replacing activities by concentrations; in some cases, the plots of R_D against $\log C_{Zn^{2+}}$ were used. The results were easily reproducible to 2–3%. In 2 *M* $NaClO_4$, for example, the average of 14 determinations of k(25°C) with C_{Zn}/

$C_{Zn^{2+}}$ ratio ranging from 0.7 to 4.5, was 2.48×10^{-3} cm.sec^{-1}, with a standard deviation of 2.5%.

In Table 2, a list is given of values of k(25°C) over the range of ionic strength $\mu = 0.1$ to $\mu = 4.0$, together with the corresponding frequency factors A, calculated from the Arrhenius equation $k = A \exp(-\Delta H^{\neq}/RT)$, using an averaged value of $\Delta H^{\neq}$ from the data of Table 1.

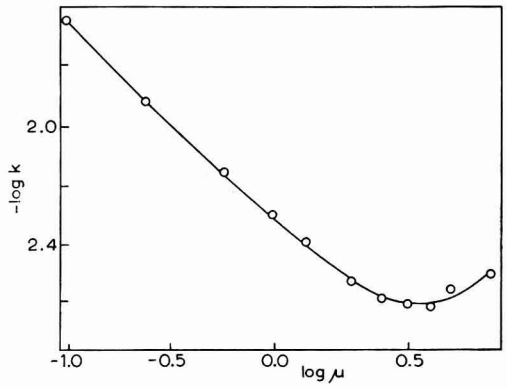

Fig. 6. The influence of ionic strength of the base electrolyte ($NaClO_4$) on the equilibrium rate constant. (25°C).

TABLE 2

RATE CONSTANT k(25°C) AND FREQUENCY FACTOR A OF $Zn^{2+}/Zn(Hg)$ EXCHANGE IN $NaClO_4$ DETERMINED BY IMPEDANCE MEASUREMENTS. (REPEATED VALUES FOR THE SAME IONIC STRENGTH WERE OBTAINED USING DIFFERENT AMALGAMS. THE VALUE OF $\mu = 2.0$ AS THE AVERAGE OF 16 DETERMINATIONS USING A WIDE RANGE Zn^{II} AND Zn(Hg) CONCENTRATIONS.)

μ	$k \times 10^3$(25°C) cm.sec^{-1}	$A \times 10^{-4}$ cm.sec^{-1}
4.0	3.52	6.93
3.0	2.83	5.57
2.4	2.47	4.88
2.4	2.51	4.96
2.0	2.48	4.89
1.6	2.62	5.18
1.2	2.99	5.89
1.2	3.04	6.00
0.8	3.99	7.87
0.8	3.93	7.75
0.6	4.89	9.64
0.4	6.86	13.5
0.4	6.86	13.5
0.2	11.9	24.1
0.1	22.7	44.7

Amalgam dissolution current

Direct-current measurements were made on polarized Zn(Hg) electrodes in $NaClO_4$ solution at 25°C. Anodic current-potential curves were recorded as described above.

These were analyzed by KOUTECKY's method[22], and the value of the parameter χ obtained. This is given by

$$\chi = (12t/7D_{Zn})^{\frac{1}{2}} \overleftarrow{k} \left(1 + \exp \frac{n\mathrm{F}}{RT}(\mathrm{V} - \mathrm{V}')\right) \tag{21}$$

where

$$\mathrm{V}' = \mathrm{V}_0 - \frac{RT}{n\mathrm{F}} \ln \gamma \tag{22}$$

and

$$\gamma = (D_{Zn^{2+}}/D_{Zn})^{\frac{1}{2}} \tag{23}$$

A plot of log $(3t/7D_{Zn})^{\frac{1}{2}} \overleftarrow{k}$ against η was drawn; k was obtained from the intercept at $\eta = 0$, and the transfer coefficient from the gradient.

The typical results shown in Fig. 7 were obtained at fairly high anodic overpotentials (up to 90 mV) in 2 M $NaClO_4$. The gradient yields the value 0.66 for the coefficient α, which is considerably greater than the value found from measurements near equilib-

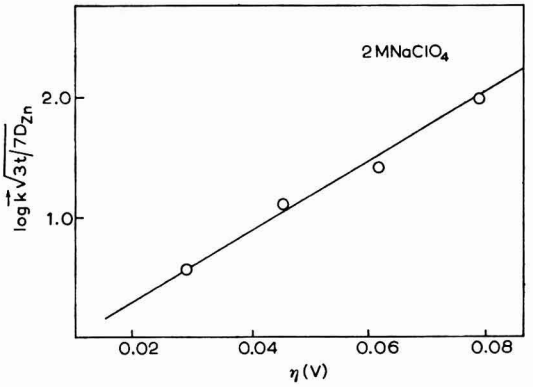

Fig. 7. Analysis of amalgam dissolution current (25°C, 2 M $NaClO_4$) (see text).

rium and at cathodic overpotentials of the same ionic strength (0.31). Previous direct-current measurements[7] on the zinc ion discharge current were in good agreement with the results of impedance measurements, so that the corresponding analysis for the anodic reaction should also be reliable. The measurements were less reproducible than those on the ion discharge current, and repetition yielded values of α in the range 0.5–0.7, with an average of about 0.6. Similarly, the values of k calculated from the intercepts were somewhat variable, but were always lower than those obtained from a.c. or d.c. measurements at cathodic potentials these; ranged from log $k = -2.8$ to -3.2. In the vicinity of the equilibrium potential, log k is -2.61 in 2 M $NaClO_4$ (*cf.* Fig. 6).

An increase of the transfer coefficient and decrease of the rate constant at anodic overpotentials are precisely what we should expect to find if the mechanism were a two-step one of the type of (10), provided that the free energy of activation of the first barrier is slightly larger than that of the second at the equilibrium potential.

We do not wish to attach too much weight to the numerical results, as the reproducibility of the measurements was not very satisfactory. However, it seems certain that α increases on proceeding to anodic overpotentials, and that it is at least greater than 0.4 for $\eta \sim 60$–90 mV. A similar high value of α (0.72) was calculated from the amalgam dissolution current in 1 M KCl with η up to 90 mV.

DISCUSSION

One point which is established is that the heat of activation $\Delta H^{\neq}$ for the $Zn^{2+}/Zn(Hg)$ exchange is, within experimental limits, unaltered over a wide range of ionic strength (0.1–3.0) in non-complexing solution. The Frumkin theory of salt effects in electrode kinetics[23] takes account of variations of total rate constant with electrolyte concentration. PARSONS[24] has recently discussed the separate effects on heats and entropies of activation, for processes in which the transition complex is located within the diffuse double layer. The dependence of activation energy on μ is influenced mainly by the temperature coefficient of the reversible potential of the system and by the proximity of this potential ot the point of zero charge. Variation of $\Delta H^{\neq}$ with μ will naturally be greatest at very low ionic strength. For this system, in which V_0 is well removed from the zero-charge point, very little variation of $\Delta H^{\neq}$ with μ is to be expected at moderate ($\geqslant 0.1$) to high ionic strength so that the variation should result primarily from change, of the frequency factor. The present results are in agreement with this. If the two-step mechanism (10) is the correct one, this would imply that the activation energies of the first and second barriers are not very different.

It is evident that the slow step in the exchange is a charge-transfer process. The two most likely mechanisms for this have been mentioned above. At moderately high ionic strengths ($\mu > 1$) the experimental results for cathodic overpotentials are consistent with either a single activation barrier, involving simultaneous transfer of two electrons, or a two-step process in which the rate-determining step is $Zn^{2+} + e \rightleftharpoons Zn^{+}$, the activation barrier for the second step $Zn^{+} + e \rightleftharpoons Zn(Hg)$ being smaller, and not rate-determining. The effects of lowering the ionic strength of the solution, and of change from cathodic to anodic overpotential, must be examined in attempting to distinguish between these alternative reaction paths.

There is no explanation in terms of any existing theory of an appreciable increase in the transfer coefficient as the ionic strength is lowered for an exchange proceeding through a single activation barrier. On the other hand, this could be understood in terms of the consecutive step mechanism as indicating a transition from rate control by the first one-electron barrier to mixed rate control by both barriers, the height of the second barrier approaching that of the first at the lower ionic strengths. The direction of this trend would be consistent with the Frumkin theory of salt effects. These are attributed in first-order approximation to alteration of the potential, with respect to that of the solution, of the plane containing the activated complex. Non-uniformity of the potential of this plane is ignored in this approximation. On the basis of the two-step mechanism we have, according to the Frukmin theory,

$$\left(\frac{\partial \ln k_1}{\partial \psi}\right)_T = -\frac{F}{RT}(2 - \beta_1) = -\frac{2F}{RT}(1 - \alpha_1) \qquad (24)$$

$$\left(\frac{\partial \ln k_2}{\partial \psi}\right)_T = -\frac{F}{RT}(1 - \beta_2) = -\frac{2F}{RT}(1 - \alpha_2) \qquad (25)$$

where k_1, k_2, α_1, α_2, β_1, β_2 are defined by equations (10)–(13). We assume both activated complexes to be located in the electrode side of the outer Helmholtz plane. From the Stern theory for a 1 : 1 electrolyte in the absence of specific adsortpion,

$$\psi = \text{const.} + \frac{RT}{F} \ln \mu \tag{26}$$

so that at ionic strengths which are small enough for equation (26) to apply,

$$\left(\frac{\partial \ln k_1}{\partial \ln \mu}\right)_T = -2(1 - \alpha_1) \tag{27}$$

$$\left(\frac{\partial \ln k_2}{\partial \ln \mu}\right)_T = -2(1 - \alpha_2)\,. \tag{28}$$

Since $\alpha_1 \leqslant \frac{1}{2}$, $\alpha_2 \geqslant \frac{1}{2}$, k_1 will increase more rapidly than k_2 as μ is lowered, so that a transition from rate control by $Zn^{2+} + e \rightleftharpoons Zn^+$ to control by $Zn^+ + e \rightleftharpoons Zn(Hg)$ might be observed at the lower ionic strengths. This would be consistent with the observed increase in α at low ionic strengths; on this interpretation, $\alpha_1 = 0.31$, $\alpha_2 > 0.51$.

If this were the correct explanation, we would also expect to observe an increase in α on changing from cathodic to sufficiently large anodic polarization. The method of analysis of a complex exchange current i^* in terms of the consecutive step mechanism is given above in equations (10)–(18). At extreme cathodic polarization, where $i_2 \gg i_1$, the polarizing current would tend to the limiting value

$$I_C = 2Fk_1\{C_O \exp - \beta_1 F\eta/RT - C_M \exp(2 - \beta_1)\, F\eta/RT\} \tag{30}$$

and at extreme anodic polarization, where $i_1 \gg i_2$, the polarizing current would tend to the limiting value

$$I_A = 2Fk_2\{C_M \exp - (1 + \beta_2)\, F\eta/RT - C_R \exp(1 - \beta_2)\, F\eta/RT\}\,. \tag{30}$$

In the first case (η negative), the height of the total activation barrier is effectively that corresponding to the first process, $Zn^{2+} + e \rightarrow Zn^+$; in this region, the measured transfer coefficient yields a vlaue for α_1. Similarly, α_2 is in principle obtainable from measurements on the far anodic side of equilibrium. The change in transfer coefficient should be more marked at low ionic strengths: however, only results at fairly high ionic strengths, with η up to + 90 mV, are available. The analysis of the amalgam dissolution current is interpreted as placing a lower limit of 0.4 on α for $\eta = 60 - 90$ mV; this is significantly greater than the value nearer equilibrium and on the cathodic side, although the difference is small. In this connection, the recent work of LOSEV[25] on combined radio-isotope and d.c. polarisation measurements on the Zn^{2+}/Zn(Hg) system is of interest. LOSEV*, working 1 N $ZnSO_4$ solutions at cathodic and

* LOSEV found it necessary to reduce the rate of the reaction by a factor of 10^2 by addition of 5×10^{-5} M tetrabutylammonium sulphate in order to study the reaction by these techniques. Electrocapillary data and studies of hydrogen overvoltage at Hg electrodes indicate that adsorption of tetrabutylammonium ion changes only slightly over the potential range covered, and the slopes of hydrogen-ion discharge curves are unaffected over a very wide range of potential in the presence of tetrabutylammonium sulphate[26–28]. There is, therefore, little doubt that in the Zn case also, the function of this salt is to change the overall rate without affecting the mechanism of the reaction; this is confirmed by the agreement with our results.

anodic overpotentials up to ± 100 mV, found $\alpha = 0.37$ for the cathodic process and $\alpha = 0.42$ at anodic potentials. These agree well with our values, and the anodic transfer coefficient is again the larger. However, the difference is small, as before. A final decision between the two mechanisms can obviously not yet be made. From the above discussion it seems likely that the critical experiment will be accurate determination of k and of α at very high anodic overpotentials, using solutions, of low ionic strength. This is outside the range of the techniques employed in the present work. Losev interprets his results as indicating that the discharge proceeds through consecutive one-electron steps, with the transfer $Zn^{2+} + e \rightarrow Zn^{+}$ rate-determining, but this should regarded as provisional.

It should be mentioned that a consecutive step mechanism for this exchange has also previously been proposed by Heyrovsky in a number of publications, on the basis of oscillographic measurements; these are summarised in ref.29. However, while HEYROVSKY's results are interesting, they are not easy to interpret in detail, and they do not provide unambiguous evidence for the suggested mechanism.

A preliminary account of the results of this work was given at the fourth Conference on Electrochemistry, Moscow, October 1–6, 1956[30].

ACKNOWLEDGEMENT

The award of a D.S.I.R. maintenance grant to one of us (J.B.) is acknowledged.

SUMMARY

The rate of the $Zn^{2+}/Zn(Hg)$ exchange reaction has been studied in $NaClO_4$ solution as a function of ionic strength and temperature by measurement of the a.c. impedance, and also by d.c. measurements of the amalgam dissolution current. The activation energy is independent of ionic strength (10.0 kcal.mole^{-1}, $\mu = 0.2$–3.0) and the rate constant increases sharply with decreasing ionic strength below $\mu = 2.0$. The transfer coefficient measured near the equilibrium potential and at cathodic overpotentials is 0.31 ± 0.01 (independent of temperature) and is larger at anodic overpotentials at moderately high ionic strengths. At low ionic strengths ($\mu < 1$) the cathodic transfer coefficient increases with decreasing ionic strength. The results can be interpreted either in terms of a consecutive-step mechanism,

$$Zn^{2+} + e \rightleftharpoons Zn^{+}$$

$$Zn^{+} + e \rightleftharpoons Zn(Hg)$$

for the exchange, with the first step rate-determining at moderately high ionic strengths, or in terms of a single two-electron rate-determining step. There is some evidence in favour of the first mechanism.

REFERENCES*

1 J. E. B. RANDLES, *Discussions Faraday Soc.*, 1 (1947) 11.
2 B. V. ERSHLER, *Zh. Fiz. Khim.*, 22 (1948) 683.
3 H. GERISCHER, *Z. Elektrochem.*, 54 (1950) 362; 55 (1951) 98.
4 H. GERISCHER, *Z. Physik. Chem. (Frankfurt)*, 197 (1951) 286.
5 J. E. B. RANDLES AND P. SOMERTON, *Trans. Faraday Soc.*, 48 (1952) 951.
6 B. V. ERSHLER AND A. ROZENTHAL, *Proc. Meeting Electrochem., Moscow 1950*, publ. 1953, p. 446.

* We are indebted to Dr. R. PARSONS for translations of the Russian papers.

[7] N. S. HUSH (unpublished work).
[8] H. GERISCHER, *Z. Physik. Chem. (Frankfurt)*, 202 (1953) 302.
[9] S. GLASSTONE, K. J. LAIDLER AND H. EYRING, *The Theory of Rate Processes*, McGraw Hill, 1941.
[10] P. VAN RYSSELBERGHE, *J. Chem. Phys.*, 17 (1949) 1226.
[11] R. PARSONS, *Trans. Faraday Soc.*, 47 (1951) 1332.
[12] H. GERISCHER, *Z. Physik. Chem. (Frankfurt)*, 202 (1953) 292.
[13] K. VETTER, *Z. Naturforsch.*, 7a (1952) 328; 8a (1953) 823.
[14] N. S. HUSH, *Trans. Faraday Soc.*, submitted.
[15] A. G. STROMBERG, *Dokl. Akad. Nauk., U.S.S.R.*, 85 (1952) 831.
[16] D. W. TURNER AND C. A. WINKLER, *Can. J. Chem.*, 29 (1951) 469.
[17] M. VAN STACKELBERG AND H. STREHLOW, *Z. Elektrochem.*, 54 (1950) 51.
[18] N. H. FURMAN AND J. COOPER, *J. Amer. Chem. Soc.*, 72 (1950) 5667.
[19] J. BLACKLEDGE, *Ph.D. thesis*, Bristol, 1956.
[20] M. I. TEMKIN, *Zh. Fiz. Khim.*, 22 (1948) 1081.
[21] J. E. B. RANDLES, *Trans. Faraday Soc.*, 48 (1952) 828.
[22] J. KOUTECKY, *Coll. Czech. Chem. Commun.*, 18 (1953) 597.
[23] A. N. FRUMKIN, *Z. Physik. Chem. (Frankfurt)*, 164 (1933) 121.
[24] R. PARSONS, *Advances in Electrochemistry, vol. 1.* Ed. Delahay, Interscience, New York, 1961' p. 1.
[25] I. P. LOSEV, *Dokl. Akad. Nauk.*, 100 (1955) 111.
[26] Z. A. IOFA, M. F. KABANOV *et al.*, *Zh. Fiz. Khim.*, 13 (1939) 1105; *Acta Physicochim., U.S.S.R.*, 10 (1939) 317.
[27] Z. A. IOFA, T. F. ANDREEVA AND N. V. NIKOLAEVA, *Proc. Meeting Electrochem., Moscow 1950*, publ. 1953, p. 294.
[28] T. F. ANDREEVA, *Zh. Fiz. Khim.*, 29 (1955) 699.
[29] J. HEYROVSKY, *Z. Elektrochem.*, 59 (1955) 802.
[30] Soviet Electrochemistry: *Proc. Fourth Conf. Electrochem., Moscow 1956*. (English transl. by Consultants Bur., New York, 1961).

MECHANISM OF THE $Zn^{II}/Zn(Hg)$ EXCHANGE

Part 2: CATALYSIS BY HALIDE AND THIOCYANATE IONS

J. BLACKLEDGE AND N. S. HUSH

Department of Physical and Inorganic Chemistry, The University, Bristol

(Received February 6th, 1963)

INTRODUCTION

In Part I[1], measurements on the $Zn^{2+}/Zn(Hg)$ exchange were reported. The exchange is known from previous work[2] to be accelerated if the base solution contains highly polarisable anions such as halide and thiocyanate ions. This is an interesting effect, and an unusual feature is that iodide ion, which has the least tendency to complex with Zn^{2+}, is more effective than chloride ion, which forms much more stable complexes, in increasing the exchange current.

In the work reported here, the mechanism of the exchange in the presence of Cl^-, Br^-, I^- and CNS^- is examined. Exchange mechanisms in the presence of ligands forming more stable complexes with Zn^{2+} (*e.g.*, NH_3, CN^-, OH^-) have been studied by GERISCHER[3].

EXPERIMENTAL

The a.c. bridge circuit, electrode assembly and technique of impedance measurements were as described in Part I. All measurements were made using aqueous solutions of Zn^{II} in the appropriate base electrolyte.

MATERIALS

B.D.H. laboratory reagent grade samples of NaI and NaBr were purified by chromatographic adsorption on activated alumina, followed by elution with water distilled from alkaline permanganate solution. The solutions obtained were carefully evaporated to dryness. This procedure was followed in order to remove traces of organic impurities. However, no measurable difference was found between the results of impedance measurements using purified and stock samples of these salts.

NaCl, KCl, NH_4CNS and $ZnSO_4$ were of Analar grade, and were used without further purification.

Preparation of Zn amalgams and $NaClO_4$ solutions, and purification of Hg and solvent were carried out by the methods described in Part I.

OVERALL KINETICS WITH HALIDE AND THIOCYANATE BASE SOLUTIONS

The first series of measurements was made using molar solutions of KCl, NaBr, NaI and NH_4CNS as base electrolytes. As in previous work, the electrochemical system (excluding the series solution resistance) is represented as a series combination of reaction resistance R_D and Warburg impedance W, in parallel with the double-layer capacity C_l[4-6]. The experimental equivalent circuit is a parallel combination of resistance R_D and C_p. The resistance R_D is related to R_p by

$$\frac{R_p}{1+\beta^2} = R_D + \frac{K}{\sqrt{\omega}} \tag{1}$$

where ω is the frequency of the applied a.c., $\beta = \omega R_p(C_p - C_l)$ and $K/\sqrt{\omega}$ is the Warburg resistance. The capacity C_l was measured at a pure mercury electrode in the absence of Zn^{II} ions in the solution. For all solutions except those containing iodide ions the dispersion of R_p over the frequency range 500–4000 cycles/sec was in good accordance with equation (1). In the presence of I^-, the value of the constant K was slightly larger than the calculated[4-6] value. However, the effect is small and for the present purpose can be ignored.

As β^2 is generally small, R_D can usually be obtained with good accuracy by plotting R_p directly against $\omega^{-\frac{1}{2}}$ and extrapolating to infinite frequency; this method has been extensively used by GERISCHER[3]. The exchange current density i_0 at given concentrations of Zn^{II} in the solution and Zn in the amalgam was calculated from R_r by the usual relationship for a two-electron process.

$$i_0 = \frac{RT}{2AF} \cdot \frac{1}{R_D} \tag{2}$$

where A is the area of the electrode and the remaining symbols have their usual significance.

The transfer coefficient α was obtained both from the variation of i_0 with Zn^{II} concentration and from the variation of i_0 with electrode potential V, at fixed amalgam concentration. Since the variation of ionic strength in a particular experiment was negligible over the range of Zn^{II} concentrations used, the relationships[7]

$$\left.\frac{\partial \ln i_0}{\partial \ln [Zn^{II}]}\right|_{[Zn]} = 1 - \alpha \tag{3a}$$

$$\left.\frac{\partial \ln i_0}{\partial V}\right|_{[Zn]} = (1-\alpha)\cdot\frac{2F}{RT} \tag{3b}$$

$$\left.\frac{\partial \ln i_0}{\partial \ln [Zn]}\right|_{[Zn^{II}]} = \alpha \tag{3c}$$

(the square brackets denoting concentration) may be assumed to be valid if the exchange current density is related to the concentration $[Zn^{II}]$, [Zn] by

$$i_0 = 2Fk\,[Zn^{II}]^{(1-\alpha)}\,[Zn]^{\alpha} \tag{4}$$

Typical plots of log i_0 *vs.* log $[Zn^{II}]$ and log i_0 *vs.* V (both at fixed amalgam concentration) are shown in Figs. 1a and 1b. Over the range of concentration studied, these

plots were in all cases linear, and the independent values of α were in good agreement. The values obtained from the potential dependence of i_0, however, showed rather more scatter, as was also found in the previous work on the $Zn^{2+}/Zn(Hg)$ exchange. The averaged values of α (25°C) are shown in Table 1.

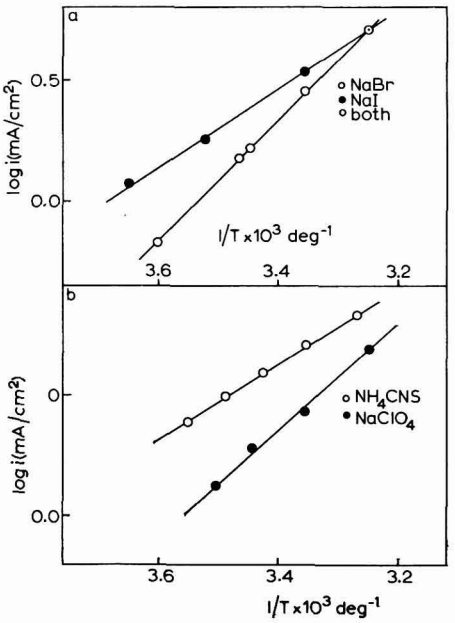

Fig. 1. Dependence of exchange currents i on Zn^{II} concentration in molar halide and thiocyanate base solutions (Fig. 1a) and on electrode potential E in molar chloride and iodide solutions (Fig. 1b). Measurements at 25°C.

TABLE 1

TRANSFER COEFFICIENTS (α) FOR $Zn^{II}/Zn(Hg)$ EXCHANGE IN 1 M HALIDE AND THIOCYANATE SOLUTIONS AT 25°C

Base electrolyte	α
KCl	0.30 ± 0.11
NaBr	0.28 ± 0.02
NaI	0.00 ± 0.07
NH_4CNS	0.40 ± 0.02

The values of α obtained by applying equation (3c) were in all cases in sufficiently good agreement with equation (4) to establish that the relative apparent orders of reaction with respect to Zn^{II} and Zn are as we have assumed. These values were not used in the averaging, as the precision was not high owing to the rather small range of [Zn] covered.

The rate constants k for the exchange process at 25°C, obtained from equation (4), using the experimental transfer coefficients, are listed in Table 2. Comparing these with the data for the exchange reaction with 1 M $NaClO_4$ as base electrolyte, it is evident that the electrode process is accelerated in the presence of all three halide

TABLE 2

OVERALL RATE CONSTANT (k), HEAT OF ACTIVATION ($\Delta H^{\neq}$) AND FREQUENCY FACTOR (A) FOR Zn^{II}/Zn(Hg) EXCHANGE IN 1 M HALIDE AND THIOCYANATE SOLUTIONS AT 25°C. THE RATE CONSTANTS ARE CALCULATED FROM THE EXPERIMENTAL EXCHANGE CURRENT DENSITIES EMPLOYING THE RELATIONSHIP $i_0 = 2Fk[Zn^{II}]^{(1-\alpha)}[Zn]^{\alpha}$.

*Base electrolyte**	*This work*		
	k $cm.sec^{-1} \times 10^3$	$\Delta H^{\neq}$ $kcal.mole^{-1}$	A $cm.sec^{-1} \times 10^{-4}$
M KCl	5.05 ± 0.05	10.0 ± 0.5	11 ± 24
M Na(K)Br	10.3 ± 0.6	11.0 ± 0.3	102 ± 120
M Na(K)I	131 ± 7	7.2 ± 0.5	2.5 ± 4.0
M NH_4(K)CNS	17.5 ± 0.2	6.9 ± 0.1	0.20 ± 0.04

*Base electrolyte**	RANDLES AND SOMERTON[2] **		
	k $cm.sec^{-1} \times 10^3$	$\Delta H^{\neq}$ $kcal.mole^{-1}$	A $cm.sec^{-1} \times 10^{-4}$
M KCl	5.18	8.6	1.0
M Na(K)Br	10.6	9.3	7.0
M Na(K)I	84	5.6	0.1
M NH_4(K)CNS	21	7.0	0.3

* Halide salts of the first cation were used in this work. RANDLES AND SOMERON used potassium salts (indicated by parentheses) throughout.

** The values of k and A listed in ref. 2 for 20°C are recalculated here for 25°C.

ions and thiocyanate ion, the effect being most pronounced in the presence of iodide ion. This is in agreement with the work of RANDLES AND SOMERTON[2]. The transfer coefficients also show a good deal of variation from one base solution to another. From the magnitude of these, we can infer that for all base solutions except NaI, the rate-determining step involves a charge-transfer activation barrier, and that if the reaction proceeds through successive one-electron steps, the rate-determining step in the discharge process is the formation of a species of oxidation state +1 from Zn^{II}. On the basis of the conclusions of Part 1, this mechanism appears to be somewhat more probable than one involving simultaneous two-electron uptake by Zn^{II}, but no clear distinction between the two alternative paths can be found from impedance measurements in the vicinity of the normal potential of the system. With 1 M NaI, the transfer coefficient is zero, which shows that in this case the rate-determining step precedes the charge transfer step(s) in a potential range close to the normal potential.

The temperature-dependence of the exchange currents, using the same base solutions, was also examined. Typical plots of log i_0 *vs.* $1/T$ are shown in Figs. 2a and 2b. The experimental activation energies $\Delta H^{\neq}$ and frequency factors A were calculated

from these plots, assuming the temperature-dependence of the rate constant k to obey the Arrhenius equation

$$k = A e^{-\Delta H^{\neq}/RT} \quad (5)$$

The results are also given in Table 2. The standard deviation in the $\Delta H^{\neq}$ determinations were of the order of 0.1–0.5 kcal/mole^{-1}. The results obtained by RANDLES AND

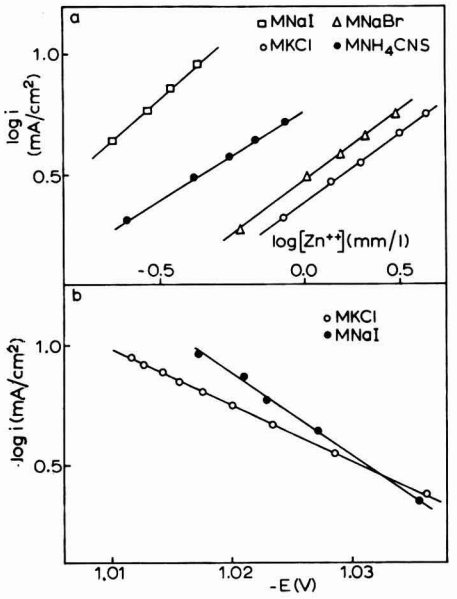

Fig. 2. Temperature-dependence of exchange currents i in molar halide, thiocyanate and perchlorate base solutions.

SOMERTON for the $Zn^{II}/Zn(Hg)$ exchange in 1 M solutions containing the same anions are listed for comparison. The rate constants (except for the reaction in presence of iodide) agree well with our values; however, the activation energies found by these authors are mostly somewhat lower (by $\sim$ 1.5 kcal/mole for the halide solutions) than ours.

For the $Zn^{2+}/Zn(Hg)$ exchange in 2 M $NaClO_4$ solution, the transfer coefficient α was found to be independent of temperature over the range 0–25°C. The value of α with 1 M KCl as base electrolyte was measured at three temperatures between 0 and 38°C (Table 3). Although the value at the highest temperature is slightly larger than the two identical values at lower temperatures, the difference hardly exceeds the estimated limits of error, and is not regarded as significant.

TABLE 3

TRANSFER COEFFICIENT (α) FOR $Zn^{II}/Zn(Hg)$ EXCHANGE IN M KCl AT DIFFERENT TEMPERATURES

Temperature, °C	α
0.8	0.30 ± 0.02
25.0	0.30 ± 0.02
38.0	0.34 ± 0.03

RATES OF EXCHANGE IN 2 *M* $NaClO_4$ IN PRESENCE OF ADDED HALIDE AND THIOCYANATE IONS

The results reported above provide information about the overall exchange kinetics, but do not enable us to draw any conclusions about the role of halide and thiocyanate ions in the reaction mechanism. A second series of measurements was therefore made in which varying concentrations up to 0.05 *M* of the halide and thiocyanate salts were added to 2 *M* $NaClO_4$. The impedance measurements were made with this mixed electrolyte solution rather than pure halide and thiocyanate solutions, in order to minimise the effect of varying ionic strength on the rate constants and on the activity coefficients of electroactive species. The rate constant (and transfer coefficient) for the simple ion exchange are very little affected by ionic strength variations over the range 2.0–2.8 in $NaClO_4$ solution.

Results of measurements at 25°C are shown in Figs. 3a and 3b, in which the logarithm of the exchange current density is plotted against that of the concentration of added anion.

There are two principal ways in which the exchange kinetics might be altered by addition of halide and thiocyanate ions.

(i) Halide and thiocyanate ions are specifically adsorbed at the Hg-solution interface. This will change the potential distribution within the double layer, which will in turn affect the rate of the simple ion-exchange process.

(ii) In the presence of these ions, reactions in which halide and thiocyanate complexes take part may be important.

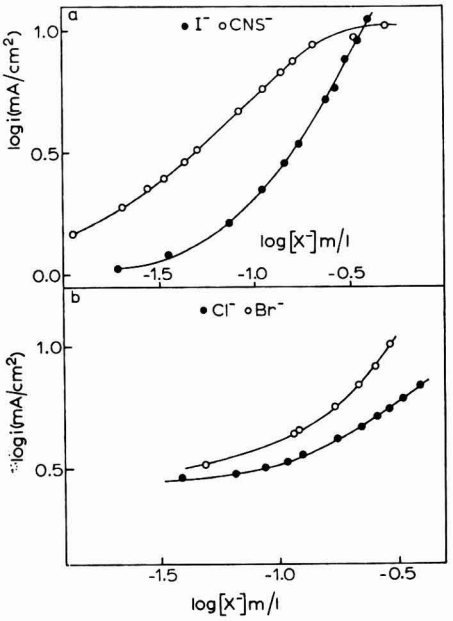

Fig. 3. Exchange currents *i* in 2 *M* $NaClO_4$ containing added halide and thiocyanate ions. Measurements at 25°C.

At low concentrations of added anions, the effect (i) should be small for this system, as the $Zn^{II}/Zn(Hg)$ equilibrium potential is always considerably negative with respect to that of the zero point of charge. In agreement with this, we find that the exchange current data for 2 *M* $NaClO_4$ + NaBr and 2 *M* $NaClO_4$ + NH_4CNS at low Br^- and SCN^- concentrations extrapolate to a value close to that determined in 2 *M* $NaClO_4$ solution alone. We shall therefore assume that at low concentrations of the additives, the rate constant of the simple ion discharge has the same value as in 2 *M* $NaClO_4$ solution and express the observed current density i as

$$i = i_s + i_c \tag{6}$$

where i_s and i_c are respectively the exchange current densities for the simple ion reaction and for a process involving complexes of Zn^{2+} with the added anions. (i_c may itself be composite.) Equation (6) will be applicable when the concentration of additive is fairly low, but must be used with caution at high concentrations, as i_s may not then remain strictly constant.

The logarithm of i_c (calculated from the observed current densities using equation 6) is plotted against $\log[X^-]$ in Figs. 4a and 4b. These results can be interpreted as follows. The general equation for an exchange process in which the activated complex contains ν anions X^- is.

$$Zn^{2+} + \nu X^- + 2e \rightleftharpoons Zn(Hg) + \nu X^- \tag{7}$$

and the exchange current density i_c for this process is

$$i_c = 2Fk_c[Zn^{2+}]^{(1-\alpha)}[Zn]^{\alpha}[X^-]^{\nu} \tag{8}$$

In this last expression, k_c is the rate constant for the complex exchange mechanism. We continue to write the rate expressions in terms of concentrations rather than activities of reacting species; variations in activity coefficients should be negligible as the variation of total ionic strength with changing $[X^-]$ is small in the presence of 2 *M* $NaClO_4$.

Introducing the dissociation constant K_c of the complex $Zn\,X_\nu^{2-\nu}$, defined by

$$K_c = [Zn^{2+}][X^-]^{\nu}/[Zn\,X_\nu^{2-\nu}] \tag{9}$$

the current density can be written as

$$i_c = 2Fk_c[Zn^{II}]^{(1-\alpha)}[Zn]^{\alpha}[X^-]^{\nu}\left[1 + \frac{[X^-]^{\nu}}{K_c}\right]^{-(1-\alpha)} \tag{10}$$

where $[Zn^{II}]$ is the total concentration of Zn in oxidation state $+2$ in the solution. In the solutions used, the condition $[X^-] \gg [Zn\,X_\nu^{2-\nu}]$ holds. The dependence of i_c on $[X^-]$ at constant $[Zn^{II}]$, $[Zn]$, and nearly constant ionic strength is then (*cf.* GERISCHER[7]):

$$\left.\frac{\partial \ln i_c}{\partial \ln [X^-]}\right|_{[Zn^{II}][Zn]} = \nu + (1-\alpha)\frac{2F}{RT}\left.\frac{\partial V}{\partial \ln [X^-]}\right|_{Zn^{II},Zn} \tag{11}$$

The last term in equation (11), which is due to the shift of equilibrium potential due to complexing of Zn^{2+}, is directly measurable. But for these weakly-complexing

anions the potential shift with $[X^-] \leqslant 0.5\ M$ is too small for accurate measurement at a dropping electrode. Using SILLEN's data[8] for the dissociation constants of the halide complexes ZnX^+ ($K_c = 1.54$, 4.0 and > 20 mole litre^{-1} for Cl^-, Br^- and I^- respectively in 3 M $NaClO_4$ at 25°C), and taking 0.5 as an average value of α, we can calculate the second term of equation (11), using the relationship:

$$\left.\frac{\partial V}{\partial \ln [X^-]}\right|_{[Zn^{II}][Zn]} = -\frac{RT}{2F}\,\nu\,\frac{[X^-]^\nu}{K_c}\left[1 + \frac{[X^-]^\nu}{K_c}\right]^{-1} \qquad (12)$$

The second term of equation (11) obtained in this way is -0.12, -0.06 and $-|<0.01$ for Cl^-, Br^- and I^- respectively at $[X^-] = 0.5\ M$ with $\nu = 1$. The corresponding values for higher ν will be much smaller. For all reactions except one involving $ZnCl^+$, the simpler equation

$$\left.\frac{\partial \ln i_c}{\partial \ln [X^-]}\right|_{[Zn^{II}][Zn]} = \nu \qquad (13)$$

is therefore an adequate approximation. In the exceptional case, equation (13) will suffice to determine ν with a precision of $\sim 10\%$; since ν is necessarily integral, this will yield an unambiguous value. As addition of thiocyanate ion also results in a barely measurable shift of the equilibrium potential in our solutions, eqn. (13) is also valid for the CNS^--catalysed exchange current.

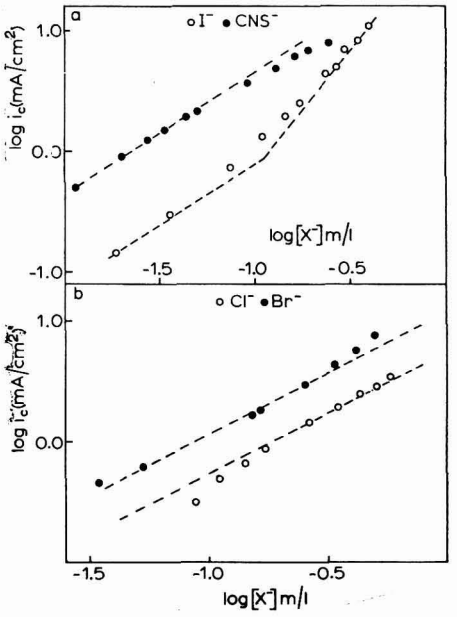

Fig. 4. Complex exchange currents i_c (obtained from measured i as described in text) in 2 M $NaClO_4$ containing added halide and thiocyanate ions. These are associated with the catalysed processes

$$Zn^{2+} + \nu X^- + 2e \rightleftharpoons Zn(Hg) + \nu X^- .$$

The broken lines are theoretical slopes (equation 13) for $\nu = 1$; the second broken line for iodide-containing solutions is drawn for $\nu = 2$. Measurements at 25°C.

The broken straight lines in Figs. 4a and 4b for the Cl^-, Br^- and CNS^- reactions represent the slope $\nu = 1$. The points for Br^- and CNS^- conform closely to this slope at all but the highest concentrations. There is some scatter in the case of Cl^- at the lowest concentrations. This is attributed to the fact that the rate constant is least affected by Cl^-, so that the small difference $i_0 - i_s$ at low $[Cl^-]$ is sensitive to experimental error. The slope in I^- solutions also conforms to $\nu = 1$ at low I^- concentration, but not at concentrations >0.1 M. Above this concentration, there is apparently a transition to a slope corresponding to $\nu = 2$, although it is possible that the effect is due to an increase in the rate constant resulting from alteration of the structure of the double layer as the surface excess of specifically adsorbed I^- increases.

We conclude, therefore, that the complex reaction proceeds through an activated complex containing one anion at low concentrations of all four anions, and possibly through a complex containing two I^- ions at iodide concentrations >0.1, in 2 M $NaClO_4$ solution.

Some confirmatory evidence for different mechanisms of the exchange process at I^- concentrations greater and less than 0.1 M in the mixed electrolyte base solution is provided by the variation of exchange current with total ionic strength. In Fig. 5, exchange currents for base solutions containing (i) 0.05 M I^- and (ii) 0.33 M I^-, and varying concentrations of $NaClO_4$, are plotted over a wide range of ionic strength (μ). At the lower I^- concentration, there is a gradual decrease of exchange current

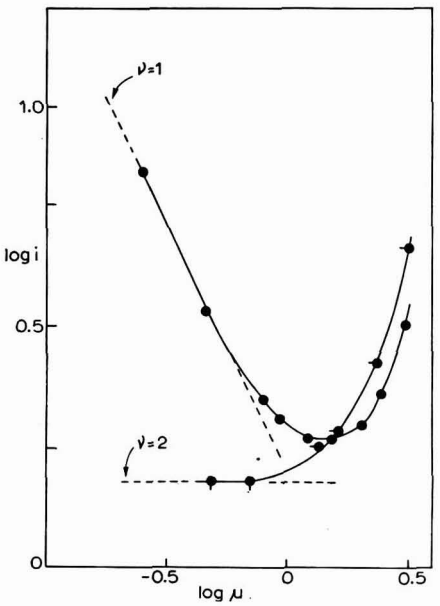

Fig. 5. Exchange currents i in $NaClO_4$ solutions containing 0.33 M NaI (points ●) and 0.05 M NaI (points ●–●), as a function of total ionic strength μ. For the first measurements, the Zn^{II} and Zn(Hg) concentrations were 0.194 and 2.4 millimole/litre respectively, and for the second, 1.39 and 5.0 millimole/litre respectively. (Measurements at 25°C.) The broken straight lines represent theoretical limiting slopes for the process

$$Zn^{2+} + \nu I^- + 2e \rightarrow Zn(Hg) + \nu I^-$$

with $\nu = 1$ and 2 respectively. (See text and equation 14.)

as the ionic strength drops. At the higher concentration, there is a similar decrease to $\mu = 1.5$, but at lower μ, the exchange current rises sharply. This marked difference can be qualitatively correlated with a difference of ν. The data of Table 1 indicate that the rate-determining step at high I^- concentrations precedes charge transfer; we assume that this is also so (*i.e.*, $\alpha \sim 0$) for the reaction at low I^- concentration. The rate-determining step is thus

$$[Zn^{2+} + \nu X^-]_i \rightarrow [Zn\, X^{2-\nu}]_p$$

where in the initial state i, the ions are located in the interior of the solution and in state p, which immediately succeeds the transition state, the complex $ZnX^{2-\nu}$ is located within the double layer. Neglecting the effect of specific adsorption, the Frumkin theory of ionic strength effects at low salt concentration[9,10] predicts a variation of rate constant with μ which is approximately

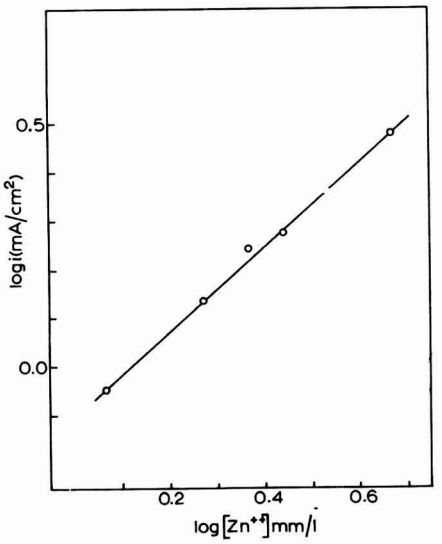

Fig. 6. Complex exchange current (25°C) in 2 M $NaClO_4$ containing 0.05 M NaI (calculated from measured current as described in text) as a function of Zn^{II} concentration.

$$\frac{\partial \ln k}{\partial \ln \mu} \approx -(2 - \nu) \tag{14}$$

On the simplest interpretation of the results of Fig. 7, $\nu = 1$ in case (i) and 2 in case (ii); the slope $\partial \ln k / \partial \ln \mu$ at low μ is thus predicted to be -1 and 0 respectively. The data of Fig. 9 for $\mu < 1.5$ are in agreement with this. Although this representation of the ionic strength effect cannot be an exact one, the qualitative predictions should be reliable.

The transfer coefficient for the reaction in 2 M $NaClO_4$ in the presence of 0.05 M I^- was determined from the variation of $\log i_c$ with $\log [Zn^{II}]$ at constant [Zn]. The plot is shown in Fig. 6. From this gradient we obtain $\alpha = 0.15 \pm 0.05$ (25°C). This

is very low, but greater than the value $\alpha = 0$ found with 1 M NaI as base electrolyte. This may represent a transition between an activation barrier preceding discharge and a charge-transfer activation barrier of nearly equal height at low I^- concentration.

The absolute values of the complex rate constants k_c may be obtained from the exchange currents i_e. The relationship is:

$$\frac{i_e}{2F[Zn^{II}]^{(1-\alpha)}[Zn]^{\alpha}[X^-]^{\nu}} = k_c\left[1 + \frac{[X^-]^{\nu}}{K_c}\right]^{-(1-\alpha)} \qquad (15)$$

As the dissociation constants K_c are large, the right-hand side of equation (15) reduces to k_c at low $[X^-]$; the correction is largest for solutions containing Cl^-, but is of the same order as the experimental error, and has been neglected. Some values

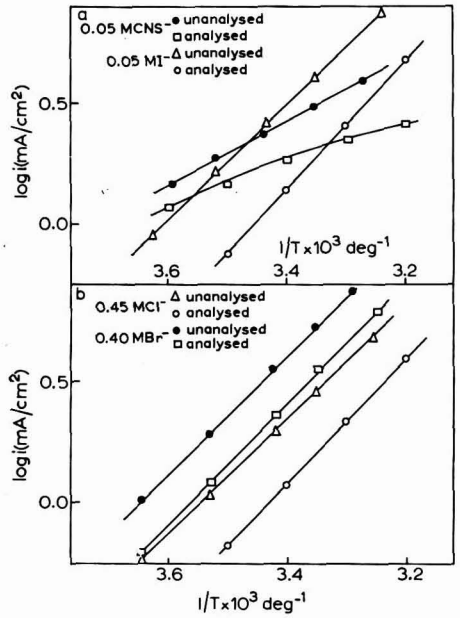

Fig. 7. Exchange currents in 2 M $NaClO_4$ containing added halide and thiocyanate ions, as a function of temperature. The measured current is plotted in the "unanalysed" curves. The exchange current accompanying the simple $Zn^{2+}/Zn(Hg)$ exchange has been subtracted from this in the "analysed" curves.

of k_c calculated in this way, using the experimental transfer coefficients, are listed in Table 4.

Within the experimental limits of accuracy, the rate constants are independent of Zn and Zn^{II} concentrations.

The temperature variation of the exchange current using the mixed electrolyte base solutions were also measured. Typical results are shown in Figs. 7a and 7b. The plots labelled 'unanalysed' are those of log i *vs.* $1/T$ and those labelled 'analysed' are those of log i_e *vs.* $1/T$. The 'analysed' slopes have been used to calculate the activation energy $\Delta H_c^{\neq}$ for the process

$$Zn^{2+} + X^- + 2e \rightleftharpoons Zn(Hg) + X^-$$

All analysed plots were linear except those for the exchange in the presence of 0.5 M CNS^-; there is appreciable curvature in this last case. Good agreement was found for values of $\Delta H_c^{\neq}$ for the halide-catalysed reactions with different $[Zn]/[Zn^{II}]$ ratios.

TABLE 4

OVERALL RATE CONSTANTS k, AND RATE CONSTANT k_c FOR THE PROCESS $Zn^{2+} + X^- + 2e \rightleftharpoons Zn(Hg) + X^-$, IN 2 M $NaClO_4$ SOLUTION + ADDED HALIDE OR THIOCYANATE. (SEE TEXT FOR METHOD OF OBTAINING k_c FROM EXPERIMENTAL EXCHANGE CURRENT.)

Base electrolyte 2 M $NaClO_4$ plus	*$[Zn]$ millimole/l*	*$[Zn^{II}]$ millimole/l*	*k $cm.sec^{-1} \times 10^3$*	*k_c $cm^4.mole^{-1}sec^{-1}$*
0.45 M NaCl	11.5	4.20	2.3	5.1
0.45 M NaCl	7.02	5.66	2.2	5.2
0.45 M NaCl	5.0	2.32	2.7	6.0
0.40 M NaBr	5.3	1.39	4.4	11
0.40 M NaBr	11.5	4.20	4.8	12
0.05 M NH_4CNS	2.56	1.85	5.0	100
0.05 M NH_4CNS	11.5	0.30_2	5.0	100
0.05 M NaI	5.30	3.74	3.0	60
0.05 M NaI	5.48	2.34	3.6	72

In the presence of 0.40 M Cl^-, $\Delta H_c^{\neq}$ was found to be 11.9 kcal.mole^{-1} with $[Zn^{II}] = 2.32$, $[Zn] = 5.00$, and 12.2 kcal.mole^{-1} with $[Zn^{II}] = 10.1$, $[Zn] = 7.02$ (concentration in millimole/l); this agreement is typical for the halide ions. The values for the CNS^--catalysed reaction, calculated from the slope at 25°C, were reproducible to about ± 0.4 kcal.mole^{-1}.

TABLE 5

AVERAGED VALUES OF RATE CONSTANT (k_c), HEAT OF ACTIVATION ($\Delta H_c^{\neq}$), AND FREQUENCY FACTOR A_c FOR PROCESS $Zn^{2+} + X^- + 2e \rightleftharpoons Zn(Hg) + X^-$ IN 2 M $NaClO_4$ SOLUTION AT 25°C.

k_c $cm^4.mole^{-1}sec^{-1}$	*$\Delta H_c^{\neq}$ kcal.mole^{-1}*	*A_c $cm^4.mole^{-1}sec^{-1} \times 10^{-9}$*	*Anion (X^-)*
5.4	12.0	3.5	Cl^-
11.5	11.8	5.4	Br^-
66	11.6	22	I^-
105	4.4	0.00018	CNS^-

Averaged values of k, $\Delta H_c^{\neq}$ and the frequency factor A for the complex reaction with $\nu = 1$ (25°C, 2 M $NaClO_4$) are shown in Table 5. The corresponding averaged values of $\Delta H^{\neq}$ calculated from the variation of total exchange current with temperature were found to be 11.1, 10.9, 10.6 and 5.9_5 kcal.mole^{-1} for the Cl^-, Br^-, I^- and CNS^--catalysed processes respectively.

The frequency factors and rate constants for this process increase in the order $Cl^- > Br^- < I^-$ in the halide series and the activation energies decrease slightly in this order. Thiocyanate ion is evidently the most effective in accelerating the exchange rate by this mechanism.

DISCUSSION

The factors determining the heat and entropy of activation of an electrode process will of course be different for each particular reaction. In spite of this it is an experimental fact that there is a remarkably constant correlation of activation energy and frequency factor for electron-exchange and ion-exchange processes of the most diverse types. In general, high activation energies tend to be accompanied by high frequency factors and low activation energies by low frequency factors. In Fig. 8, we have plotted the $\Delta H^{\neq}$ and log A values obtained by RANDLES and co-workers[2,10] for a large number of electron-exchange and ion-exchange processes. These were mostly obtained with 1 M base solutions; the frequency factors are calculated from observed exchange currents at 20°C, and are all formally of the same dimensions ($cm.sec^{-1}$). There is a definite trend towards a quasi-linear relationship between the

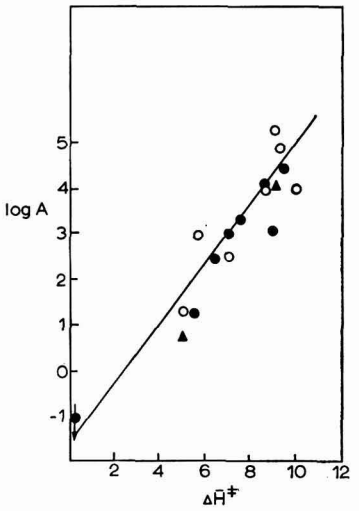

Fig. 8. Correlation between frequency factor A ($cm.sec^{-1}$ at 20°C) and heat of activation $\Delta H^{\neq}$ ($kcal.mole^{-1}$) for electrode processes*. Points ⊙: ion-exchange processes at Hg surface. Points ●: electron-transfer processes at Hg surface. Points ▲: electron-transfer processes at Pt surface.

two quantities $\Delta H^{\neq}$ and log A in these data. The equation of the line in the figure, which represents the average slope, is:

$$\Delta H^{\neq} = 1.54 \log A + 2.3 \qquad (16)$$

($\Delta H^{\neq}$ in $kcal.mole^{-1}$, A in $cm.sec^{-1}$)

This is evidence of a broad general relationship between heats and entropies of activation for quite diverse electrode processes (at the same temperature and not too dissimilar ionic strength of base electrolyte). As a result of this parallelism, large individual variations of heat and entropy of activation are accompanied by relatively smaller variations in the free energy of activation. It is perhaps not surprising that such a correlation is found for simple electron-transfer processes at electrodes. In

* Data from refs. 2 and 10.

these processes, in which all reacting species are on the solution side of the interface, the activation energy is primarily a function of differences of ion-solvent interaction energies in initial, final and transition states. It is well-known that heats and entropies of solvation of ions in aqueous solution show a general parallelism. This has a simple physical interpretation; indeed, the simple Born electrostatic theory[11], in which the solvent is regarded as a structureless dielectric, predicts the ratio $\Delta H_{solv}/\Delta S_{solv.}$ to be the same for all ions. It is perhaps more unexpected that heats and entropies of ion-exchange processes (in which there is mass transfer across the metal-solution interface) should apparently conform to the same general trend. However, this correlation is encouraging, as it suggests that a relatively simple theory of the activation process for both types of reaction will be able to account for the broad features of the experimental results.

Similar plots of $\Delta H^{\neq}$ *vs.* log A for the overall $Zn^{II}/Zn(Hg)$ exchange in 1 *M* halide solutions (data from Table 1) and also for the process $Zn^{2+} + X^- + 2e \rightleftharpoons Zn(Hg) + X^-$ (data from Table 4) can be constructed, with a different intercept (as the dimensions of A are different) for the second set. In both cases, there is an undoubted trend in the expected direction, although the very small variations of $\Delta H^{\neq}$ ($\sim$0.4 kcal.mole^{-1}) within the halide-catalysed reactions of the second set are not in this order.

The theory of the detailed mechanism of ion-exchange processes is not yet sufficiently developed for it to be possible to assign an unambiguous physical basis to the catalysis of the $Zn^{2+}/Zn(Hg)$ process by halide and thiocyanate ions. The effect is not due simply to stabilisation, by ion-pair formation, of the Zn^{2+} ion in a state preceding the discharge step(s), as the free energies of association of Zn^{2+} with X^- to form ZnX^+ are all positive for the X^- ions, and increase in the order Cl^-, Br^-, I^-, which is also the order of increasing effectiveness of the anion in catalysing the reaction (*cf.* also discussion in ref. 2). Similar small catalytic effects by halide ions have been observed in homogeneous electron-transfer processes[12], and an interpretation of these has been proposed by HUSH[13]. It is difficult to extend this theory to heterogeneous processes of the kind studied here, as (i) specific adsorption may be important and (ii) more information is needed about the ion-electrode distance in the transition state.

In Part 1, it was pointed out that experimental results for the simple ion-exchange process are consistent either with a mechanism in which the rate-determining step in discharge is the formation of Zn^+ ion, bonded to the metal surface, from Zn^{2+} in solution, or with one in which both electrons are gained in the same step. The present results do not resolve this problem. It is interesting to note, however, that the free energy change accompanying the process

$$\tfrac{1}{2}\,Zn^{2+}(aq.) + X^-(aq.) + \tfrac{1}{2}\,Zn(c) \rightarrow ZnX(g) \qquad (17)$$

is 10 kcal.mole^{-1} lower for ZnI than for ZnCl (data from ref. 14), which would be consistent with the relative catalytic efficiencies of I^- and Cl^- ions if a two-step mechanism were assumed.

ACKNOWLEDGEMENT

The award of a D.S.I.R. maintenance grant to one of us (J.B.) is acknowledged.

SUMMARY

The faradaic admittance at dilute Zn amalgam electrodes in aqueous solutions containing Zn^{II} has been measured using as base electrolytes solutions containing halide and thiocyanate ions. It is known from previous work by RANDLES and SOMERTON that the rate of the $Zn^{II}/Zn(Hg)$ exchange is accelerated in the presence of these anions. Measurements have been made using (i) 1 *M* halide and thiocyanate solutions and (ii) 2 *M* $NaClO_4$ solutions containing small varying amounts of added halide or thiocyanate, as base electrolyte solutions. The reaction orders with respect to Zn^{II}, Zn and X^- have been established. In 2 *M* $NaClO_4$, the reaction proceeds through the parallel paths

$$Zn^{2+} + 2e \rightleftharpoons Zn(Hg)$$

$$Zn^{2+} + X^- + 2e \rightleftharpoons Zn(Hg) + X^-$$

(where X^- is Cl^-, Br^-, I^- or CNS^-) at low X^- concentration. At high iodide concentration there is evidence that the predominant reaction is

$$Zn^{2+} + 2I^- + 2e \rightleftharpoons Zn(Hg) + 2I^- .$$

(All reactions listed might be composite, and proceed through two consecutive one-electron steps).

The rate constants, transfer coefficients, activation energies and frequency factors for the anion-catalysed processes have been obtained by an analysis of the observed exchange currents.

The variations of activation energy $\Delta H^{\neq}$ and frequency factor A observed in these reactions are related to an approximate correlation of the type $\delta \Delta H^{\neq} \approx \delta \log A$ that appears to hold very generally for the rate constants of electrode processes, measured under similar experimental conditions.

REFERENCES

1 N. S. HUSH AND J. BLACKLEDGE, *J. Electroanal. Chem.*, 5 (1963) 420.
2 J. E. B. RANDLES AND P. SOMERTON, *Trans. Faraday Soc.*, 48 (1952) 951.
3 H. GERISCHER, *Z. Physik. Chem. (Frankfurt)*, 202 (1953) 302.
4 J. E. B. RANDLES, *Discussions Paraday Soc.*, 1 (1947) 11.
5 B. V. ERSHLER, *Zh. Fiz. Khim.*, 22 (1948) 683.
6 D. C. GRAHAME, *J. Electrochem. Soc.*, 99 (1952) C 370.
7 H. GERISCHER, *Z. Physik. Chem. (Frankfurt)*, 202 (1953) 292.
8 L. G. SILLEN AND W. LILJEQVIST, *Svensk. Kem. Tidskr.*, 56 (1944) 85.
9 A. N. FRUMKIN, *Z. Physik. Chem. (Frankfurt)*, 164 (1933) 121.
cf. PARSONS, *Trans. Faraday Soc.*, 47 (1951) 1332.
10 J. E. B. RANDLES AND P. SOMERTON, *Trans. Faraday Soc.*, 48 (1952) 951.
11 A. BORN, *Z. Physik. Chem.*, 1 (1920) 45.
12 J. SILVERMAN AND R. W. DODSON, *J. Phys. Chem. (Frankfurt)*, 56 (1952) 846.
13 N. S. HUSH, 1963 (to be published).
14 *Selected Values of Chemical Thermodynamic Properties*, U.S. National Bureau of Standards, 1952.

CYCLIC VOLTAGE SWEEP CHRONOAMPEROMETRY WITH A PLATINUM MICROELECTRODE

Z. KUBLIK

Department of Inorganic Chemistry, University of Warsaw, Poland

(Received February 6th, 1963)

The recording of cyclic, repetitive current-voltage curves is well suited to the study of the products of the electrode reactions. Chronologically the cyclic technique, connected with the dropping mercury electrode, was for the first time used by HEYROVSKÝ AND FOREJT[1], but ŠEVČIK[2] was the first who introduced in this field the triangular voltage sweep. To reduce the unfavourable influence of changes of area of the dropping electrode it was however necessary to use the fast voltage sweeps as well as oscillographic recording.

Next in the papers of ČERMAK[3] and KEMULA AND KUBLIK[4] it was shown, that well defined cyclic current-voltage curves could be obtained for slow polarisation rates too, if instead of dropping mercury electrode the stationary mercury electrode was used. It was shown too, that under such conditions it was much easier to study the particular stages of the electrode reactions as well as the secondary chemical processes. According to the nomenclature of electroanalytical methods proposed by DELAHAY, CHARLOT AND LAITINEN[5] this technique should be called cyclic voltage sweep chronoamperometry.

There are many papers on this subject, in which mercury microelectrodes are employed, but literature data concerning the use of solid microelectrodes in this field are scarce. Only ADAMS *et al.*[6] applied cyclic technique to the study of electrode reactions of various organic systems using platinum or carbon paste electrodes. Applying a special potentiostatic device CROFT[7] studied the formation and properties of insoluble oxide films on cadmium and silver electrodes. Similarly WILL AND KNORR[8], as well as BREITER[9] recorded oscillographically the cyclic, potentiostatic current-potential curves studying the adsorption and the desorption of the hydrogen and the oxygen on platinum and other metals.

The rare use of solid electrodes in cyclic electrochemical techniques is probably caused by the familiar opinion, that on such electrodes, before recording every new curve, special conditioning of the electrode must be carried out. The purpose of the present work was therefore to find whether this opinion is right and to what extent solid microelectrodes are suited for the cyclic techniques.

EXPERIMENTAL

The platinum microelectrode was a wire 0.3 mm in diameter sealed into a glass tube and fused at the end to a sphere. The real surface area of the electrode was 2.2 mm^2,

and was found by comparison of current-voltage curves of the same solution using the electrode being studied and the hanging mercury electrode with known surface area. The platinum electrode was stored in 8 *M* HNO_3 and before use treated anodically to evolution of oxygen. The formed oxide film was then removed from the surface by shortcircuiting *vs.* the S.C.E. (saturated calomel electrode). The previously described hanging mercury electrode[10] with a surface area 1.8 mm^2 was used. As a nonpolarizable reference electrode the S.C.E. of the surface area, equal to 12 cm^2, was used. In the salt bridge there was usually a 1 *M* solution of KCl. The resistance of the cell was about 2000 ohms, which at a current equal to ± 5 μA gave ± 10 mV for the ohmic drop. Solutions were deaerated by the nitrogen washed through a column containing sulfuric acid solution of vanadous sulfate and zinc amalgam. The cyclic current-voltage curves were recorded using Radiometer PO4 polarograph. The rate of voltage sweep was 0.8 V/min.

RESULTS

Residual currents. The utility of an electrode in various kinds of voltammetry depends considerably on residual currents. The curves representing residual currents for platinum microelectrode in 0.1 *N* H_2SO_4 solution are given in Fig. 1. Curve 1 was taken using the low sensitivity of the polarograph. Under these conditions the curve is pretty flat in the potential range from -0.2 V to $+1.4$ V. At a potential more negative than -0.2 V hydrogen evolution and at a potential more positive than $+1.4$ V oxygen evolution takes place.

Curve 2 was recorded for the same solution at much higher sensitivity. In this case the curve is more complex and generally similar to the curves obtained by WILL AND KNORR[8] and BREITER[9], who investigated the chemisorption of hydrogen and oxygen

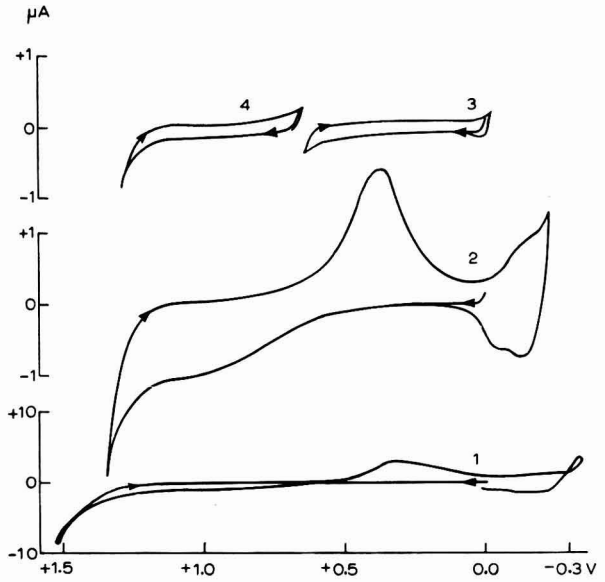

Fig. 1. Cyclic current-voltage curves recorded for 1 *M* H_2SO_4 solution. The platinum electrode had a surface area of 2.2 mm^2.

on the platinum electrodes. The rise of the cathodic and anodic currents at potentials more negative than 0 V is due to the adsorption and desorption of hydrogen. The rise of the anodic current at potentials more positive than 0.65 V is connected with chemisorption of oxygen. During the subsequent cathodic sweep the adsorbed oxygen layer is irreversibly reduced forming a cathodic peak at about 0.4 V.

Between 0 and +0.6 V neither hydrogen nor oxygen is adsorbed. In this region the residual current is fairly low and for given electrode equal to about 0.1 μA. This quantity is however about ten times greater than the capacity current found at hanging mercury electrode with nearly the same surface area.

The residual current observed in the potential range +0.7– +1.3 V can be considerably diminished in the second and subsequent cycles if the electrode is polarized in this potential range only (Fig. 1, curve 4). In this case the reduction potential of chemisorbed oxygen layer is not attained, so that the same oxygen layer is attached to the platinum surface in each successive run.

The curves obtained for neutral solutions containing SO_4^{2-} and ClO_4^- ions are similar to those given in Fig. 1. For solutions containing Cl^- ions the positive range of the potential is a little shorter because Cl_2 is evolved at a less positive potential than O_2.

Comparison of results obtained on platinum and mercury electrodes. It might be expected that the results obtained on both kinds of electrodes will be similar, if the products of the electrode reaction are soluble in solution and that differences will appear, if the products remain at the platinum surface as an insoluble deposit or if they diffuse into the bulk of the mercury drop.

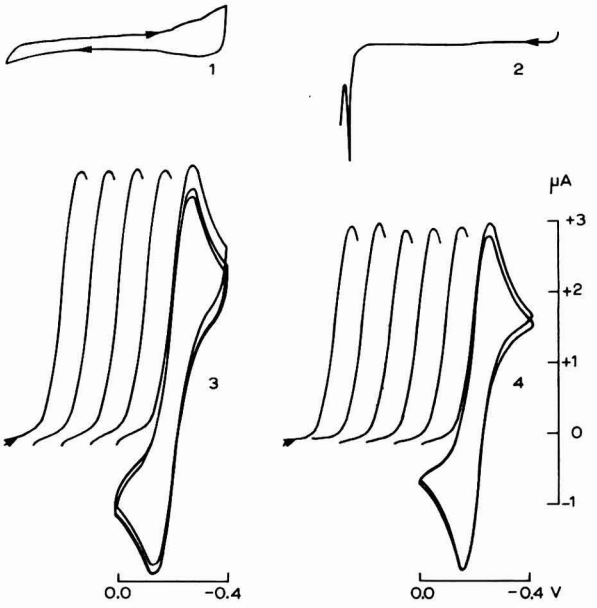

Fig. 2. Current-voltage curves recorded for 0.08 M $Na_2C_2O_4$ and 0.01 M H_2SO_4 solutions containing: 1 and 2 — 0; 3 and 4 — 2×10^{-3} M Fe^{3+} ions; successive curves start from 0.0 V. Curves 1 and 3 — platinum microelectrode; curves 2 and 4 hanging mercury drop electrode.

The curves shown in Fig. 2 are recorded for oxalate complexes of ferric iron, *i.e.* for a case where products are soluble in a solution. As was expected, the curves obtained by means of both electrodes are very similar in a shape, though those obtained on platinum are a little more drawn-out.

The separation of the peaks, *i.e.* the difference $E_{pa} - E_{pc}$ (where E_{pa} is the potential of the anodic peak and E_{pc} the potential of the cathodic one) according to the FRANKENTHAL AND SHAIN[11] equation can be a measure of the reversibility. For electrodes and voltage sweep rates used in the present work the value $E_{pa} - E_{pc}$ predicted by a theory should be equal to 68 mV and 34 mV for one- and two-electron reversible transfer respectively. Though the Frankenthal and Shain equation is not strictly valid for the segment of the cyclic curve where the secondary reaction takes place, nevertheless the deviation caused by this incorrectness is small. For strictly reversible systems studied on hanging mercury electrode the experimental values agree within a few milivolts with the values predicted by the theory. The experimentally found value of $E_{pa} - E_{pc}$ for oxalate complexes of Fe(III), after subtraction of corrections for inertia of recording device and correction for the ohmic voltage drop, is equal to 70 and 120 mV, for curves taken using mercury and platinum electrodes respectively. The electrode reaction on platinum is therefore not so reversible as on mercury. We must, however, pay attention to the fact, that in the potential range where this reaction takes place the platinum is partially covered by adsorbed hydrogen layer.

As can be seen from Fig. 2 the reproducibility is fairly good, when every new curve was taken using a new mercury drop or, in the case of platinum, when before every

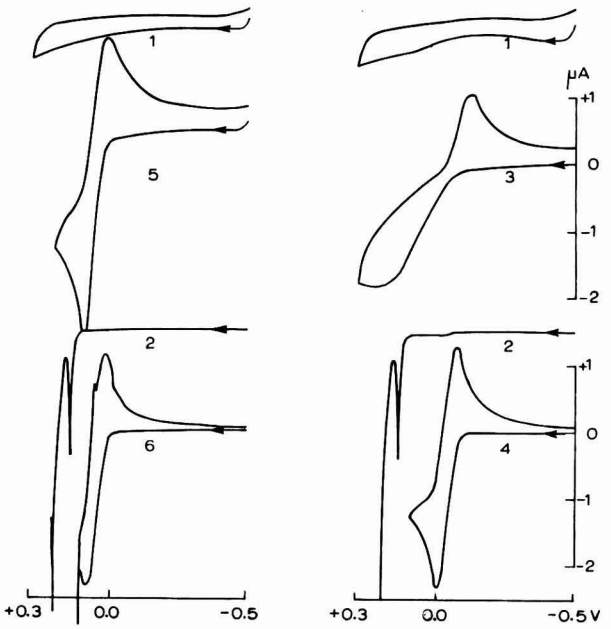

Fig. 3. Current-voltage curves recorded for 1/15 M Na_2HPO_4 solutions containing: 1 and 2 — 0; 3 and 4 — 5×10^{-4} M p-hydroquinone; 5 and 6 — 5×10^{-4} M p-phenylenediamine. Curves 1, 3 and 5 — platinum microelectrode; curves 2, 4 and 6 — hanging mercury drop electrode.

run, the electrical circuit was disconnected and the solution stirred to remove concentration differences. When the curves were recorded cyclically the second and further runs differ slightly from the first one.

Another example of reaction, in which products are soluble in solution, is the system *p*-phenylenediamine/*p*-quinonediimine (Fig. 3, curves 5 and 6). In this case both curves are reversible, though the reaction on mercury is a little disturbed by processes connected with anodic dissolution of mercury.

The *p*-benzoquinone/*p*-benzohydroquinone system gives at the mercury electrode in buffered solution with pH = 8.3, reversible curves too (Fig. 3, curve 4), but on platinum a distinct irreversibility appears, particularly in the anodic run (Fig. 3, curve 3). These irreversible curves have not only greater difference $E_{pa} - E_{pc}$, but also lower height of peaks. The irreversibility is much more marked in old solutions. Successive cyclic polarisation does not cause much difference. Only the second and the subsequent runs differ slightly from the first one.

The curves obtained for Cu^{2+} ions, *i.e.*, for a case in which the products are soluble in mercury and insoluble in platinum, are represented in Fig. 4. The electrode reaction on mercury corresponds to a reversible 2-electron reaction. The height of the cathodic peak rises proportionally to the concentration of Cu^{2+} ions in solution (curves 3, 5 and 7). The anodic peak is a little greater than the cathodic one due to the enrichment of copper atoms in mercury drop.

The reactions which take place on platinum (curves 4, 6 and 8) are much more complex. There are two systems of peaks. The first cathodic peak appearing at more positive potential rises proportionally to the concentration of Cu^{2+} ions, but only for

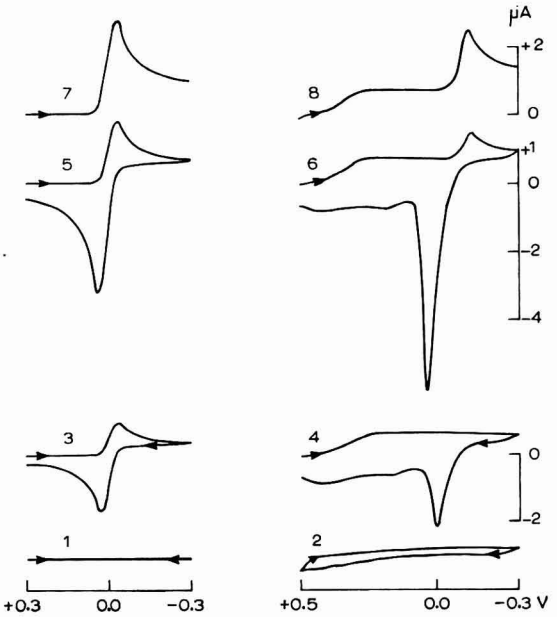

Fig. 4. Current-voltage curves recorded for 0.1 *M* K_2SO_4 solutions containing various amounts of $CuSO_4$: 1 and 2 — 0; 3 and 4 — 2.5×10^{-4} *M*; 5 and 6 — 5×10^{-4} *M*; 7 and 8 — 7.5×10^{-4} *M*. Curves 1, 3, 5 and 7 — hanging mercury drop electrode. Curves 2, 4, 6 and 8 — platinum microelectrode.

the concentrations lower than $2.5 \times 10^{-4} M$. This peak corresponds to the deposition of copper monolayer on platinum and therefore the increase of its height stops when the monolayer is completely deposited. For the same reason the poorly defined anodic part of this system can reach only limited height. The process is favoured by binding energy between copper and platinum atoms and therefore it takes place at a more positive potential than the deposition reaction on mercury.

The second, less positive, cathodic peak appears distinctly only after the first peak reaches its maximal height. Both peaks of this system are well defined and the anodic peak is even higher than corresponding peak observed on mercury. The potential difference between $E_{pa} - E_{pc}$ is greater than corresponding value obtained on mercury and this value rises with the increasing concentration of Cu^{2+} ions in solution.

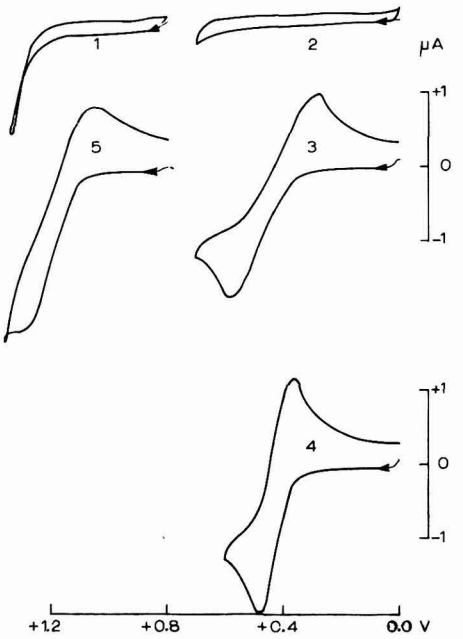

Fig. 5. Cyclic current-voltage curves recorded using platinum microelectrode for 0.5 M H_2SO_4 solutions containing: 1 and 2 — 0; 3 — $5 \times 10^{-4} M$ KBr; 4 — $1 \times 10^{-2} M$ KBr; 5 — $5 \times 10^{-4} M$ KI; 6 — $1 \times 10^{-2} M$ KI.

It should be noted that similar effects, *i.e.* the formation of two peaks during anodic stripping of nickel accumulated on platinum electrode, were observed by Nicholson[12].

Investigation in the positive potential range. The electrode reactions which take place in the potential range more positive than anodic dissolution of mercury could be investigated on the platinum electrode only. The results obtained in this potential region for bromide and iodide ions are shown in Fig. 5. The curves taken for a dilute solution of bromide ions were well defined (curve 3) with the difference $E_{pa} - E_{pc}$ equal to 70 mV, which corresponds to a reversible, one electron reaction. The

curves obtained for more concentrated solutions (curve 4) were drawn out due to ohmic voltage drop.

The curves obtained for solution containing iodide ions were, especially in more concentrated solutions (curve 6), not so well defined as the corresponding curves for bromide ions. The anodic part of the curve was drawn out and little disturbances were visible on it. Besides that, the cathodic peak was higher than corresponding peak for bromine reduction. All these disturbances were probable caused by adsorption of iodine on the electrode surface. In this case again the repetitive, cyclic polarisation did not cause much more difference.

Well defined curves can be obtained for systems $Fe(CN)_6^{4-}/Fe(CN)_6^{3-}$ and Fe(II)/Fe(III), for which in potasium chloride solution the values $E_{pa} - E_{pc}$ were equal to

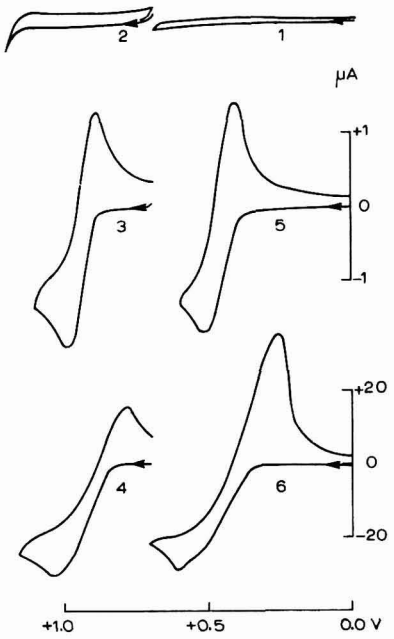

Fig. 6. Cyclic current-voltage curves recorded using platinum microelectrode for 0.5 M H_2SO_4 solutions containing: 1 and 2 — 0; 3 — 1.1 × 10^{-3} M Fe^{2+} ions; 4 — 1.1 × 10^{-3} M $K_4Fe(CN)_6$; 5 — 1 × 10^{-3} M Ce^{3+} ions.

70 mV. In sulphuric, acid medium the system $Fe(CN)_6^{4-}/Fe(CN)_6^{3-}$ was almost reversible (Fig. 6, curve 4), though it appeared at slightly more positive potential. On the other hand, as can be seen from curve 3 (Fig. 6), the peaks of the system Fe(II)/Fe(III) are more drawn out. In this case the value $E_{pa} - E_{pc}$ corresponds to 250 mV.

Deviations from reversibility were also found for the system Ce(III)/Ce(IV) (Fig. 6, curve 5), for which in sulphuric acid medium the value $E_{pa} - E_{pc}$ was found to be 200 mV. In this case yet another deviation from reversibility appeared, namely the height of the cathodic peak was smaller than the height expected for a pure diffusion process.

Irreversible systems. In the above mentioned experiments the reversibility of simple, 1- or 2-electrons reactions was mainly studied. However, as it was shown in papers of KEMULA AND KUBLIK[4], the technique used gives good results during investigation of products formed in complex multielectron reactions. The following experiments show that similar results can be obtained on solid electrodes too.

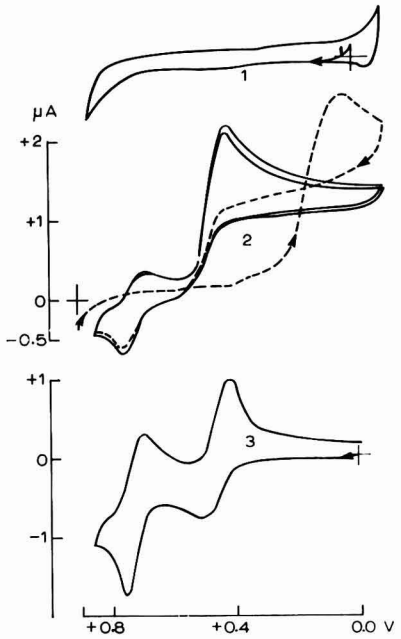

Fig. 7. Cyclic current-voltage curves recorded using platinum microelectrode for 0.1 *M* HCl solutions containing: 1 — 0; 2 — 2.5 × 10^{-4} *M* KIO_3; 3 — 2.5 × 10^{-4} *M* KI.

Fig. 7 represents the curves obtained for HCl solution containing IO_3^- ions (curve 2) and I^- ions (curve 3). In the latter case the picture is comparatively simple and almost unchanging during multiple cyclic polarisation. Two reversible systems of peaks correspond to reactions:

$$2\,I^- \rightleftharpoons I_2 + 2e \qquad (1)$$

$$I_2 \rightleftharpoons 2I^+ + 2e \qquad (2)$$

The second reaction takes place only in solution containing excess of Cl^- ions.

The pictures obtained for solutions containing IO_3^- ions are more complex. In the first cathodic run, recorded from 0.9 V (broken line), the rise of the cathodic peak starts at 0.2 V, which corresponds to the reduction of IO_3^- to I^- ions. However, already in the anodic segment of the first cycle, the reduction ceased not at 0.2 V, but at 0.5 V.

In the second and subsequent cycles the reduction current starts not at 0.2 V, as in the first cycle, but at 0.5 V, what corresponds to the reduction of iodine to iodide ions. Further runs differ only slightly from the second one. Stirring of the solution with the electrical circuit disconnected re-establishes the whole sequence again. This behaviour is due to the secondary chemical reactions taking place in the vicinity of the electrode. In the first part of the cathodic run IO_3^- ions are reduced to I^- ions. Iodide ions react however chemically with IO_3^- ions forming iodine, which

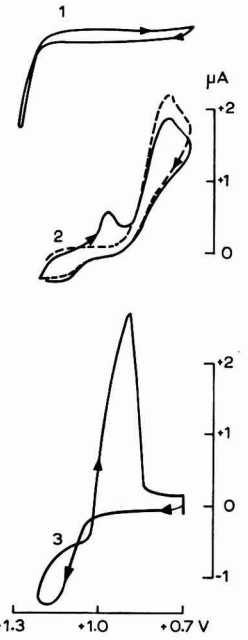

Fig. 8. Cyclic current-voltage curves recorded using platinum microelectrode for 0.05 M K_2SO_4 and 0.01 M H_2SO_4 solutions containing: 1 — 0; 2 — 1×10^{-3} N $KMnO_4$; 3 — $1 \times 10^{-}$ N $MnSO_4$.

in turn is reduced at a potential less positive than 0.5 V, forming iodide ions again. So, I^- and IO_3^- ions are continually consumed in the secondary, chemical reaction and therefore the peak of the anodic oxidation of I^- can not be seen at all and the reduction peak of IO_3^- ions appears only in the first run. On the other hand the system I/I^+ is quite well visible, because the components of this system do not react chemically with IO_3^- ions.

A similar conclusion that during the course of electrolysis the predominant reaction occurring at the electrode changes from IO_3^- reduction to iodine reduction was previously drawn by ANSON[13] on the ground of his chronopotentiometric studies of the reduction of IO_3^- ions.

Another example of multielectron irreversible reaction is the reduction process of permanganate ion. Fig. 8 represents the curves obtained for weakly acid solutions containing Mn(II) ions (curve 3) and permanganate ions (curve 2). In the anodic sweep Mn(II) ion was oxidized and a well defined peak arose. The products formed in the anodic process were reduced in the subsequent cathodic sweep forming a new

peak. This peak was steeper and greater than the corresponding anodic peak which could be explained by an assumption that products formed in the anodic process were insoluble in solution and therefore they accumulated at the electrode surface. The accumulation can be still greater, if the electrolysis at a constant potential sufficient to the oxidation of Mn(II) ions is performed. For the case where there is only a little solid deposit on the electrode surface the difference $E_{pa} - E_{pc}$ was equal to 120 mV, but this value rose with the increasing amount of the deposit on the electrode surface.

All these facts point out that in cathodic process the reduction of MnO_2 takes place, though this species cannot be directly formed in the electrode process.

Curve 2 was taken for solution containing MnO_4^- ions. The first cathodic run shown as a broken line from +1.2 V shows only the reduction peak of MnO_4^- ion. The product formed during this reaction is oxidized in the subsequent anodic run at roughly the same potential as Mn(II) ions on the curve 3. The products formed in this anodic reaction behave similar to the products formed during anodic oxidation of Mn(II), *i.e.*, they give similar cathodic peak. So, from the comparison of the curves 2 and 3, it follows that during the recording of current-voltage curves for solutions containing MnO_4^- ions the system Mn(II)/Mn(IV) arises.

From the fact that on the curve 2 the peak of Mn(II) oxidation is quite well visible it follows that, unlike to the reaction between IO_3^- and I^-, the reaction between MnO_4^- and Mn(II) does not occur very fast.

With increasing concentration of sulphuric acid the reduction of MnO_4^- ion as well as oxidation of Mn(II) ion is shifted towards more positive potential and the current of system Mn(II)/Mn(IV) becomes smaller and at last in 1 *M* H_2SO_4 it disappears completely.

The reaction between MnO_4^- and Mn^{2+} ions taking place in the bulk of the solution was studied by DESIDERI[14], who used the bubbling platinum electrode. This author supposed that for acidity equal to 0.1 *M* the reaction leads to the formation of MnO^{2+} and Mn(III), *i.e.*, to soluble species.

Almost all above described experiments, except several curves represented in Fig. 1, were carried out either in the potential region, where the platinum electrode behaves as an ideally polarizable electrode or in the region where chemisorption of oxygen takes place, *i.e.* under conditions, where the residual currents were fairly low (Fig. 1, curves 3 and 4). When it was necessary to record the curves in the wider potential range the curves obtained were not so well defined due to the effects connected with the formation and removal of chemisorbed oxygen layer.

CONCLUSIONS

From the experiments described it follows that the platinum microelectrode can be successfully used in cyclic electrochemical techniques. The cyclic current-voltage curves obtained were reproducible and well defined even for systems with many intermediates as well as for systems in which the deposits are formed on the electrode, as for example in the case of Cu^{2+} reduction and Mn^{2+} oxidations. Some limitations arise during the work in the potential range where the formation and the removal of the chemisorbed oxygen layer takes place. From the comparative studies carried out in the potential range where both the platinum and the mercury electrode could be applied it follows that the reversibility of reactions on mercury is always better than on platinum.

SUMMARY

The utility of the platinum microelectrode to the cyclic voltage sweep chronoamperometric technique was studied for various solutions containing Fe^{2+}, $Fe(CN)_6^{4-}$, Cu^{2+}, Ce^{3+}, Br^-, I^-, IO_3^-, Mn^{2+} and MnO_4^- ions as well as hydroquinone and *p*-phenylenediamine. For some cases the comparative curves were taken by means of the mercury and platinum microelectrode.

REFERENCES

1 J. HEYROVSKÝ AND J. FOREJT, *Z. physik. Chem.*, 193 (1943) 77.
2 A. ŠEVČIK, *Collection Czechoslov. Chem. Commun*, 13 (1948) 349.
3 V. ČERMAK, *Collection Czechoslov. Chem. Commun*, 23 (1958) 1471; 24 (1959) 831.
4 W. KEMULA AND Z. KUBLIK, *Bull. Acad. Polon. Sci.* Cl. III, 6 (1958) 653; *Roczniki Chem.*, 32 (1958) 941; *Nature*, 182 (1958) 799.
5 P. DELAHAY, G. CHARLOT AND H. A. LAITINEN, *Anal. Chem.*, 32 (1960) 103A.
6 C. OLSON, H. Y. LEE AND R. N. ADAMS, *J. Electroanal. Chem.*, 2 (1961) 396.
T. MIZOGUCHI AND R. N. ADAMS, *J. Am. Chem. Soc.*, 84 (1962) 2058.
Z. GALUS AND R. N. ADAMS, *J. Am. Chem. Soc.*, 84 (1962) 2061.
Z. GALUS AND R. N. ADAMS, *J. Am. Chem. Soc.*, 84 (1962) 3207.
7 G. T. CROFT, *J. Electrochem. Soc.*, 106 (1959) 278.
8 F. WILL AND C. A. KNORR, *Z. Elektrochem.*, 64 (1960) 258, 270.
9 M. W. BREITER, *J. Electrochem. Soc.*, 109 (1962) 42.
10 W. KEMULA AND Z. KUBLIK, *Anal. Chim. Acta*, 18 (1958) 104.
11 R. P. FRANKENTHAL AND I. SHAIN, *J. Am. Chem. Soc.*, 78 (1956) 2669.
12 M. M. NICHOLSON, *Anal. Chem.*, 32 (1960) 1058.
13 F. C. ANSON, *J. Am. Chem. Soc.*, 81 (1959) 1554.
14 P. G. DESIDERI, *J. Electroanal. Chem.*, 4 (1962) 359.

SÉPARATION DE RADIOÉLÉMENTS PAR ÉLECTROPHORÈSE SUR PAPIER À HAUTE TENSION

J.-P. ADLOFF ET R. BERTRAND

Centre de Recherches Nucléaires, Département de Chimie Nucléaire, Strasbourg-Cronenbourg, France

(Reçu le 23e janvier, 1963)

L'électrophorèse sur papier a trouvé de nombreuses applications en radiochimie: séparation de radioéléments naturels et artificiels, détermination de l'état chimique d'ions radioactifs sans entraîneurs en solutions très diluées, analyse des composés chimiques radioactifs résultant de réactions Szilard et Chalmers. En général, l'application de champs électriques d'une dizaine de volts par centimètre assure le succès de l'opération en un temps raisonnable. Plusieurs auteurs[1,8] ont souligné récemment les avantages offerts par l'utilisation de tensions beaucoup plus élevées: l'augmentation de la vitesse de migration des ions et le gain de temps qui en résulte, limitent considérablement l'effet de diffusion. De plus, lorsqu'ils sont soumis à un gradient de potentiel de 200 volts par cm, les ions peuvent parcourir en quelques minutes une distance de 10 à 15 cm, suffisante pour séparer des espèces de mobilités très voisines. C'est pourquoi la technique d'électrophorèse sur bande de papier avec un champ électrique intense nous a semblé particulièrement adaptée à la séparation rapide de radioéléments de courtes périodes.

Les exemples de séparation de composés minéraux par électrophorèse à haute tension sont encore peu nombreux. GROSS[2] a séparé les éléments alcalins en une trentaine de minutes avec un champ de 100 volts/cm; l'électrolyte était une solution 0,1 *M* de carbonate d'ammonium. Le même auteur a séparé rapidement des métaux lourds complexés par l'acide citrique, ainsi que les acides halogénés[3]. MICHL[1] a obtenu en 90 min, avec un champ de 46 volts/cm, une bonne séparation de Th, Y et des terres rares Nd, Ce, Pr, en présence d'acide lactique. Les métaux du groupe du cuivre ont été séparés par PUCAR[4] et des mélanges de phosphates par SANSONI ET BAUMGARTNER[5]. Ce sont BAILEY ET YAFFE[6] qui ont introduit l'électrophorèse à haute tension en radiochimie; ces auteurs ont réussi à séparer en moins de 30 minutes, des radioéléments en filiation: ^{90}Sr–^{90}Y, ^{140}Ba–^{140}La, ^{99}Mo–^{99m}Tc, ^{210}Pb–^{210}Bi–^{210}Po. Le champ électrique était de 100 à 180 V/cm et l'électrolyte une solution d'un acide organique complexant. Plus récemment H. VAN DIJK *et al.*[7] ont pu séparer des radioéléments de courte période par électrophorèse dans un champ de 30 à 60 V/cm en tenant compte des zones basique et acide qui se forment par réaction électrochimique au voisinage des électrodes.

Plusieurs dispositifs d'électrophorèse à haute tension ont été décrits[8,9,10,11]. Le problème essentiel du refroidissement de la bande électrophorétique, a été discuté par GROSS[8]. La vitesse de migration augmente avec la tension appliquée; l'intensité du courant traversant la bande s'élève dans le même rapport, mais la chaleur dégagée par le passage du courant augmente avec le carré de l'intensité. Il est nécessaire d'évacuer rapidement cette énergie, puisqu'une élévation de la température entraîne une diminution de la résistance de l'électrolyte et par conséquent une nouvelle augmentation de l'intensité. Les conditions de l'électrophorèse sont alors mal définies et peu reproductibles.

PARTIE EXPÉRIMENTALE

L'appareil que nous avons réalisé est inspiré de celui décrit par GROSS[8]. La chaleur dégagée pendant l'électrophorèse est évacuée par une circulation d'eau ou d'un liquide réfrigérant dans deux plaques d'aluminium appuyant uniformément sur la bande de papier. L'isolement électrique des plaques est assuré par des feuilles minces de chlorure de polyvinyle entre lesquelles est glissée la bande électrophorétique. La température du papier est en moyenne de 15°C. La haute tension est fournie par une générateur de tension continue 0–5 kV avec un débit maximal de 500 mA. Les dimensions des bandes de papier (Arches n°302) sont 44 × 3 cm. La position des radioéléments, après électrophorèse, est déterminée par déplacement de la bande de papier sous un détecteur approprié (compteur α ou β, scintillateur) et les isotopes séparés sont identifiés par leur rayonnement et leur période. Dans le cas de radioéléments de courtes périodes (30 minutes ou moins) ou d'activités faibles, la bande de papier est découpée cm par cm. L'évolution de l'activité des divers échantillons est déterminée à l'aide d'un compteur très sensible ou d'une installation de comptage à faible bruit de fond, ce qui permet de tracer les histogrammes de l'activité de la bande à un instant donné.

RÉSULTATS

(1) Des exemples de séparation de radioéléments de courtes périodes sont groupés dans le tableau 1. Dans tous les cas, le champ électrique est de 80 V/cm. Les déplace-

TABLEAU 1

CIT, OX, EDTA, NTA: SELS D'AMMONIUM DES ACIDES CITRIQUE, OXALIQUE, ÉTHYLÈNE DIAMINE TÉTRACÉTIQUE, NITRILOTRIACÉTIQUE; CONCENTRATION 0.05 *M*

Produit de départ	*Radioélément séparé*	*Période*	*Durée de l'électrophorèse*	*Electrolyte*	*Position du radioélément séparé*
^{211}Pb (AcB)	^{207}Tl (AcC'')	4.76 min	5 min	Ac. citrique	+ 10.8 cm
				EDTA	+ 2.4 cm
				NTA	− 3.6 cm
^{212}Pb (ThB)	^{208}Tl (ThC'')	3.1 min	5 min	Ac. citrique	+ 10 cm
			8 min	OX	+ 7.5 cm
^{211}Pb (AcB)	^{211}Bi (AcC)	2.16 min	5 min	HCl 0,5 *N*	− 1 cm
^{137}Cs	^{137m}Ba	2.6 min	2 min	CIT	− 1 cm

ments des ions sont comptés à partir du point de dépôt, avec le signe + pour une migration vers la cathode, et le signe — dans le cas inverse.

(2) La séparation des descendants en filiation de radioéléments naturels, est représentée schématiquement sur la Fig. 1. L'électrophorèse de ^{227}Ac, ^{228}Ra et ^{210}Pb en équilibre avec leurs dérivés, a été réalisée dans différents milieux complexants: sels d'ammonium des acides citrique (CIT), nitrilotriacétique (NTA) et éthylènediaminetétraacétique (EDTA). Seules ont été représentées les positions des radio-

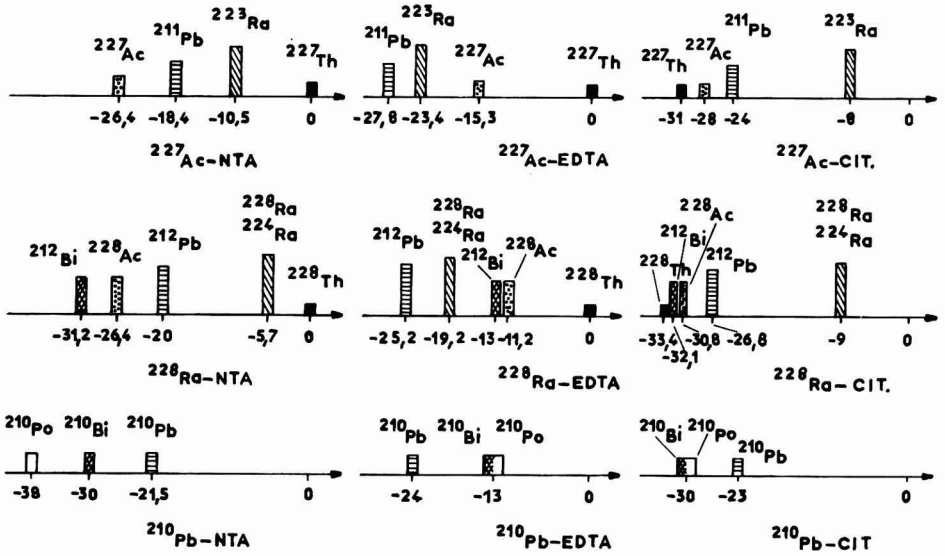

Fig. 1. Séparation par électrophorèse à haute tension des descendants de ^{227}Ac, ^{228}Ra et ^{210}Pb. Concentration des électrolytes 0.05 *M*. Tension 5000 volts; durée 35 min; température 15°C.

éléments de période supérieure à 30 minutes: pour ^{227}Ac: ^{227}Th(RAc), ^{223}Ra (AcX), ^{211}Pb (AcB); pour ^{228}Ra (MThI): ^{228}Th (RTh), ^{224}Ra (ThX), ^{228}Ac (MThII), ^{212}Pb (ThB) et ^{212}Bi (ThC); pour ^{210}Pb (RaD): ^{210}Bi (RaE) et ^{210}Po (RaF).

(3) Séparation et migration du francium[12].

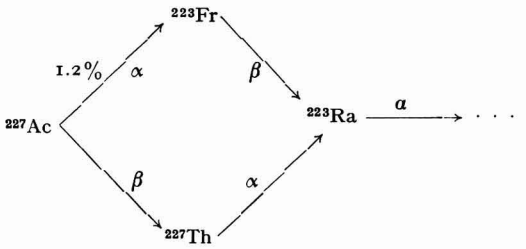

Le principal isotope du francium est ^{223}Fr ou AcK provenant de la désintégration par émission d'un rayonnement α, de 1.2% des atomes de ^{227}Ac:

^{223}Fr se désintègre avec une période de 21 minutes. Plusieurs méthodes de séparation du francium ont été décrites: précipitations chimiques répétées en présence d'entraîneurs[13], entraînement du francium par des hétéropolyacides[14], extraction par solvants[15], chromatographie sur papier ordinaire[16] et sur papiers imprégnés d'échangeur d'ions minéraux[17,18] ou sur une colonne de bleu d'outremer[19]. Aucune de ces méthodes ne répond entièrement et simultanément aux deux conditions exigées pour la préparation de francium radiochimiquement pur: *rapidité*, en raison de la courte période du radioélément, et *spécificité*, la chaîne principale de la famille de l'actinium conduisant à ^{227}Th, ^{223}Ra, ^{211}Pb et ^{207}Tl, présents en quantités cent fois plus importantes.

L'électrophorèse à haute tension permettant de satisfaire la première condition, il suffit de choisir un électrolyte pour lequel le déplacement du francium n'interfère pas avec celui des isotopes de Ac, Th, Ra, Pb et Tl. A l'encontre des alcalins, ces derniers éléments peuvent former des complexes avec certains acides organiques.

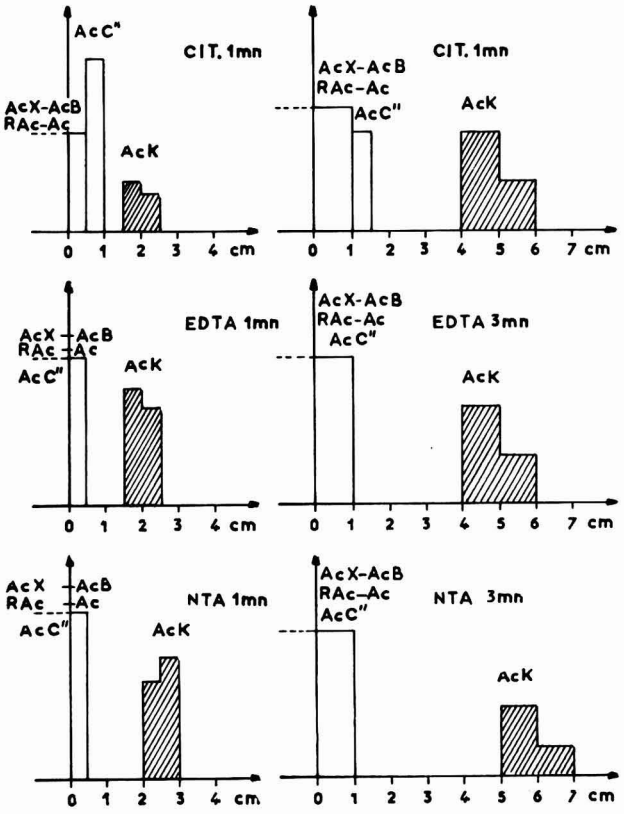

Fig. 2. Electrophorégrammes de ^{227}Ac en équilibre avec ses descendants (partie cationique). En abscisse: déplacement à partir du point de dépôt; en ordonnée: activité en unités arbitraires. Concentration des électrolytes: 0.05 *M*; champ appliqué: 80 V/cm; température 15°C.

Il est donc possible de réaliser un milieu dans lequel le francium migre seul et rapidement vers la cathode, tous les autres éléments, complexés, se déplaçant vers l'anode. La partie cationique de l'électrophorégramme d'actinium en équilibre radioactif avec tous ses descendants est représentée sur la Fig. 2. La séparation du francium est encore excellente en 30 secondes; dans tous les cas l'efficacité de la séparation a été contrôlée par la mesure de la période du francium.

Il nous a semblé intéressant de comparer la mobilité du francium à celle des autres éléments alcalins. Le francium se déplace plus rapidement que le sodium (Fig. 3), mais il migre à la même vitesse que le césium (Fig. 4). GROSS[2] a déterminé les vitesses relatives de migration de K^+, Rb^+ et Cs^+ (0.962 : 1.000 : 0.988) en effectuant une

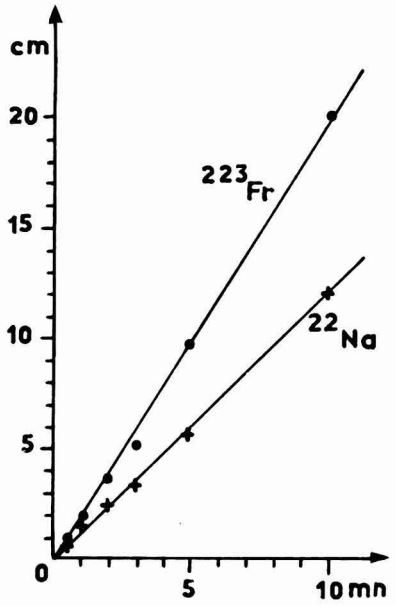

Fig. 3. Déplacements de Fr^+ et Na^+. Electrolyte: citrate d'ammonium 0.05 *M*; champ: 80 V/cm; température 15°C.

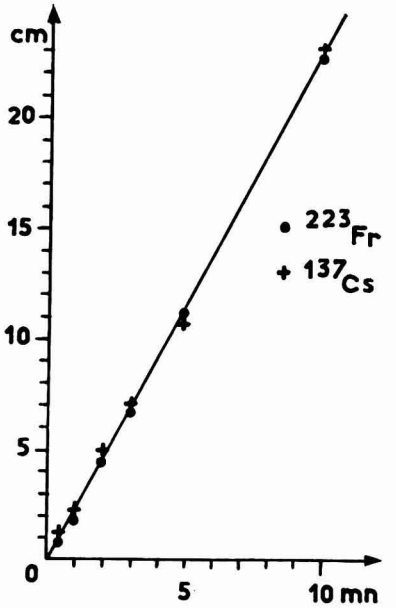

Fig. 4. Déplacements de Fr^+ et Cs^+. Electrolyte: sel d'ammonium de EDTA 0.05 *M*; champ: 80 V/cm; température 15°C.

électrophorèse en présence de carbonate d'ammonium 0.1 *M*, pH 8.9, dans un champ électrique de 100 V/cm. Dans ces mêmes conditions la vitesse de migration du francium est égale à celle du césium. Les mobilités de ces deux éléments sont très voisines, comme le suggère le rapport des rayons ioniques de Fr^+ et Cs^+, évalué à 1.07[20].

RÉSUMÉ

L'électrophorèse sur papier dans un champ électrique élevé (80 V/cm) en présence d'acides organiques complexants, permet la séparation rapide de radioéléments de courtes périodes. Le francium a été isolé de l'actinium en équilibre avec tous ses descendants.

SUMMARY

Paper electrophoresis in a high electric field (80 V/cm) in the presence of complexing organic acids permits rapid separation of radio elements of short half-life. Francium has been separated from actinium in equilibrium with its disintegration products.

BIBLIOGRAPHIE

1 H. MICHL, *J. Chromatog.*, 1 (1958) 93.
2 D. GROSS, *Nature*, 180 (1957) 596.
3 D. GROSS, *Chem. Ind. (London)*, (1957) 1597.
4 Z. PŮCAR, *Anal. Chim. Acta*, 17 (1957) 476 et 485.
5 B. SANSONI ET L. BAUMGARTNER, *Z. Anal. Chem.*, 158 (1957) 241.
6 R. A. BAILEY ET L. YAFFE, *Can. J. Chem.*, 38 (1960) 1871.
7 H. VAN DIJK, F. P. IJSSELING ET H. LOMAN, *Anal. Chim. Acta*, 27 (1962) 563.
8 D. GROSS, *J. Chromatog.*, 5 (1961) 194.
9 A. E. PASICKA, *Can. J. Biochem. Physiol.*, 39 (1961) 1313.
10 J. C. ARIAS ET A. Q. MUSSO, *Soc. Ci. Nat. La Salle*, 21 (1961) 49.
11 Z. PRUSIK ET B. KEIL, *Coll. Czech. Chem. Commun.*, 25 (1961) 2049.
12 J. P. ADLOFF ET R. BERTRAND, *Compt. Rend.*, 254 (1962) 2575.
13 M. PEREY, *Thèse*, Paris 1946.
14 E. K. HYDE, *J. Amer. Chem. Soc.*, 74 (1952) 4081.
15 R. MUXART, M. LEVI ET G. BOUISSIERES, *Compt. Rend.*, 249 (1959) 1000.
16 M. PEREY ET J. P. ADLOFF, *Compt. Rend.*, 236 (1953) 1163 et 240 (1955) 1389.
17 J. P. ADLOFF, *J. Chromatog.*, 5 (1961) 366.
18 H. J. SCHROEDER, *Radiochim. Acta*, 1 (1962) 27.
19 W. HERR ET H. J. RIEDEL, *Radiochim. Acta*, 1 (1962) 32.
20 A. K. LAVROUKHINA, *Usp. Khim.*, 27 (1958) 1209.

INTERPRETATION OF TOTALLY IRREVERSIBLE CHRONOPOTENTIOMETRIC WAVES

C. D. RUSSELL* AND J. M. PETERSON**

Gates and Crellin Laboratories of Chemistry California Institute of Technology (Pasadena, Cal., U.S.A.)

(Received February 12th, 1963)

INTRODUCTION

The simplest case in chronopotentiometry is the case of direct discharge of a single species under conditions of linear diffusion. If the discharge is totally irreversible the theoretical potential-time curve, derived by DELAHAY AND BERZINS[1] and confirmed experimentally by DELAHAY AND MATTAX[2], is the following:

$$E = \frac{RT}{\alpha n_a F} \ln\left(\frac{nFck}{i}\right) + \frac{RT}{\alpha n_a F} \ln\left[1 - \left(\frac{t}{\tau}\right)^{1/2}\right] \quad (1)$$

where E is the electrode potential, t the time measured from the beginning of the pulse of constant current, n the number of electrons involved in the over-all electrode reaction, n_a the number of electrons involved in the rate-determining discharge process, k the rate constant for $E = 0$, α the transfer coefficient, i the current density, c the bulk concentration of the species undergoing discharge, R the gas law constant, T the absolute temperature, and F Faraday's constant. τ is the "transition time",

$$\tau = \frac{n^2 F^2 c^2 D}{4i^2} \quad (2)$$

where D is the diffusion coefficient of the discharging species. The rate constant and transfer coefficient may be obtained from the slope and E-intercept of a plot of E *versus* log $[1 - (t/\tau)^{1/2}]$. DELAHAY AND MATTAX[2,3] used this method to obtain rate constants and transfer coefficients for several electrode reactions, but the method has largely been neglected as a means of measuring electrochemical kinetic parameters.

A major difficulty in using this method is the determination of an accurate transition time, which must be known to construct the plot. The transition time is not precisely defined in a typical chronopotentiogram (*cf.* Fig. 2) due to the capacitance of the double layer and to the commencement of secondary reactions. Empirical graphical procedures have been suggested for determining the transition time from

* Present address: *Department of Chemistry, Harvard University (Cambridge, Mass.).*
** Present address: *Institute of Theoretical Science, University of Oregon (Eugene, Oregon).*

an experimental chronopotentiogram (see below). The transition time can also be chosen as the time required to reach an arbitrarily predetermined potential.

The quantity τ defined by eqn. (2) may be regarded as the "true" transition time which one desires to measure. This will have the property $i\tau^{1/2}/c$ = constant if the diffusivity of the discharged species is constant, and constancy of $i\tau^{1/2}/c$ has been the usual criterion for the validity of the technique used to determine the transition time. No critical comparison of the different techniques has been published. This communication will compare various methods of obtaining transition times and rate parameters from chronopotentiometric waves, as applied to the wave for the reduction of iodate on mercury in alkaline solution. Several new methods are presented and the results are compared with a least-squares analysis by digital computer.

EXPERIMENTAL

Reagents. The electrolysis solution (0.00420 *M* KIO_3, 0.890 *M* NaOH) was prepared from reagent grade chemicals and doubly distilled water, the first distillation being from basic permanganate. All glassware contacting the solution was cleaned with sulfuric acid-potassium dichromate cleaning solution. Comparison tests using all-glass equipment, including a glass electrolysis cell, showed that the solutions could be stored in polyethylene bottles without picking up any surface-active organic material which affected the measurements.

The mercury used was either technical grade mercury which had been treated in an "oxifier" and then agitated by air bubbles under a dilute solution of nitric acid and hydrogen peroxide for twelve hours, or Mallinckrodt triply distilled mercury. In either case it was forced through sintered glass directly into the electrolysis cell. No difference was found between the two preparations.

Apparatus. The electrolysis cell is illustrated in Fig. 1. A polyethylene vessel was

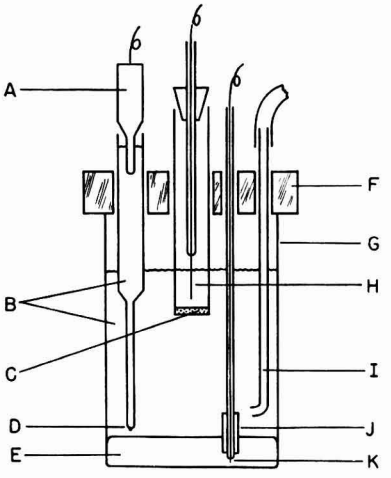

Fig. 1. Electrolysis cell. A. Saturated calomel electrode (fiber bridge); B. Test solution; C. Fine porosity fritted glass; D. Soft glass bead in pyrex stem; E. Mercury pool; F. Glass plate; G. Polyethylene beaker; H. Platinum wire electrode; I. Nitrogen inlet tube (raised during measurement; J. Teflon jacket; K. Platinum wire contact.

used, to avoid penetration of solution between the mercury and the wall of the vessel. When a glass vessel was tried, even if great care was used in delivering the solution to the cell to avoid wetting the walls below the mercury level, only the first chronopotentiogram was undistorted. (Waves of very irregular shape were obtained at high current densities using the glass cell; water was driven visibly between glass and mercury by the pulse of current.) Contact with the mercury pool was made by a platinum wire sealed in a glass tube which was covered with Teflon electrical spaghetti to prevent penetration of water between the mercury and the glass. The saturated calomel reference electrode was separated from the electrolysis cell by a salt bridge containing the same solution as in the cell. Ohmic drop between the mercury pool and the reference electrode was measured and found negligible. The area of the mercury pool was calculated from the transition time for the reduction of a standard Pb^{+2} solution.

The current source was a Wenking potentiostat (Elektronische Werkstätten, Göttingen) connected so as to control the potential across a resistor in series with the cell. The chronopotentiograms were recorded on a Moseley Model 3 S Autograf x-y-time recorder isolated by a follower amplifier of the DeFord type[4] constructed with George A. Philbrick Company plug-in amplifiers.

Procedure. The solution was deaerated 20 min. with Linde High Purity Dry Nitrogen (presaturated with water) and two chronopotentiograms were recorded.

RESULTS AND DISCUSSION

A typical chronopotentiogram is reproduced in Fig. 2 and points calculated from eqn. (1) are also plotted on the same coordinates using parameters which give the best least-squares fit. The least squares treatment was performed on a digital com-

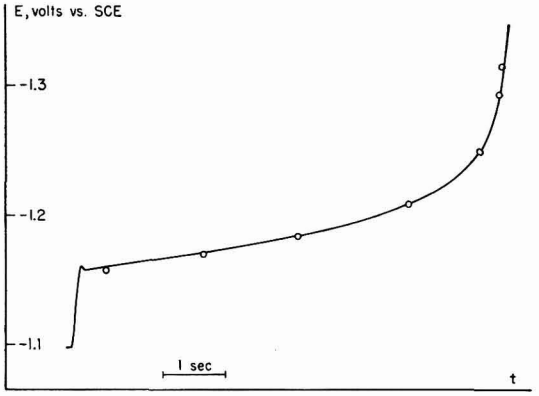

Fig. 2. Experimental chronopotentiogram and calculated points. Solution containing 0.004 *M* KIO_3, 0.9 *M* NaOH. Current density 0.25 mA/cm^2.

puter. The calculated points fit nearly the whole experimental curve within the accuracy of measurement. Table 1 lists the least-squares parameters for a series of measurements.

TABLE 1

INTERPRETATION OF CHRONOPOTENTIOMETRIC WAVES BY VARIOUS METHODS

Run No.	*Least Squares*			*Delahay and Mattax*	*Reinmuth*	*Kuwana*	*Eqn. 2*		*Eqn. 3*		*Eqn. 4*
	$E_{1/4}$	$n\alpha$	τ	τ	τ	τ	$\tau\,(a)$	$\tau\,(b)$	$n\alpha\,(a)$	$n\alpha\,(b)$	$n\alpha(c)$
1	1.170	0.899	6.83	6.64	6.69	6.79	6.83	6.79	0.915	0.957	1.00
2	1.172	0.881	6.84	6.44	6.54	6.75	6.82	6.71	0.936	0.992	1.00
3	1.174	0.917	6.81	6.61	6.67	6.82	6.80	6.71	0.937	1.003	0.99
4	1.176	0.941	6.80	6.60	6.65	6.82	6.78	6.73	0.948	0.999	1.01
5	1.169	0.900	6.94	6.75	6.80	6.96	6.91	7.01	0.921	0.943	0.96
6	1.170	0.934	6.86	6.69	6.74	6.88	6.87	6.86	0.938	0.937	0.95
7	1.172	0.904	6.62	6.39	6.45	6.65	6.60	6.54	0.938	0.975	1.00
8	1.173	0.934	6.65	6.45	6.54	6.68	6.61	6.60	1.030	0.989	1.04

(a) $E_1 = 1.180$ V, $E_2 = 1.230$ V, $E_3 = 1.280$ V
(b) $E_1 = 1.170$ V, $E_2 = 1.210$ V, $E_3 = 1.250$ V
(c) Least-squares τ was used in calculation

Transition times calculated by the graphical methods of DELAHAY AND MATTAX[2] and of REINMUTH[5] are also listed in Table 1. The procedures are as follows.

Method of DELAHAY AND MATTAX[2] (Fig. 3a). Tangent lines AC and BD are drawn to the linear portions of the wave preceding and following the potential pause. Two more lines, AB and CD, are drawn parallel to the time axis forming a trapezoid. A fifth line, EF, is drawn through points E and F lying one fourth of the distance from C to D and From A to B respectively. GH is drawn through the intersection of EF with the curve, parallel to the time axis. The transition time then corresponds to the distance GH. DELAHAY AND MATTAX also describe a method for handling waves with very poorly defined potential breaks at the end of the potential pause, which we shall not consider here.

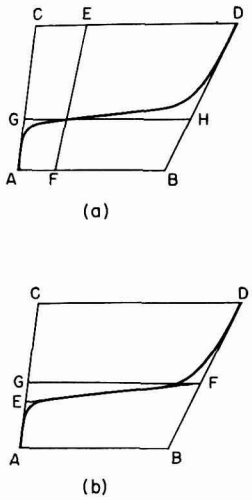

Fig. 3. Graphical determination of transition time. (a). Method of DELAHAY AND MATTAX; (b). Method of REINMUTH.

Method of REINMUTH[5] (Fig. 3b). Tangent lines AC, BD, and EF are drawn to the linear portions of the wave preceding and following the potential pause and to the linear part of the wave near its inflection. A line, GF, is then drawn through the intersection of EF and BD, parallel to the time axis, and its length corresponds to the transition time.

Another graphical method is simply to lay a straightedge along the steep part of the curve following the potential pause and select the point at which the curve becomes straight as the transition time. (Through there is no theoretical reason for the curve to become linear, it generally does so.) This method has not appeared in print but since we have first seen it used by T. KUWANA it will be called the method of KUWANA. It gave the best results of the graphical methods (Table I).

An algebraic method for calculating the transition time can be based on the equation

$$\tau^{1/2} = \frac{t_2 - t_1^{1/2} t_3^{1/2}}{2t_2^{1/2} - t_1^{1/2} - t_3^{1/2}} \qquad (3)$$

which follows exactly from eqn. (1). Here (t_1, E_1), (t_2, E_2), and (t_3, E_3) are points of the chronopotentiogram chosen such that $E_3 - E_2 = E_2 - E_1$. The advantage of this method is that it is based on points from the central part of the curve where secondary effects (double layer capacity, secondary reactions) are unimportant. Best results are obtained if points fairly close to the steep regions are used, however, as Table 1 shows. Care must be taken in using this equation to carry enough significant figures since cancellation of errors between numerator and denominator occurs; if the times are known to three significant figures, four significant figures must be carried through the calculation. Error analysis showed that the calculated value of τ is more sensitive to the errors in t_3 (where $t_3 > t_2 > t_1$) than in t_1 or t_2. For the data treated here, an error in t_3 (at $E = 0.13$) is multiplied by 1.5 in the calculated value of τ.

A similar equation may be derived for the transfer coefficient α in terms of the same three points.

$$n\alpha = \frac{RT}{F(E_1 - E_2)} \ln \left[\frac{t_3^{1/2} - t_2^{1/2}}{t_2^{1/2} - t_1^{1/2}} \right] \tag{4}$$

Values of $n\alpha$ calculated from this equation are given in Table 1.

A graphical method for calculating the transfer coefficient can be based on the fact that central part of a totally irreversible chronopotentiometric wave is nearly linear. It can be shown from eqn. (1) that the wave has an inflection point at $t = \tau/4$, where the slope has the minimum value

$$\frac{dE}{dt} = \frac{2RT}{\alpha n F \tau} \tag{5}$$

This slope can readily be found with a straightedge, since according to eqn. (1) it is constant to within $\pm$ 5% from 0.15 τ to 0.38 τ. Values of the transfer coefficient obtained from eqn. (5) are listed in Table 1. This method requires that a value for τ be obtained independently.

A final means of interpreting a totally irreversible chronopotentiometric wave is to choose by trial and error the value of τ which results in the most linear plot of E against $\log [1 - (t/\tau)^{1/2}]$. Figure 4 shows the sensitivity of the log plot to the assumed value of τ. Apparently τ can be determined this way to within several percent.

In all of the chronopotentiograms which were recorded the initial rise to the potential pause was too rapid for the recorder to follow. For this reason a vertical rise was assumed in the application of all methods for determining the transition time. (CA was drawn vertically, for example, in Fig. 3.) For the rest of the curve the rate of voltage change fell within the limits prescribed by the recorder manufacturer for 0.5% accuracy; lack of distortion was verified by monitoring the error signal from the recorder feedback amplifier. The rapid rise to the potential pause indicates negligible distortion over most of the wave from the effect of double-layer capacitance, since the ratio of charging current for the double layer to the total current during the potential pause is equal to the ratio of the slope of the curve during the potential pause to its slope preceding the potential pause if the double layer capacity is assumed constant. This ratio was less than 1% over most of the wave. If a large double-layer capacitance is present so that line CA cannot be drawn vertically in the methods

of Fig. 3, its deviation from the vertical will tend to shorten the calculated transition time and counteract in part the opposite effect of the capacitance to lengthen the transition time. It does not simply undercompensate by a factor of approximately two as REINMUTH[5] suggests, however, for the charging current during the potential pause depends on and is proportional to the rate of change of potential rather than having the constant value assumed by REINMUTH. It might be helpful to correct the

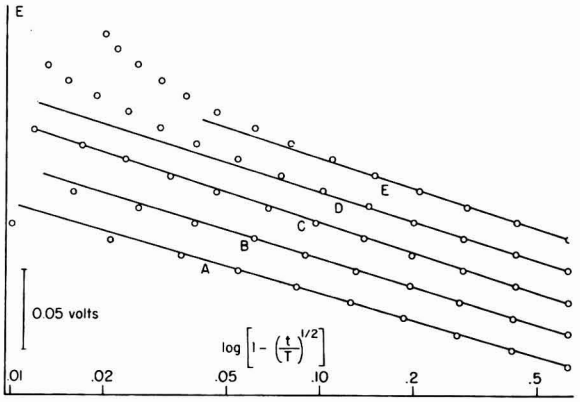

Fig. 4. Sensitivity of logarithmic plot to assumed value of transition time. By least squares analysis, $\tau = 6.80$, $n\alpha = 0.941$.
A. $\tau = 6.60$ s. assumed, $n\alpha = 1.04$ calculated from slope of line
B. $\tau = 6.70$, $n\alpha = 1.00$
C. $\tau = 6.80$, $n\alpha = 0.94$
D. $\tau = 6.90$, $n\alpha = 0.99$
E. $\tau = 7.00$, $n\alpha = 0.96$

current by subtracting the charging current estimated from the ratio of the slopes of AC and EF (Fig. 3b) but the simple eqn. (1) no longer applies strictly and any effort to use it must involve some arbitrariness. It is desirable, when measuring kinetic parameters, to avoid conditions under which the charging current is significant.

We regard the least-squares procedure as the most reliable of the methods used here. Comparing the least-squares value for τ with those obtained by the other methods, the best results were obtained using the method of KUWANA or, if E_1, E_2, and E_3 covered a wide enough range on the chronopotentiogram, by using eqn. (3). The method of REINMUTH gave somewhat poorer results, and the method of DELAHAY AND MATTAX, poorer results still. None of the methods of determining $n\alpha$ proved entirely satisfactory, and even the least-squares $n\alpha$ calculated from different chronopotentiometric waves obtained under the same experimental conditions was not very reproducible. (The values of τ did not reproduce from run to run either, due to variations in the exposed area of mercury. Variation in τ is expected; variation in $n\alpha$ is not.) Better results for $n\alpha$ were obtained by using eqn. (4) than by using eqn. (5).

In the case studied the best simple methods of determining τ and $n\alpha$ were the use of the graphical method of KUWANA and the use of eqn. (4), respectively. These are simpler and faster than methods previously suggested. Equation (5) offers a still quicker way of determining $n\alpha$ than eqn. (4). Its poor showing in Table I may be attributable to the small slope of the chronopotentiogram at the quarter wave potential (*cf.* Fig. 2) which could not be measured with great accuracy. Expanding

the voltage scale when the data were recorded would remedy this. Equation (3) may be preferred by some as a method of determining the transition time because of its straightforward theoretical justification, although it is somewhat more trouble to apply than the method of KUWANA. Probably the most reliable method of hand calculation, though by far the most laborious, is the trial-and-error procedure exemplified in Fig. 4.

While conventional practice is to calculate the rate constant from the extrapolated potential at $t = 0$, it can just as well be calculated from the quarter-wave potential using the formula:

$$k = \frac{2i}{n\mathrm{F}c} \exp\left(-\frac{\alpha n\mathrm{F}}{RT} E_{\frac{1}{4}}\right) \tag{6}$$

This is the same formula as that used to calculate the rate constant from the potential at $t = 0$, except for a factor of 2 corresponding to the fact that when $t = \tau/4$ half of the reactant at the electrode surface has been consumed. The quarter-wave potential can be read directly from the chronopotentiogram. An advantage of calculating the rate constant from the quarter-wave potential and $n\alpha$ from the quarter wave slope is that the calculations are based on the central part of the wave where the influence of the double-layer capacity and other secondary effects are at a minimum. (The end portions of the wave must be used to determine the transition time, however, and an error in τ will introduce errors into $E_{\frac{1}{4}}$ and $n\alpha$.) On balance this procedure seems comparable in accuracy to those previously published and much simpler.

Rate constants for the reduction of iodate in 1 M NaOH at a mercury electrode can be estimated from published graphical data. The value $k = 10^{-2.5}$ cm/sec at -1.150 V *vs.* SCE is obtained from the polarographic data of GIERST[6] for 0.9 M sodium hydroxide solution. Gierst measured $n\alpha = 0.87$[7] (misprinted 0.67 in reference[6]). We estimate from the data of DELAHAY AND MATTAX[3] (measured chronopotentiometrically) that $n\alpha = 0.85$ for 1.0 M sodium hydroxide solution. The values calculated from the least-squares parameters of Table I are $k = 10^{-3.03}$ cm/sec, $n\alpha = 0.91$. These data have not been corrected for the double layer effect[6].

It should be remarked that the practice of reporting rate constants based on the normal hydrogen electrode as reference voltage introduces a large roundoff error into the data unless the quarter-wave potential is near zero. This results from the fact that the rate constant referred to zero potential (N. H. E.) has a large exponential factor exp $[(\alpha n\mathrm{F}/RT)\, E_{\frac{1}{4}}]$ which causes the principal error in the calculated rate constant to be that arising from the error in α. After *rounding off* the calculated rate constant accordingly, it is impossible to recalculate the original quarter-wave potential from the reported constant to the accuracy with which it was originally measured. Thus information is permanently lost in the calculation. It is better to report a rate constant based on a non-zero reference potential which is near the quarter-wave potential, so that the exponential factor involving α is small.

SUMMARY

Methods for obtaining transition times and rate parameters from totally irreversible chronopotentiometric waves are compared and applied to data for the reduction of iodate on mercury in alkaline solution. Several new methods are presented and the

results are compared with a least-squares analysis by digital computer. Rate data are given.

ACKNOWLEDGEMENTS

We appreciate the assistance of R. S. Deverill with the computer programming. This work was partially supported by the U.S. Army Research Office (Durham) under Grant No. DA-ARO(D)-31-124-G315.

REFERENCES

1 T. BERZINS, P. DELAHAX, *J. Am. Chem. Soc.*, 75 (1953) 4205.
2 P. DELAHAX, C. C. MATTAX, *J. Am. Chem. Soc.*, 76 (1954) 874.
3 P. DELAHAX, C. C. MATTAX, *J. Am. Chem. Soc.*, 76 (1954) 5314
4 D. D. DEFORD, *Symposium on Electroanalytical Techniques*, 133rd American Chemical Society Meeting, San Francisco, April, 1958.
5 W. H. REINMUTH, *Anal. Chem.*, 33 (1961) 485.
6 L. GIERST, *Transactions of the Symposium on Electrode Processes*, Philadelphia (1959), E. Yeager, ed., John Wiley & Sons, Inc., New York, p. 109.
7 L. GIERST, private communication.

THE LIFETIME OF COMPLEX IONS IN IONIC LIQUIDS: AN ELECTRODE KINETIC STUDY

J. O'M. BOCKRIS, D. INMAN,* A. K. N. REDDY** AND S. SRINIVASAN

The Electrochemistry Laboratory, University of Pennsylvania, Philadelphia 4, Penna.

(Received March 12, 1963)

INTRODUCTION

In a previous publication[1], the formation constants of cadmium-containing complex ions in the molten solvent $NaNO_3$–KNO_3 at 263°C, were presented. These formation constants were obtained by the analysis of potential-time relations under conditions of constant current. The total cadmium concentrations (free and complexed cadmium) were low ($\sim 10^{-3}$ mole Kg^{-1}), the ligand concentrations at least ten times the total cadmium concentration and the applied current densities relatively small.

The present investigation is concerned with chronopotentiometric studies at higher cadmium concentrations.

EXPERIMENTAL

The apparatus and technique have been described elsewhere[1].

RESULTS

The plots of the square root of the transition time (τ) against the reciprocal of the current for the $NaNO_3$–KNO_3 melts containing $CdNO_3$ and KBr are shown in Figures 1 to 3.

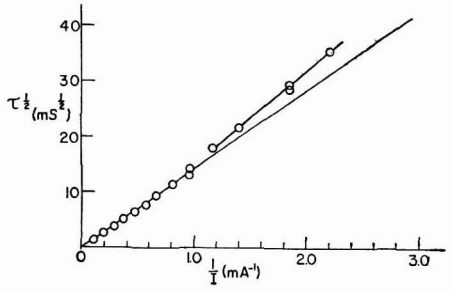

Fig. 1. $\tau^{1/2}$ against $1/I$ for $C_{Cd^{2+}} = 4.98 \times 10^{-3}$ mole Kg^{-1}. $C_{KBr} = 1.09 \times 10^{-2}$ mole Kg^{-1}.

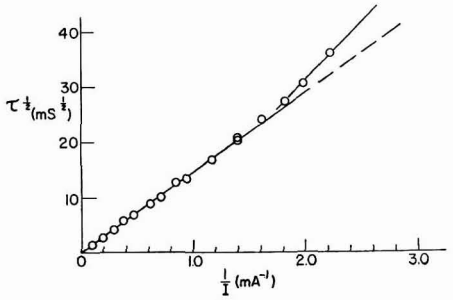

Fig. 2. $\tau^{1/2}$ against $1/I$ for $C_{Cd^{2+}} = 5.38 \times 10^{-3}$ mole Kg^{-1}. $C_{KBr} = 2.06 \times 10^{-2}$ mole Kg^{-1}.

* Present address: *Chemistry Department, The University, Reading, England.*
** On leave of absence from the *Central Electrochemical Research Institute, Karaikudi-3, S. India.*

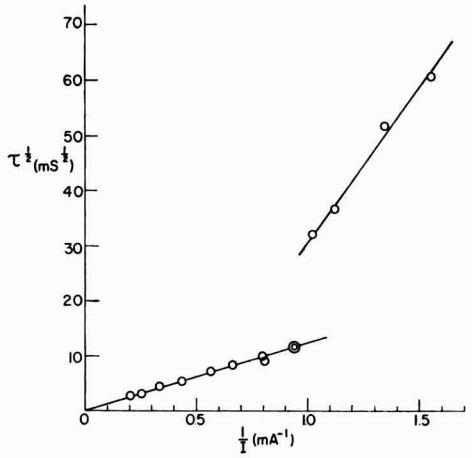

Fig. 3. $\tau^{1/2}$ against $1/I$ for $C_{Cd^{2+}} = 4.82 \times 10^{-3}$ mole Kg^{-1}. $C_{KBr} = 9.21 \times 10^{-2}$ mole Kg^{-1}.

DISCUSSION

The most significant feature of the results is the fact that the $\tau^{1/2}$ *vs.* $1/I$ plots exhibit two well-defined linear sections. The lower section (pertaining to the higher current densities) passes through the origin; the upper section has a different slope and when extrapolated yields an intercept on the $\tau^{1/2}$ axis.

The interpretation of the upper section is straight-forward. The function $i\tau^{1/2}$ decreases with an increase in current density, and hence some homogeneous reaction precedes the charge transfer reaction. This homogeneous reaction can only be the dissociation of a cadmium-containing complex[1]. Thus the overall process can be written:

$$CdBr_3^- \underset{k_3^-}{\overset{k_3^+}{\rightleftharpoons}} CdBr_2 \underset{k_2^-}{\overset{k_2^+}{\rightleftharpoons}} CdBr^+ \underset{k_1^-}{\overset{k_1^+}{\rightleftharpoons}} Cd^{++} \rightleftharpoons Cd(Hg) \qquad (1)$$

The theoretical analysis of processes of the type $A \underset{k^-}{\overset{k^+}{\rightleftharpoons}} B \overset{ne}{\rightarrow} C$ has been developed by DELAHAY AND BERZINS[2], who utilized an ingenious transformation of variables (KOUTECKY AND BRDICKA[3]) in solving the boundary value problem. For the case of an electrode reaction preceded by a second-order chemical reaction of the type: $A \underset{k^-}{\overset{k^+}{\rightleftharpoons}} B + C \overset{ne}{\rightarrow} D$ (B is a substance which cannot be reduced at the same potential as C), it is necessary to make a slight modification for the expression for τ, the transition time. We shall write

$$\tau^{1/2} = \frac{\pi^{1/2} D^{1/2} nFc^\circ}{2i} - \frac{\pi^{1/2} K c_B^\circ}{2(k^+ + k^- c_B^\circ)^{1/2}} \operatorname{erf}[z] \qquad (2)$$

where

$$z = (k^+ + k^- c_B^\circ)^{1/2} \tau^{1/2}$$

c° is the sum of the bulk concentrations of all species containing C (*i.e.*, $c^\circ = c_A^\circ + c_C^\circ$). The diffusion coefficient D is an effective value, it being necessary to write $D \approx D_A^\circ \approx D_C^\circ$ in order to facilitate solution of the boundary value problem.

c_B° is the bulk concentration of B. The quantities K, k^+ and k^- are discussed below.

When the homogeneous reaction preceding the charge transfer reaction is the dissociation of a complex (with coordination number > 1), then the above theoretical analysis is only approximately valid. This is because the complex ion, in our case $CdBr_3^-$, dissociates in a stepwise manner with the formation of intermediates ($CdBr_2$ and $CdBr^+$). Each consecutive step is characterized by two rate constants as shown in eqn. (1). If these rate constants are sufficiently different, then it can be assumed that the overall dissociation of the complex involves essentially one rate-determining step. In applying eqn. (2) to the electrolytic reduction of such complexes, K, k^+ and k^- refer to the slow step in the dissociation of the complex; K is not the over-all formation constant of the complex. It must also be borne in mind that values of k^+ and k^- obtained in this approximate manner are too low because the effect of various consecutive steps is accounted for by assuming one single slow step.

For a given reaction in solution, k^+ and k^- are constants, but τ for the overall reaction varies with applied current density. At low current density, τ is large and the argument of the error function can be taken as greater than 2. When $z > 2$, erf $(z) = 1$ and eqn. (2) reduces to

$$\tau^{1/2} = \frac{\pi^{1/2} D^{1/2} n F c^\circ}{2i} - \frac{\pi^{1/2} K c_B^\circ}{2(k^+ + k^- c_B^\circ)^{1/2}} \tag{3}$$

showing that when $\tau^{1/2}$ is plotted against $1/i$, a straight line is obtained with slope equal to $\pi^{1/2} D^{1/2} n F c^\circ/2$ and intercept equal to $-[\pi^{1/2} K c_B^\circ/2(k^+ + k^- c_B^\circ)^{1/2}]$.

This is the equation that applies to the upper linear section of the $\tau^{1/2}$ *vs.* $1/i$ plot, – the low current density region. It enables the calculation of the rate constants of the rate-determining step in the dissociation of the complex provided K is known for this step. We do not, however, have independent knowledge of the particular step which determines the rate of breakdown of the complex. A way out of this difficulty is given below.

At high values of i, the transition times are small and the approximation used to obtain eqn. (3) cannot be applied. That is, the error function cannot be put equal to unity. It can however be expanded thus:

$$\text{erf } (z) = \frac{2}{\pi^{1/2}} \left[z - \frac{z^3}{3 \times 1!} + \frac{z^5}{5 \times 2!} \cdots \right] \tag{4}$$

At high current densities, τ is small and z may be assumed to be less than unity. Thus, taking only the first term on the right-hand side of eqn. (4), eqn. (2) gives

$$\tau^{1/2} = \frac{\pi^{1/2} D^{1/2} n F c^\circ}{2i} - K c_B^\circ \tau^{1/2} \tag{5}$$

or

$$\tau^{1/2} = \frac{\pi^{1/2} D^{1/2} n F c^\circ}{2(1 + K c_B^\circ)} \left(\frac{1}{i}\right) \tag{6}$$

which is equation of a $\tau^{1/2}$ *vs.* $1/i$ plot passing through the origin – the lower linear section of Figs. 1 to 3. (Hence the assumption that z is less than unity is valid in this region). The term $(1 + K c_B^\circ)$ distinguishes this equation from Sand's equation.

From eqns. (3) and (6), we obtain the ratio of the slopes of the upper and lower sections of the $\tau^{1/2}$ *vs.* $1/i$ plots.

$$\frac{\text{upper slope}}{\text{lower slope}} = 1 + Kc_B^\circ \tag{7}$$

In the cadmium system under study, $c_B^\circ = [Br^-]$.

Hence,

$$\frac{\text{upper slope}}{\text{lower slope}} = 1 + K\left[Br^-\right] \tag{8}$$

Equation (8) suggests a novel method of identifying the slow step in the dissociation of the complex. If the formation constants for the various stages in the dissociation are independently known, we can calculate the ratio of the slope, and by comparison of the calculated and experimental slope ratios, the rate-determining step for the dissociation can be identified, provided the ligand concentration is in considerable excess.

In the present exploratory study, the most favourable conditions for testing the above analysis are found in the experiments shown in Figure 3, which will now be considered. From the observed slope ratio of 4.7, using eqn. (8), we have $K = 40$. It is been previously reported[1] that K_1 for $Cd^{2+} + Br^- \rightleftharpoons CdBr^+$ is 100 ± 50, K_2 for $CdBr^+ + Br^- \rightleftharpoons CdBr_2$ is 65 ± 33, and K_3 for $CdBr_2 + Br^- \rightleftharpoons CdBr_3^-$ is 8 ± 3. Hence, $CdBr_2$ is the most likely species involved in the slow dissociation step, *viz.*, $CdBr_2 \underset{k_2^-}{\overset{k_2^+}{\rightleftharpoons}} CdBr^+ + Br^-$.

Using the value of $K = 40$, the slope ratios can be calculated and compared with the observed slope ratios (see Table 1). It is seen that there are considerable discrepancies between the calculated and observed ratios in the case of experiments with low bromide ion concentrations, *i.e.*, $[Br^-] = 1.09 \times 10^{-2}$ and 2.06×10^{-2} mole Kg^{-1}, which is to be expected in view of the fact that a good percentage of the added Br^- will be bound as complex.

The rate constant for this dissociation step can be calculated using eqn. (3) since the quantities $K_2 = k_2^-/k_2^+$ and the intercept $-\pi^{1/2}K[Br^-]/2(k_2^+ + k_2^-[Br^-]^{1/2}$ are experimentally known. The value of the rate constant k_2^+ thus calculated is 3.5 sec^{-1}.

TABLE 1

EXPERIMENTAL AND CALCULATED SLOPE RATIOS WITH VARIATION OF $[Br^-]$

$[Br^-]$ (*in mole* Kg^{-1})	*upper slope* (*in* $sec^{1/2}$ *amp.* $\times 10^4$)	*lower slope* (*in* $sec^{1/2}$ *amp.* $\times 10^4$)	*upper slope* / *lower slope*	
			calculated	*observed*
1.09×10^{-2}	5.45	4.39	1.44	1.2
2.06×10^{-2}	5.92	4.58	1.82	1.3
9.21×10^{-2}	17.72	3.79	—	4.7

CONCLUSIONS

(I) The ratio of the slopes of the $\tau^{1/2}$ *vs.* $1/i$ lines can be used to establish the rate-controlling step in a series of homogeneous chemical reactions preceding the elec-

trode reaction. Such an identification of the slow dissociator is not possible without a two-section plot. Hence, the present study permits a more complete analysis of processes wherein the charge transfer reaction is preceded by a series of chemical reactions.

Whether it is experimentally possible to obtain a two-section $\tau^{1/2}$ *vs.* $1/i$ plot depends on the values of the rate constants of the slow step in the chemical reaction. The value of $(k^+ + k^- [\mathrm{Br}])^{1/2}$ should be low enough to permit the current (operating on the transition time) to swing the argument of the error function (in equation 2) to values above and below 2 giving a $i\tau^{1/2}$ function which is dependent and independent on i respectively. τ, however, should be much larger (say 100 times) than the double layer charging time. Hence, the condition for securing a two-section plot is $k^+ + k^- [\mathrm{Br}^-] << $ about 300. Since many reactions do satisfy this condition, it appears that such $\tau^{1/2}$ *vs.* $1/i$ plots can be obtained using low enough concentrations, if the currents required are experimentally accessible.

(II) In recent discussions, doubts have been expressed with regard to the existence of complex ions in molten salts[4] or at least the possibility of strictly defining them. The present study, by establishing the occurrence of a rate-determining dissociation reaction, provides clear proof of the existence of complexed cadmium ions in the $CdNO_3$-KBr system in molten KNO_3-$NaNO_3$.

This point may be stressed by computing the lifetime of the particular complex which has been established as rate-controlling for the dissociation reaction. For a uni-molecular reaction the lifetime can be defined thus:

$$T = \frac{1}{k_2^+}$$

Using the average value of $k_2^+ = 3.5$ sec^{-1}, the lifetime $T^{av}_{CdBr^{2-}} = 0.28$ sec. The time during which Cd^{2+} and Br^- ions would "remain in contact", were they not covalently bound, would be (as can be shown by a consideration of the jump time in diffusion of similar species in molten salts) many powers of ten less than this.

ACKNOWLEDGEMENTS

The authors wish to thank the A.E.C. for financial support (Contract No. AT(30-1) 1769) and Dr E. BLOMGREN for stimulating discussions.

SUMMARY

For the system formed by the addition of KBr to $Cd(NO_3)_2$ in liquid $NaNO_3$-KNO_3 at 263°C, the relation of the square root of the transition time to the reciprocal of the current density shows two sections. Analysis of this behavior shows that Cd exists probably as $CdBr_2$ in solution under the given conditions and has a lifetime of about 0.3 sec.

REFERENCES

1 D. INMAN AND J. O'M. BOCKRIS, *Trans. Faraday Soc.*, 57 (1961) 2308.
2 P. DELAHAY AND T. BERZINS, *J. Am. Chem. Soc.*, 75 (1953) 2486.
3 J. KOUTECKY AND R. BRDICKA, *Colln. Czech. Chem. Comm.*, 12 (1947) 337.
4 M. BLANDER, *J. Phys. Chem.*, 63 (1959) 1262.

Short Communication

Potentiometric Study of the Reaction between Silver Nitrate and Cadmium Chloride in Fused Alkali Nitrate

Using a concentration cell of the type $Ag|Ag^{+}_{(c)} + 1000$ g melt$||Ag^{+}_{(c')} + Cl^{-}_{(x)} +$ 1000 g melt$|Ag$, FLENGAS AND RIDEAL[1] conducted potentiometric titrations of silver by halide and cyanide ions in the eutectic melt of $(Na + K)NO_3$. They determined the solubility product constants for the corresponding silver salts precipitating in the above fused medium.

Employing the same cell, we have verified the applicability of the Nernst equation for the $Ag|Ag^{+}$ electrode

$$\Delta E = \frac{RT}{nF} \log (C_{Ag^+}/C'_{Ag^+})$$

in melts of pure sodium and potassium nitrates and in their eutectic mixture (KNO_3 54.5%) at a constant temperature of 350°C. Results show that a single straight line passing through the origin represents the variation of the cell E.M.F. with the concentration of the silver ion, irrespective of the composition of the melt and whether the silver salt is in the form of a nitrate or sulphate (*vide* Fig. 1). This further reveals an

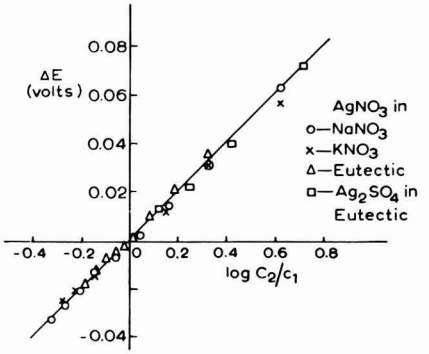

Fig. 1. Verification of the Nernst equation for electrode potential in concentration cells of $Ag|Ag^{+}$ in fused alkali nitrates at 350°.

absence of junction potential and solvation effects and that the activity coefficient of the silver ion is close to unity independent of its concentration in the range studied, *viz.* 12 to 250 meq/1000 g melt. For a comparison, the same concentration cell was studied in aqueous media of saturated solutions of sodium nitrate and of potassium

nitrate. Fig. 2 shows deviations from linearity attributable to hydration effects and to the variation of the activity coefficient of the silver ion with concentration, unlike in fused media reported here.

Next the precipitation of silver chloride was studied potentiometrically by adding weighed amounts of NaCl and $CdCl_2$ as titrants. Results with NaCl show that the salt is fully dissociated. The solubility product constant of AgCl comes out to be $(1.6 \pm 0.2) \times 10^{-4}$ at 350° in all the three fused media, *viz.* molten $NaNO_3$, KNO_3

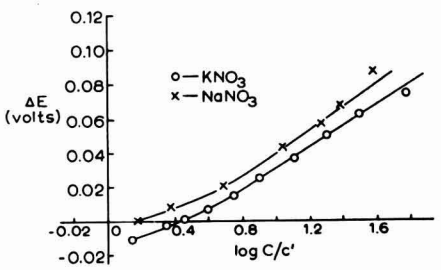

Fig. 2. Variation of the electrode potential in concentration cells of $Ag|Ag^+$ in saturated aqueous solutions of alkali nitrate at room temperature.

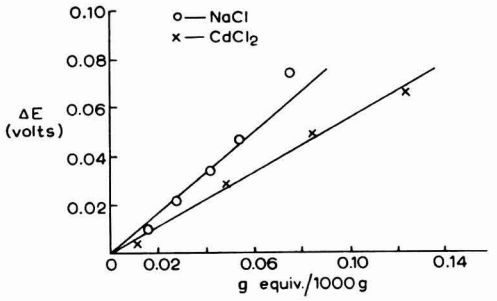

Fig. 3. Variation of the cell E.M.F. as a function of the amounts of NaCl and $\frac{1}{2}$ $CdCl_2$ added to precipitate AgCl in fused (Na + K)NO_3 medium at 350°.

and their eutectic mixture. This value for the solubility product agrees with the earlier result of FLENGAS AND RIDEAL[1] and is about a million times greater than the value for aqueous medium at ordinary temperature.

Results with cadmium chloride, however, show that this salt is in effect incompletely dissociated. This is revealed by Fig. 3 where we have plotted the cell E.M.F. as a function of the stoichiometric amount of NaCl and of $\frac{1}{2}$ $CdCl_2$ added. From the relative slopes of the two lines, it is clear that the effective degree of dissociation of $CdCl_2$ is about 0.65 (relative to NaCl = 1). This is presumably due to the formation of complexes which reduces the concentration of free chloride ions. Complexes of the type $CdCl_4^{2-}$ and even $CdCl_6^{4-}$ have been postulated earlier to account for the deviations from additivity in molar refractivity and electrical conductance of binary mixtures involving cadmium chloride in the fused state[2,3].

Department of Chemistry,
University of Poona (India)

H. J. ARNIKAR
D. K. SHARMA

[1] S. N. FLENGAS AND E. K. RIDEAL, *Proc. Roy. Soc.*, A233, (1956) 443.
[2] H. BLOOM AND E. HEYMANN, ibid, A188 (1947) 392.
[3] J. O'M BOCKRIS, *et al.*, *Trans. Farad. Soc.*, 55 (1959) 1580.

(Received February 21, 1963)

Book Reviews

Electrochemistry of Fused Salts, by I. K. DELIMARSKI AND B. F. MARKOW (translated from the Russian by A. PEIPERL), Sigma Press, 1961, xi + 353 pages, $12.50.

Interest in molten electrolyte systems is again growing among scientists, probably because better methods of investigation are now available. However, there has been no comprehensive textbook for this branch of electrochemistry, so that the present work by two of the most experienced scientists in the field of molten salts is warmly welcomed.

The subject is well treated, and the theoretical and practical aspects nicely balanced. Many carefully chosen examples make the theory easier to understand. The eight chapters deal with electrical conductance, transfer, galvanic elements, decomposition and electrode potential, solubility of metals, electrolysis, and polarisation and polarography. The last chapter will be of particular interest to analysts. Some industrial applications are also mentioned.

G. MILAZZO, Istituto Superiore di Sanità, Roma

J. Electroanal. Chem., 5 (1963) 483

Pharmaceutical Analysis, edited by TAKERU HIGUCHI AND EINAR BROCHMANN-HANZZEN, Interscience Publishers, Inc. New York and London, 1961, ix + 854 pages, 28.50, £10.15s.

This volume consists of contributions by chemists, both from university and industry, who are specialists in the field of pharmaceuticals and who have direct experience of the latest developments.

The thirteen chapters include an introductory one, and take into consideration the following substances: hydroxybenzoic acid and related compounds; carbohydrates and glycosides; steroids; sulphonamides and sulphones; carbamic acid and urea derivatives; amino acids; alkaloids and other nitrogenous bases; analgesics and antipyretics; antibiotics; vitamins and metal-organic compounds. A chapter deals with acid–base potentiometric analysis in glacial acetic acid. Various aspects of analytical determinations are discussed and the advantages and disadvantages of all methods are considered.

The authors have taken into consideration only those methods which have been thoroughly tested by the American pharmaceutical industry and the theoretical basis of each method is specified. The treatment of instrumental analysis, which can be found easily in more general textbooks describing merely physical, has been omitted.

This book is intended mainly for specialists in chemical drugs analysis and allows a choice of techniques for the determination of small quantities of oligodynamic drugs. It will be a useful addition to the libraries of those laboratories interested in the production and control of drugs and raw materials and will also be useful to students specialising in the pharmaceutical field.

MARIO COVELLO, University of Naples

J. Electroanal. Chem., 5 (1963) 483

Méthodes d'Analyse C.E.T.A.M.A. Méthodes 1 à 100, Presses Universitaires de France, 1962, 450 pages.

This is a collection of analytical methods used and recommended by the Commission for Analytical Methods of the French Atomic Energy Authority. These methods are for the most part, not new, but the procedures described are those which have been found to give the best reproducibility of analytical results and the minimum error. All methods are presented in a standard form: object and field of application, principle, apparatus, reagents, procedure. A short comment is sometimes added.

J. Electroanal. Chem., 5 (1963) 483

Developments in Applied Spectroscopy, Vol. 1, edited by W. D. ASHBY, Plenum Press, New York, 1962, 247 pages, $ 9.

This volume contains thirty-nine of the papers presented at the 12th annual symposium on spectroscopy held in Chicago, May 15–18, 1961. Twenty are given in their full text and the remaining nineteen as abstracts. The topics dealt with are X-ray spectroscopy, ultraviolet and visible spectroscopu, infrared and raman spectroscopy. Most of the papers are concerned with analytical problems, some with instrumental or methodological subjects, and a few, in abstract form, with theoretical problems, special spectroscopic techniques and nuclear magnetic resonance. No account is given of the discussions which presumably took place at the meeting, following the reading of the papers.

J. Electroanal. Chem., 5 (1963) 484

Analytik organischer Verbindungen by DR. STG. VEIBEL, Akademie-Verlag, Berlin, 1960, XX + 320 pages, D.M. 24.

This book serves as a training manual for undergraduate students of organic chemistry for identifying organic, synthetic or natural substances and is, in addition, an excellent handbook for practical analytical work in organic chemistry.

The lay-out of the book follows the classical scheme: the first chapter is devoted to methods for identifying organic substances as such, the second to qualitative and quantitative determination of elements and the third to preliminary methods of examination of the chemical and physical properties of an unknown substance. Little space, however, is devoted to the important topic of absorption spectroscopy.

Qualitative and quantitative analysis of functional groups are treated in the fourth chapter, together with the preparation of selected functional derivatives; this chapter is by far the most extensive (pp. 48–285) and is extremely useful and informative.

Analytical qualitative and quantitative methods suitable for unsaturated compounds are treated separately in the fifth chapter and specific methods for hydrocarbons in the last chapter.

This comprehensive, relatively concise and exhaustive handbook will be very useful for both the student and the more experienced chemist.

C. CASINOVI, Istituto Superiore di Sanità, Roma

J. Electroanal. Chem., 5 (1963) 484

Electronics for Scientists. Principles and experiments for those who use instruments, by H. V. MALMSTADT AND C. GENKE, W. A. Benjamin, Inc., New York, 1962, xi + 619 pages, $ 10.75.

Educational courses, particularly those for chemists, have not included until comparatively recently the study of electronics. A knowledge of electronics is indispensable for the full understanding, maintenance and use of numerous instruments for control and analysis, which are nowadays an essential part of the chemical laboratory equipment. Books dealing specifically with electronics for laboratory use are nevertheless scarce, although the subject has now become a necessary part of practical training. This book is, therefore very welcome, especially as it requires very little background knowledge in the reader, so that even the not so young can follow the principles of electronics from the beginning to their application to every kind of laboratory problem.

The nine chapters are devoted to: electrical measurements (40 pp.), power supplies (50 pp.) amplification by vacuum tubes and transistors (64 pp.), amplifier circuits (62 pp.), oscillators (28 pp.), comparison measurements (40 pp.), servo systems (50 pp.), operational amplifiers for measurement and control (56 pp.) and electronic switching and timing and digital counting systems (72 pp.). At the end of each chapter, references, problems and experiments augment and clarify the text. The writing is very clear and there are many diagrams and drawings to assist the reader. Three supplements and four appendices complete the book.

G. MILAZZO, Istituto Superiore di Sanità, Roma.

J. Electroanal. Chem., 5 (1963) 484

Bibliografia polarografica, (1959) Part II, Supplement No. 12A, by L. JELLICI, L. GRIGGIO AND E. FORNASARI, Consiglio Nazionale delle Ricerche, Rome, 1961, 76 pages, $2.00, lire 1000.

The papers published in Supplement No. 12 (see *J. Electroanal. Chem.*, 3 (1962) 83) have been rearranged according to subject.

The publication is of interest to those workers in all branches of chemistry in which polarography has been used successfully.

J. Electroanal. Chem., 5 (1963) 485

Treatise on Analytical Chemistry, Part II: *Analytical Chemistry of the Elements*, Vols. 2 and 9, I. M. KOLTHOFF, P. J. ELVING AND E. B. SANDELL, Interscience Publishers, Inc., New York and London, 1962, xx + 471, xvi + 491 pages, £6.15s. per vol.

The fields of interest of these two volumes are somewhat different. Volume 2 deals with some of the more common elements, *e.g.* Fe, Co, Ni, and Si, plus the less common metals Ga, In and Tl, whilst Volume 9 is devoted to uranium and the artificial transuranic elements (neptunium, plutonium, americium, curium, berkelium, californium, einsteinium, fermium, mendelevium, nobelium, and lawrencium) and will, therefore, be of practical interest to relatively few specialists. Nevertheless, Volume 9 is important because it summarises the analytical aspects of these elements' chemical behaviour for the first time, and also gives a general survey of their history, occurrence, synthesis, properties, general behaviour, and handling in the laboratory.

The contributors and their subjects are: HIROSHI ONISHI (Ga, In and Tl) 106 pages; H. R. SHELL (Si) 100 pages; J. R. MUSGRAVE (Ge) 40 pages; L. M. MELNIK (Fe) 64 pages; J. M. DALL AND C. V. BANKS (Co) 66 pages, and (Ni) 64 pages; G. L. BOOMAN AND J. R. WATERBURY (transuranium and transcurium elements) 252 pages.

The general arrangement of these two volumes is very similar to that adopted in the previously published volumes of this series (*J. Electroanal. Chem.*, 3 (1962) 221 and 4 (1962) 63).

GIULIO MILAZZO, Istituto Superiore di Sanità, Roma

J. Electroanal. Chem., 5 (1963) 485

Solvolytic Displacement Reactions, by ANDREW STREITWIESER, Jr., McGraw-Hill Series in Advanced Chemistry, McGraw-Hill, London, 1962, pp. ix + 214. 39s.

This book is a direct (uncorrected) reprint of an article published in Chemical Reviews in 1956, together with a twenty-two page supplement covering recent developments in the more important topics. Most of the rate measurements discussed have been made in organic or aqueous-organic solvent mixtures. Interpretations of the role of the solvent in these recactions are necessarily of a very qualitative kind. Such factors as the molecular volume of the solvent, the hydrogen bonding capacity of the solvent towards displaced groups, and 'solvent polarity' as estimated from charge-transfer absorption spectra are discussed. The rapidly-accumulating body of experimental kinetic work emphasises the need for more extensive data on the electrochemistry of non-aqueous solutions, and for theoretical work on the state of the solute in solvents of tis kind – particularly in mixed solvents.

N. S. HUSH, The University, Bristol

J. Electroanal. Chem., 5 (1963) 485

Ions in Hydrocarbons, by A. GEMANT, Interscience Publishers Inc., New York and London, 1962, viii + 261 pages, 945.

It is usually supposed that electrochemistry is confined to the study of solvents with high dielectric constants (water, alcohols etc.) and of molten electrolytes. This assumption, however, imposes an unnecessary limitation with the result that little interest has been shown in extending electrochemical research and its technological developments, in other directions. It is true that outstanding experimental difficulties have to be overcome when working with solvents of very low dieletric constant, but the author of this monograph shows, as a result of his own work, how it is possible to obtain useful results in this unexplored section of electrochemistry.

The most interesting part of this monograph is that which calls attention to the many interesting problems in this field which are worthy of study and which are also likely to be satisfactorily resolved. In addition, various other topics and the experimental data resulting from them, are logically discussed, although some of the results can only be considered as qualitative or semi-quantitative.

The contents are divided into eight sections devoted respectively to: relationship with other fields (22 pages); hydrogen ion (32 pages); ions of amino-aliphatic acids in solutions (46 page); ions from the oxidation of ortho-substituted aromatics (36 pages); ions from ozonolysis of aromatics (48 pages); metal-complex ions (8 pages); election transfer ions (24 pages) and radiolytic ions (8 pages). This short summary of the subjects dealt with shows the usefulness of this monograph which has been read with interest and with pleasure by the reviewer.

G. MILLAZZO, Istituto Superiore di Sanità, Roma

J. Electroanal. Chem., 5 (1963) 485–486

Methods of Organic Elemental Analysis, by G. INGRAM, Chapman and Stall, London, 1962, xvi + 511 pages, 75s.

Considerable advances in organic microanalysis have been made since Pregl, in 1912, developed his methods for the determination of those elements usually found in organic compounds. A vast amount of literature has consequently accumulated and several text-books on the subject are available.

This book, however, has been constructed in a rather different way from the usual reference work. It devotes considerable space to discussions on the merits of the various methods in current use as well as giving full working details. As result, only elemental analysis has been dealt with and the determination of functional groups has been omitted.

The book is divided into three sections. The methods for the determination of common elements in organic compounds are given in Part I and the methods for the determination of metallic and other non-metallic elements in Part II. Part III is concerned with the techniques of analysis on a microgram scale.

A comprehensive selection of original literature is appended to each chapter. The printing and binding are excellent and the drawings are accurate and of a very high standard.

On the whole we think that the author has achieved his purpose (stated in the preface) to present a text of elemental microanalysis which is useful both to the student and the professional analyst.

L. MANZONI, University of Rome

J. Electroanal. Chem., 5 (1963) 486

Comprehensive Biochemistry, Sect. I, Vol. 2, Organic and Physical Chemistry, by M. FLORKIN AND E. H. STUTZ, Elsevier Publishing Co., Amsterdam, 1962, xii + 328 pages, Dfl. 40.

Volume I appeared in the collection of *Comprehensive Biochemistry* and is also devoted to organic and physical chemistry.

Nowadays, a background knowledge of theoretical organic chemistry is needed for the full appreciation of biochemistry and the interpretation of biochemical phenomena. Drs. Bender and Breslow have given a very clear account of the mechanism of organic reactions together with many relevant biochemical samples, so that the original purpose of the book is always kept well to the fore.

Dr. Stein has developed the physico-chemical aspect of molecules in solution with special reference to polymers and proteins and discusses methods for the determination of protein shapes and structures. He also describes diffusion and osmosis. Particularly detailed treatment is given to the physico-chemistry of membranes.

It is difficult to obtain a complete idea of the whole work from an examination of this volume alone, but the treatment of all the topics dealt with in this part is definitely of a very high standard and should be useful to biochemists in the resolving of their problems.

G. B. MARINI BETTOLO, Istituto Superiore di Sanità, Roma

J. Electroanal. Chem., 5 (1963) 486

Announcement

ELECTROANALYTICAL CHEMISTRY COURSE

Chemistry Department
Sir John Cass College, Jewry Street, Aldgate, London, E.C.3
September 9th–14th, 1963

To be conducted by DR. K. E. JOHNSON, B.Sc., Ph.D., A.R.C.S., D.I.C., and MR. J. V. WESTWOOD, M.Sc., F.R.I.C.

A week's course of postgraduate lectures and selected practical work will be held in the Chemistry Department. Admission to the lectures is unrestricted, but the practical course is limited to twelve persons.

Programme. — Two lectures will be given each morning from Monday to Friday, 9.30 a.m. to 12.30 p.m., and practical work each afternoon from 1.30 to 5.30 p.m., (except on Friday, 13th September) and Saturday, 14th September, from 9.30 to 12.30 p.m.

Morning coffee, midday lunch and afternoon tea will be served each day, and lunch will be provided on Saterday, 14th September.

The Friday afternoon will be devoted to a colloquium at which talks will be given by Professor G. J. HILLS on *Electrochemistry of Molten Salts*, MR. E. BISHOP on *Differential Electrolytic Potentiometry*, and DR. G. C. BARKER on *R.F. Polarography*. A dinner will follow in the evening at which all members of the course will be present.

Lecture Syllabus. — Basic principles of electrode potentials, pH, buffers and potentiometric titrations. Coulometry, Conductometry and H.F. titrations, Electrolysis and mass transfer processes, Polarography. Applications to aqueous, organic and molten salt systems. Amperometry. Cathode ray and A.C. polarography. Controlled potential and controlled current electrolyses. Chronopotentiometry. Kinetics of electrode processes.

Practical Course. — A selected range of experiments in the fields covered by the lecture course will be given. A choice of experiments and equipment available will be possible.

Applications. — These should be sent to MR. J. V. WESTWOOD, Senior Lecturer, Department of Chemistry, on or before 1st June, 1963.

Fees. — For complete course, including meals £ 15.
For lectures only, including meals £ 7.

SUBJECT INDEX

AUTHOR INDEX

BOOK REVIEWS

(according to titles)

BOOK REVIEWS

(according to authors)

CONTENTS

ELSEVIER PUBLISHING COMPANY, AMSTERDAM
Printed in The Netherlands by
NEDERLANDSE BOEKDRUK INRICHTING N.V., 'S-HERTOGENBOSCH